Electronic Supporting Information

For

Highly efficient phenalenyl-copper bifunctional photoredox catalyst for direct arylation of arenes and heteroarenes C–H bonds

Krishnendu Paramanik,[a] Nilaj Bandopadhyay,[a] Suraj Kumar Agrawalla,[b] Chandra Shekhar Purohit,[b] Bhaskar Biswas,*[a] and Hari Sankar Das*[a]

[a] Krishnendu Paramanik, Nilaj Bandopadhyay, Bhaskar Biswas, Hari Sankar Das
Department of Chemistry, University of North Bengal, Darjeeling 734013, India
E-mail: bhaskarbiswas@nbu.ac.in, harisankardas@nbu.ac.in
[b] Suraj Kumar Agrawalla, Chandra Shekhar Purohit, School of Chemical Sciences, National Institute of Science Education and Research, Bhubaneswar, Orissa-751005, India.

Email: bhaskarbiswas@nbu.ac.in, harisankardas@nbu.ac.in

Table of Contents

1. Materials and methods:

Every chemical and solvent was bought from a commercial supplier and used exactly as supplied. The ligands 9-hydroxy-1-phenalenone (HO,O−PLY),[1] 5-bromo-9-hydroxy-1-phenalenone (HO,O−PLY−Ph)[2] and the metal precursor Cu(BPY)Cl_2[3] were prepared according to the literature methods. ^{1}H and ^{13}C{^{1}H} NMR spectra were carried out on a Bruker advance 400 MHz spectrometer. The elemental (C, H, and N) analyses were performed using a Perkin Elmer 2400 CHN microanalyzer. Electrospray ionization mass spectra (ESI) were recorded on a Q-tof-micro quadruple mass spectrometer. Electronic absorption spectra were performed on a HITACHI U-2910 UV-Vis spectrophotometer. IR spectra were obtained using an FTIR-8400S SHIMADZU spectrophotometer. EPR spectroscopic measurements were executed on a Magnettech GmbH EPR Spectrometer MiniScope MS400. Cyclic voltammetry was accomplished in DMSO with 0.1 M Bu_4NClO_4 as electrolyte using a three-electrode configuration (Ag/AgCl reference electrode, glassy-carbon working electrode, Pt counter electrode) and a K-Lyte 1.2 potentiostat.

2. Characterization of HO, O-PLY and HO, O-PLY-Ph ligands:

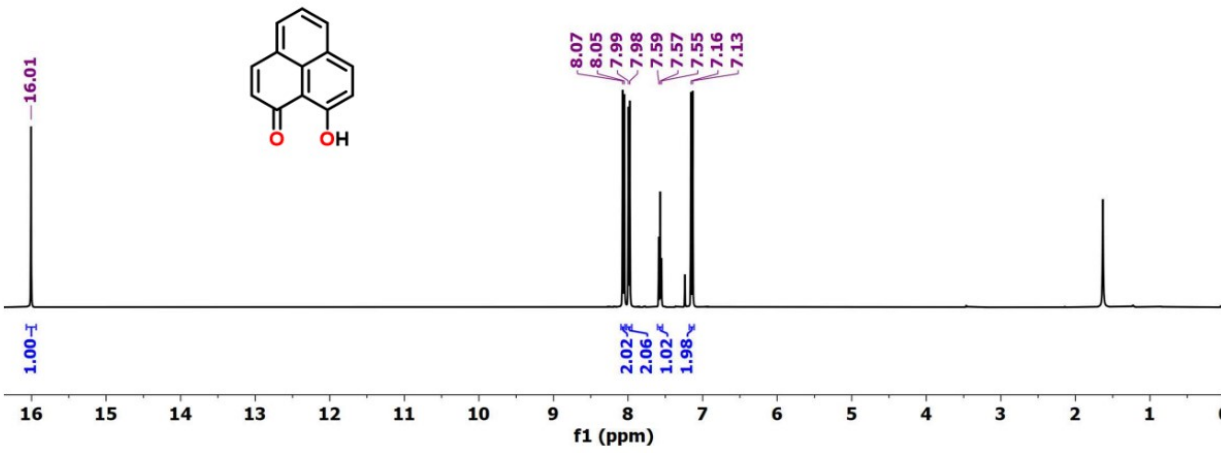

Figure S1: ^{1}H NMR spectra of ligand HO,O-PLY.

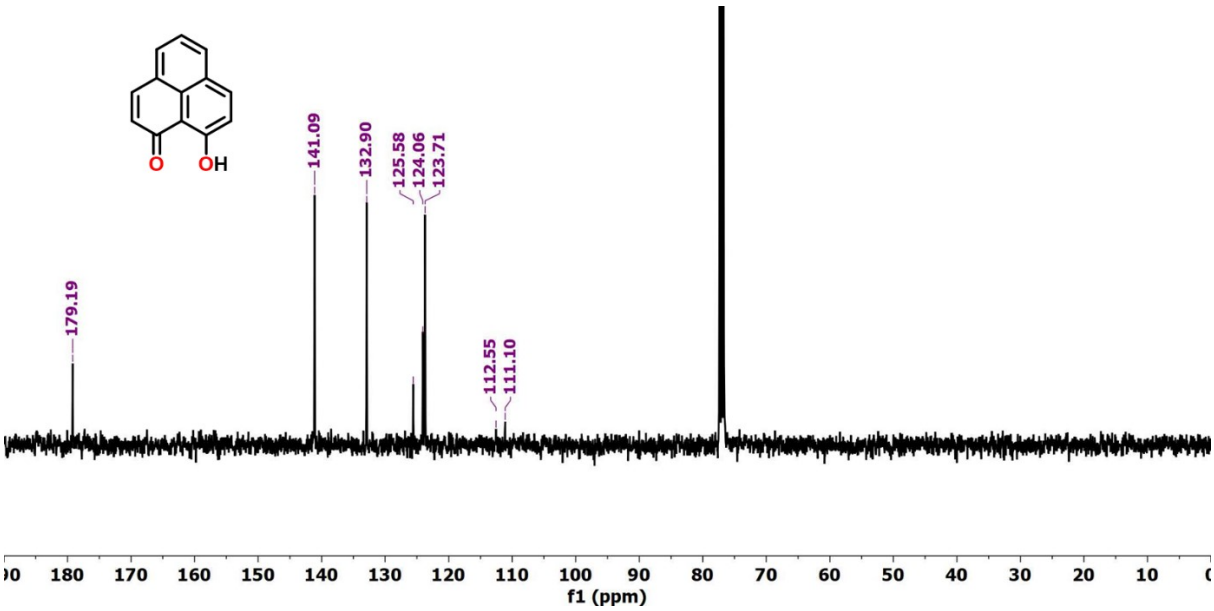

Figure S2: ^{13}C NMR spectra of ligand HO,O-PLY.

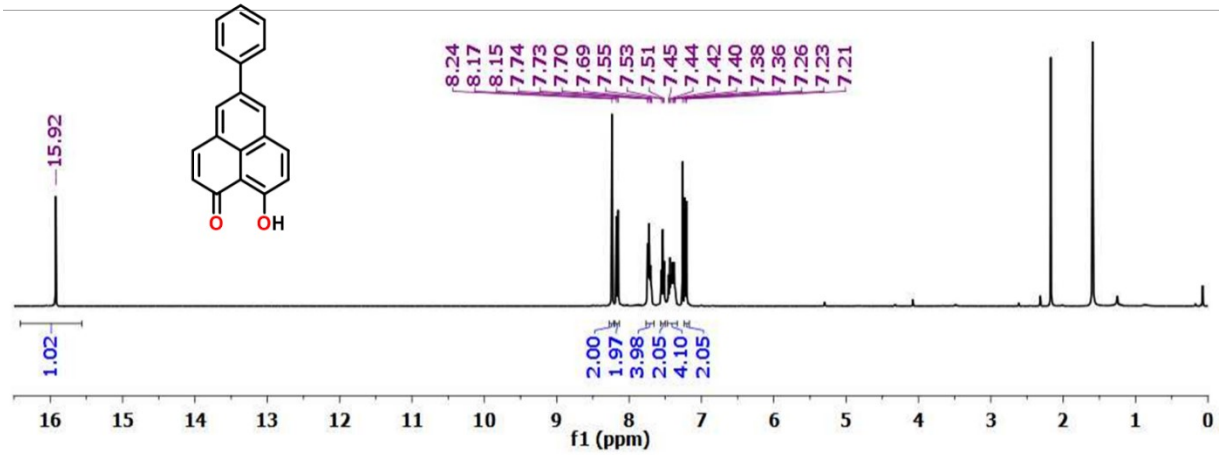

Figure S3: ^{1}H NMR spectra of ligand HO,O-PLY-Ph.

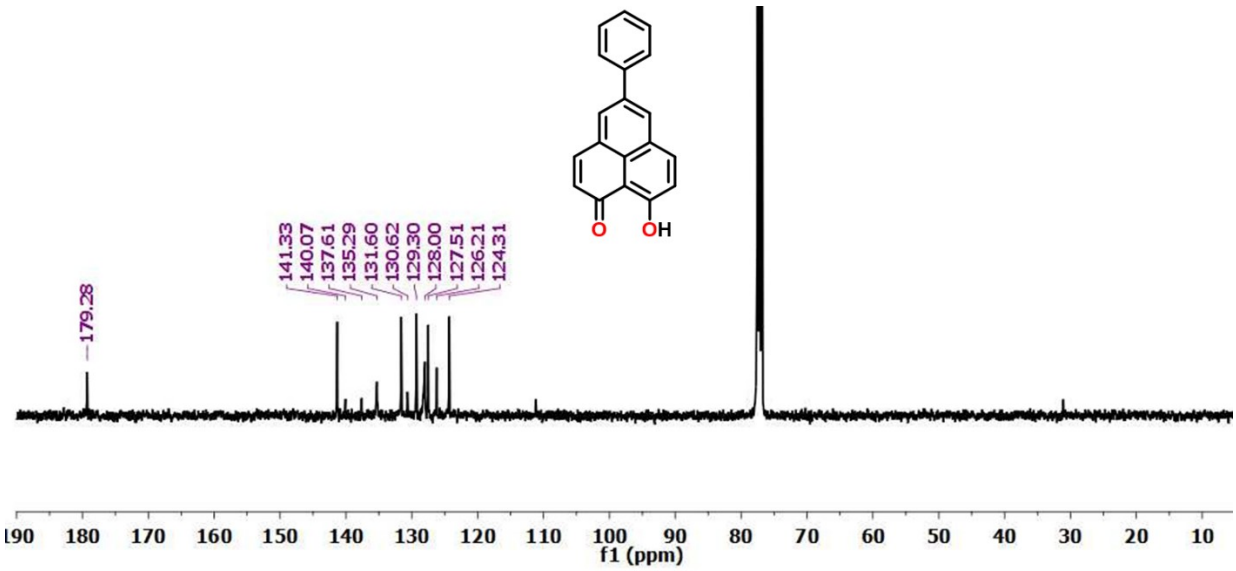

Figure S4: ^{13}C NMR spectra of ligand HO,O-PLY-Ph.

3. Characterization of precursor-complex [Cu(BPY)Cl_2]:

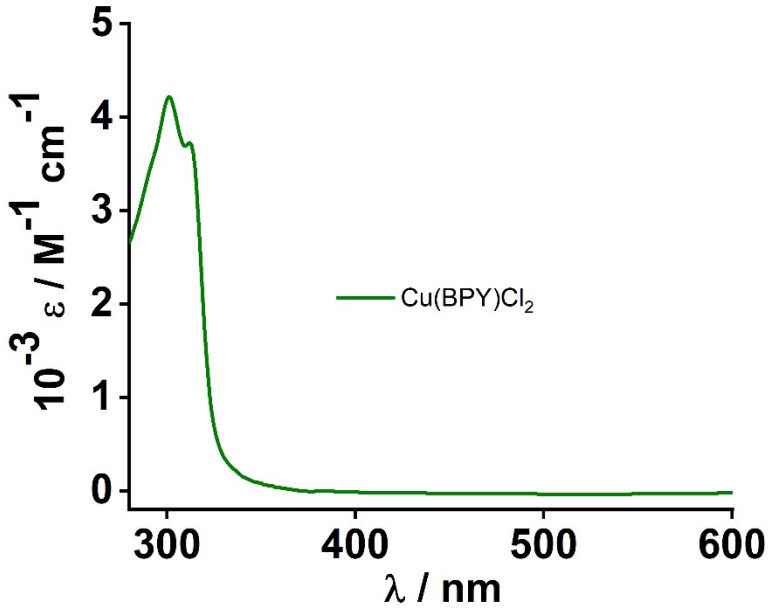

Figure S5: UV-VIS spectra of precursor-complex Cu(BPY)Cl_2 in methanol.

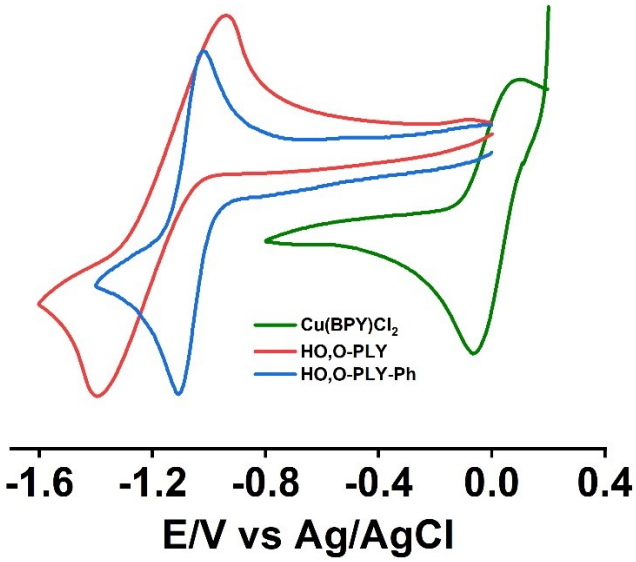

Figure S6: Cyclic Voltammogram of precursor-complex $Cu(BPY)Cl_2$, HO,O-PLY and HO,O-PLY-Ph in DMSO/0.1 M Bu_4NPF_6 at 298 K vs Ag/AgCl.

4. Synthesis and characterization of Complex 1:

4.1 Synthesis of [(BPY)Cu^{II}(O,O-PLY-Ph)Cl], 1:

To a stirred methanolic solution (5 mL) of ligand HO,O−PLY-Ph (98 mg, 0.36 mmol) and NEt_3 (100 µL, 0.72 mmol), a 8 mL DMF solution of $Cu(BPY)Cl_2$ (104.4 mg, 0.36 mmol) was added dropwise. Subsequently, the reaction mixture was refluxed at 90°C in the air for 6 h followed by ether diffusion at room temperature resulting in dark green solid precipitation. The precipitate was filtered, washed with ethanol followed by diethyl-ether, and dried in a vacuum, leading to pure complex **1**, used in catalysis without further purification. Yield: 141 mg, 74%. Elemental analysis calc. (%) for 3($C_{29}H_{19}ClCuN_2O_2$), 5(H_2O): C 62.59, H 4.04, N 5.03; found: C 62.37, H 3.94, N 4.89; ESI-MS: (m/z): calc. for $C_{29}H_{19}ClCuN_2O_2$: 525.0431 $[M]^+$; found: 525.0432. UV-vis (DMSO) λ_{max}/nm (ε in $M^{-1}cm^{-1}$): 343(16975), 358(30701), 405(3288), 427(6853), 452 (8616).

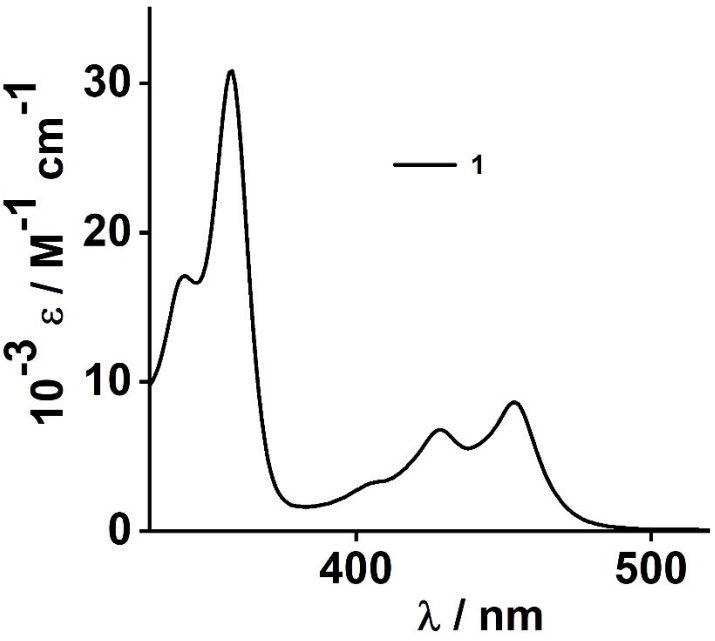

Figure S7: UV-Vis Spectra of complex **1** in DMSO**.**

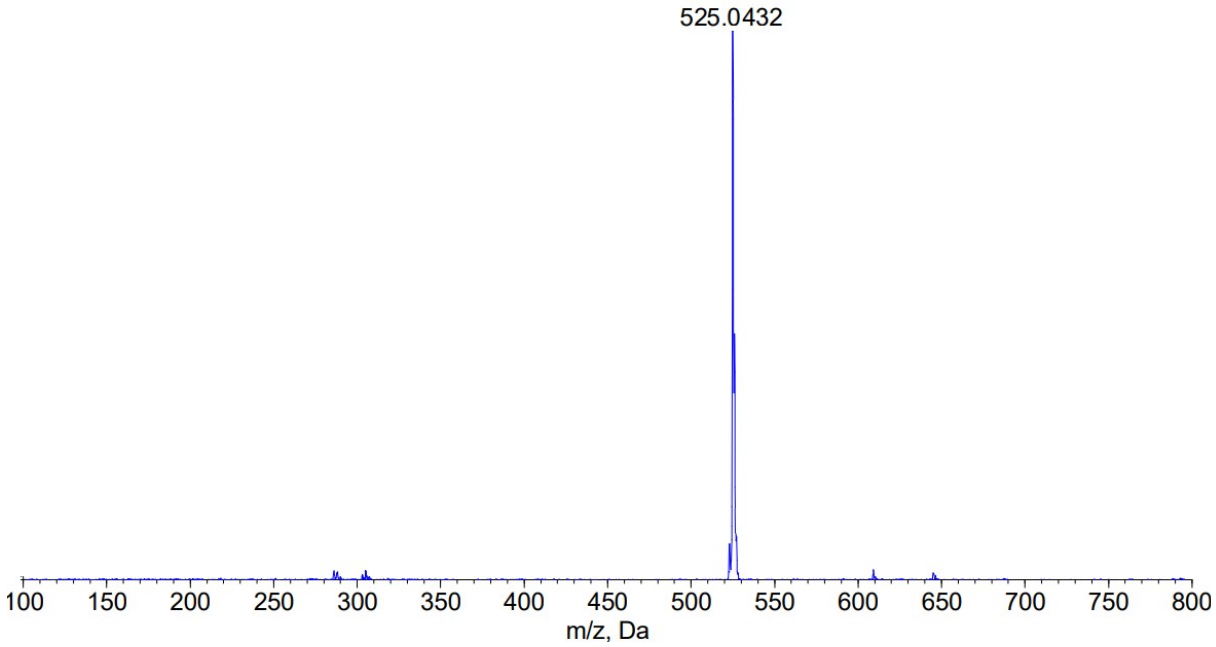

Figure S8: ESI-MS spectrum of complex **1**

4.2. Synthesis of [(BPY)Cu^{II}(O,O-PLY)Cl], 2:

Complex **2** was synthesized following the procedure for **1** by using ligand HO,O-PLY (71 mg, 0.36 mmol), NEt_3 (100 µL, 0.72 mmol), and precursor complex $Cu(BPY)Cl_2$ (104.4 mg, 0.36 mmol). The compound was isolated as a deep-green precipitate and used for catalysis without further purification. Yield: 118 mg, 73%. Elemental analysis calc. (%) for $C_{23}H_{15}ClCuN_2O_2$: C 61.34, H 3.36, N 6.22; found: C 61.49, H 3.42, N 6.07; ESI-MS: (m/z): calc. for $C_{23}H_{15}ClCuN_2O_2$: 414.0435 $[M-Cl]^+$; found: 414.0423. UV-vis (DMSO) λmax/nm (ε in $M^{-1}cm^{-1}$): 342(16795), 357(30612), 428(6794), 453(8675).

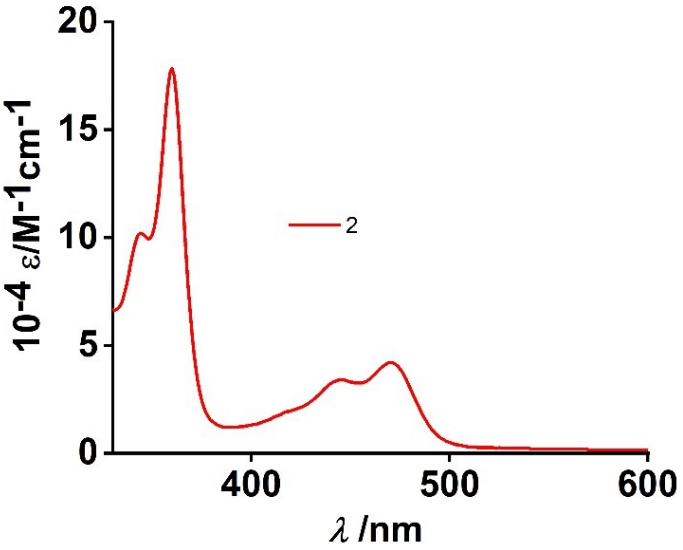

Figure S9: UV-Vis Spectra of complex **2** in DMSO.

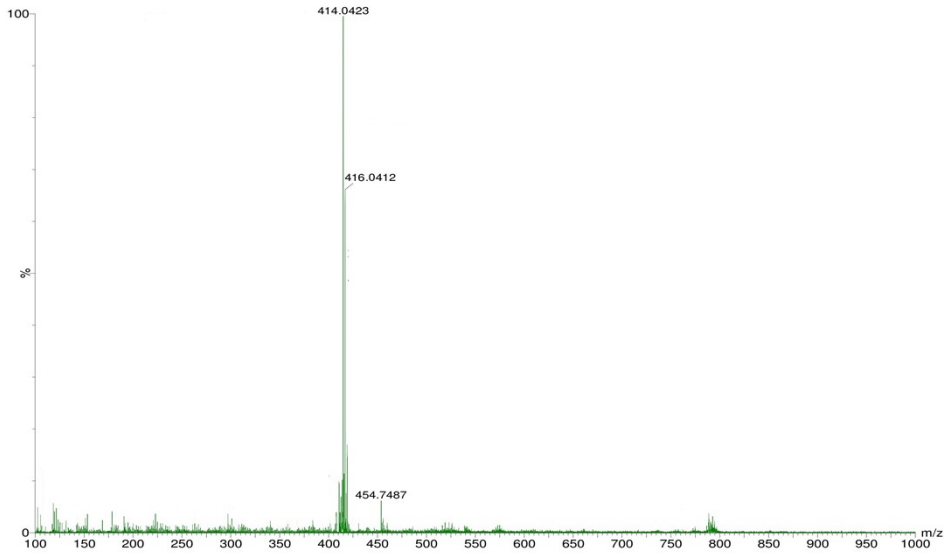

Figure S10: ESI-MS spectrum of complex **2**.

5. X-ray diffraction studies of 1:

For X-ray diffraction studies, single crystals of complexes **1** were obtained by diethyl-ether diffusion into the concentrated DMF solutions. Data collections were made on a Bruker-Kappa APEX II CCD diffractometer equipped with a 1K charge-coupled device (CCD) area detector employing a graphite monochromated Mo-Ka radiation (k¼ 0.71073 Å) at 100.0(2) K. The cell parameters and the reduction and correction of the collected data were determined by SMART SAINTPLus software, respectively,[4,5] followed by SADABS absorption corrections[6]. Finally, the crystal structures were solved by the direct method with the SHELXL-97 program package[7]. The refinement by the full-matrix least-squares method was executed on all F2 data with SHELXL-97. For all non-hydrogen atoms, anisotropic refinement was performed. Subsequently, the additional hydrogen atoms were positioned using the riding model. The molecular graphics were created using the Mercury software.

Supplementary crystallographic data are available free of charge from The Director, CCDC, 12 Union Road, Cambridge, CB2 1EZ, UK (fax: +44-1223-336033; E-mail: deposit@ccdc.cam.ac.uk or www: http://www.ccdc.cam.ac.uk) upon request, quoting deposition number CCDC 2421685 for complex **1**.

Table S1: X-ray structural data of complex **1**

Parameters	Complex **1**
Empirical formula	$3(C_{29}H_{19}ClCuN_2O_2)$, $5(H_2O)$
Formula weight	1669.53
T (K)	100
Wavelength (Å)	1.54184
Crystal system	Triclinic
Space group	P-1 (No. 2)
Unit cell dimensions	
a (Å)	11.9198 (2)
b (Å)	13.4821 (2)
c (Å)	22.5889 (4)
α (°)	84.990 (2)
β (°)	84.584 (1)
γ (°)	82.389 (1)
V (Å3)	3572.03 (10)
Z	2
ρ (gm cm^{-3})	1.552
Absorption coefficient (mm^{-1})	2.653
F (000)	1714
Theta range for data collection	3.3 to 75.6
Index ranges (h, k, l)	-14: 13 ; -16: 16 ; -28: 28
Reflections collected	55458
Independent reflections	14375
R(int)	0.075
Final R indices [I>0.0 sigma(I)]	R1 = 0.0770, wR2 = 0.1833,
Largest diff. peak and hole	2.35 and -2.56 e. $Å^{-3}$

Table S2: Selected X-ray crystallographic bond lengths (Å) and bond angles (°) of complex **1**.

Bond angles (°)			
Cl1–Cu1–O1	97.89 (7)	O2–Cu1–N2	90.59 (10)
Cl1–Cu1–O2	98.28 (7)	N1–Cu1–N2	80.68 (11)
Cl1–Cu1–N1	93.17 (8)	Cu1–O1–C1	124.8 (2)
Cl1–Cu1–N2	101.37 (8)	Cu1–O2–C11	125.9 (2)
O1–Cu1–O2	92.18 (10)	Cu1–N1–C20	124.6 (2)
O1–Cu1–N1	92.74 (10)	Cu1–N1–C24	115.3 (2)
O1–Cu1–N2	159.93 (10)	Cu1–N2–C25	115.0 (2)
O2–Cu1–N1	166.80 (11)	Cu1–N2–C29	125.7 (2)

Bond lengths (Å)			
Cu1–Cl1	2.528 (10)	O2–C11	1.276 (4)
Cu1–O1	1.950 (2)	N1–C24	1.348 (4)
Cu1–O2	1.913 (2)	N2–C29	1.350 (4)
Cu1–N1	1.995 (3)	N1–C20	1.340 (5)
Cu1–N2	2.018 (3)	N2–C25	1.342 (4)
O1–C1	1.270 (4)		

6. Experimental procedures for arylation of C–H bonds:

6.1. Optimization of photocatalytic C–H arylation of thiophene:

A mixture of catalyst (x mol%), Thiophene (0.96 mmol) and chlorobenzene diazonium salts (0.32 mmol) in 1 mL of DMSO was placed in a test tube. The reaction mixture was stirred at room temperature with irradiation of 30 W blue LED under air for 24 h. The arylated product was extracted using ethyl acetate (3 x 5 mL) and dried over anhydrous sodium sulphate. The solvent was removed under reduced pressure, and the obtained crude product was purified by column chromatography on silica gel (60-120 mesh) using a hexane/ethyl-acetate (100:1) mixture to yield the pure desired mono-arylated product.

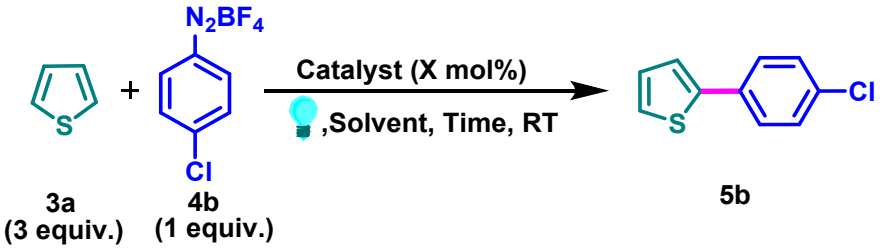

Scheme S1: Photocatalytic C–H arylation of thiophene using chlorobenzene diazonium salt.

6.2. General procedure for photocatalytic C–H arylation of arenes and heteroarenes:

A mixture of catalyst **1** (5 mol%, 0.016 mmol), arene (0.96 mmol for thiophene and furan, 1.6 mmol for benzenes, toluene, xylene, nitro-benzene and mesitylene) and aryldiazonium salts (0.32 mmol) in 1 mL of DMSO was placed in a test tube. The reaction mixture was stirred at room temperature with irradiation of 30 W blue LED under air for 24 h. The arylated product was extracted using ethyl acetate (3 x 5 mL) and dried over anhydrous sodium sulphate. The solvent was removed under reduced pressure, and the obtained crude product was purified by column chromatography on silica gel (60-120 mesh) using a hexane/ethyl-acetate mixture to yield the pure desired mono-arylated product.

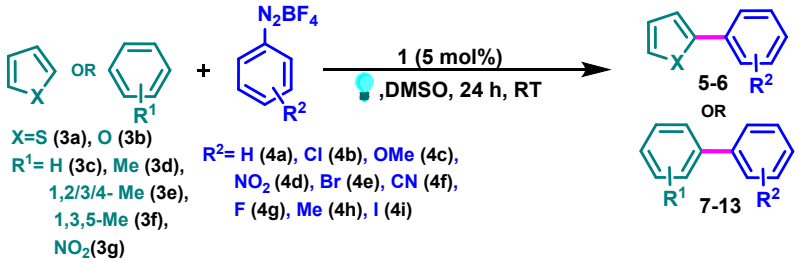

Scheme S2: Photocatalytic C–H arylation of arenes and heteroarenes using aryl diazonium salt.

6.3. Gram scale synthesis of 6c:

A mixture of catalyst (137 mg, 0.26 mmol), furan (1.13 mL, 15.6 mmol) and nitro-benzene diazonium salts (1g, 5.2 mmol) in 6 mL of DMSO was placed in a test tube. The reaction mixture was stirred at room temperature with irradiation of 30 W blue LED under air for 24 h. The arylated product was extracted using ethyl acetate (3 x 25 mL) and dried over anhydrous sodium sulphate. The solvent was removed under reduced pressure, and the obtained crude product was purified by column chromatography on silica gel (60-120 mesh) using a hexane/ethyl-acetate mixture to yield the pure desired mono-arylated product with 87% yield (856 mg).

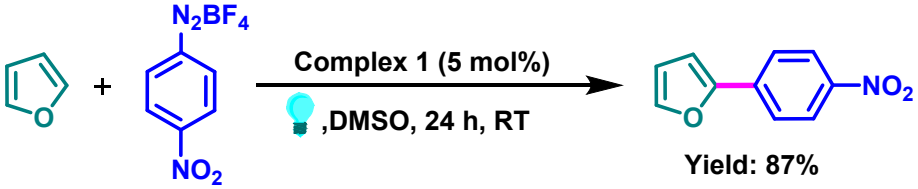

Scheme S3: Gram scale synthetic scheme of **6c**.

6.4. Gram scale synthesis of 13a:

A mixture of catalyst (116 mg, 0.22 mmol), nitro benzene (2.3 mL, 22.5 mmol) and chloro-benzene diazonium salts (1g, 4.5 mmol) in 6 mL of DMSO was placed in a test tube. The reaction mixture was stirred at room temperature with irradiation of 30 W blue LED under air for 24 h. The arylated product was extracted using ethyl acetate (3 x 25 mL) and dried over anhydrous sodium sulphate. The solvent was removed under reduced pressure, and the obtained crude product was purified by column chromatography on silica gel (60-120 mesh) using a hexane/ethyl-acetate mixture to yield the pure desired mono-arylated product with 78% yield (812 mg).

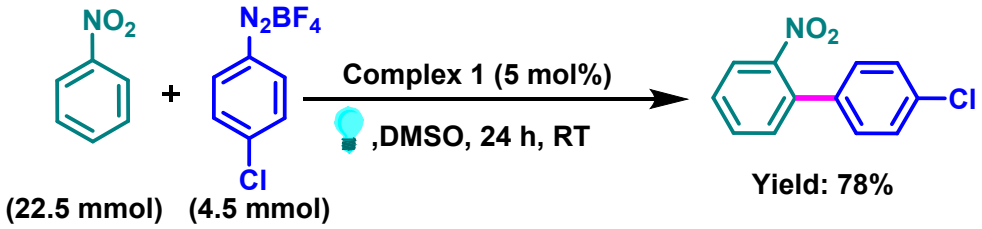

Scheme S4: Gram scale synthetic scheme of **13a**.

7. Mechanistic studies:

7.1. Procedure for reactions in the presence of radical scavenger TEMPO:

A mixture of catalyst (0.016 mmol), furan (0.96 mmol), cyano-benzene diazonium salts (0.32 mmol), and the required amount of TEMPO in 1 mL of DMSO was placed in a test tube. The reaction mixture was stirred at room temperature with irradiation of 30 W blue LED under air for 24 h. The arylated product was extracted using ethyl acetate (3 x 5 mL) and dried over anhydrous sodium sulphate. The solvent was removed under reduced pressure, and the obtained crude product was purified by column chromatography on silica gel (60-120 mesh) using a hexane/ethyl-acetate mixture to yield the pure desired product.

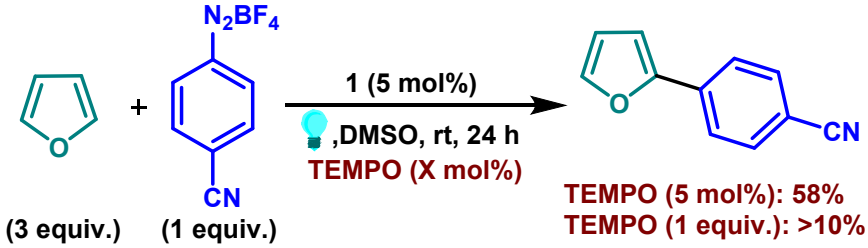

Scheme S5: **1** catalyzed C–H arylation of furan in the presence of TEMPO.

7.2. Procedure for TEMPO trapped intermediate:

A mixture of catalyst (0.16 mmol), cyano-benzene diazonium salts (0.32 mmol), and TEMPO (0.32 mmol) in 1 mL of DMSO was placed in a test tube. The reaction mixture was stirred at room temperature with irradiation of 30 W blue LED under air for 24 h. The arylated product was extracted using ethyl acetate (3 x 15 mL) and dried over anhydrous sodium sulphate. The solvent was removed under reduced pressure, and the obtained crude product was purified by column chromatography on silica gel (60-120 mesh) using a hexane/ethyl-acetate mixture to yield the pure desired compound **14** with 64% yield. The compound **14** was characterized by NMR spectroscopy (Figure S, S) and X-ray crystallography.

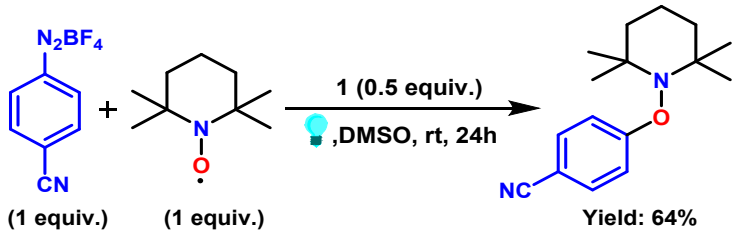

Scheme S6: Trapping of aryl radicals using TEMPO.

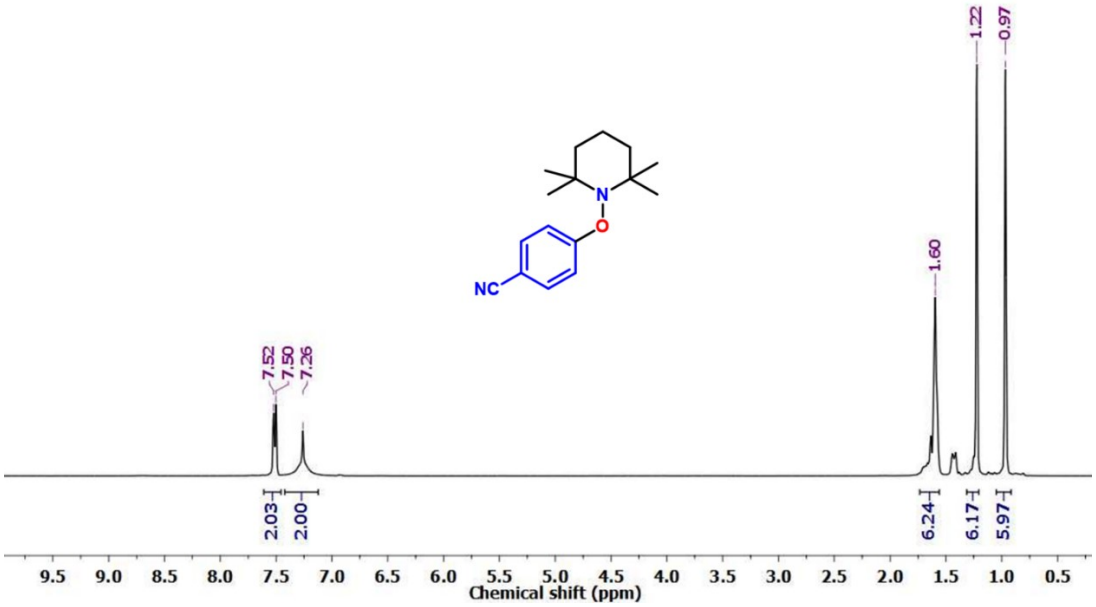

Figure S11: ^{1}H NMR spectra of TEMPO-trapped radical (**14**).

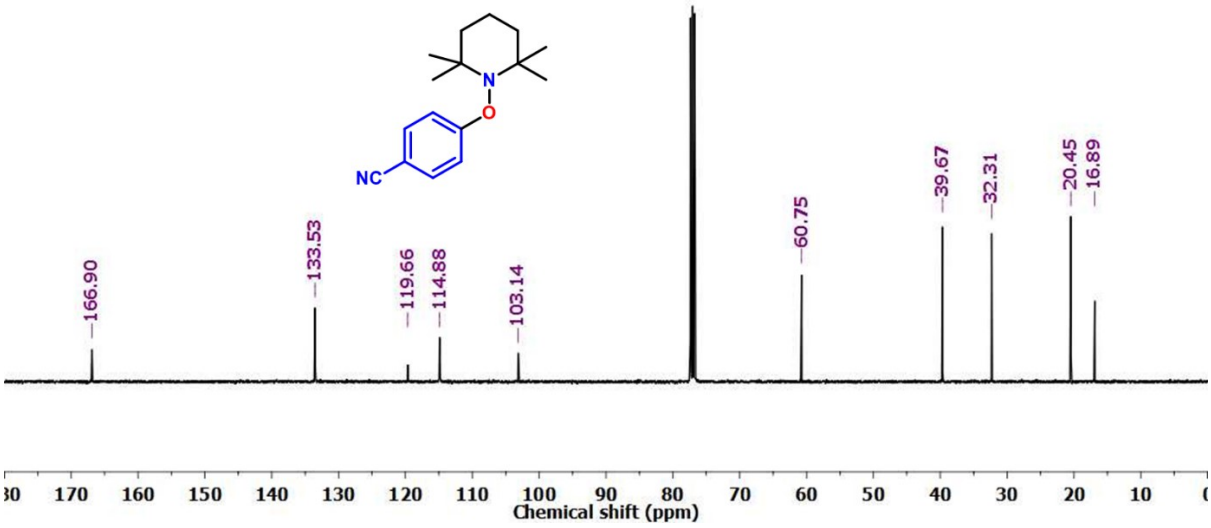

Figure S12: ^{13}C NMR spectra of TEMPO-trapped radical (**14**).

7.3. Photoluminescence study of O,O-PLY-Ph with 4b:

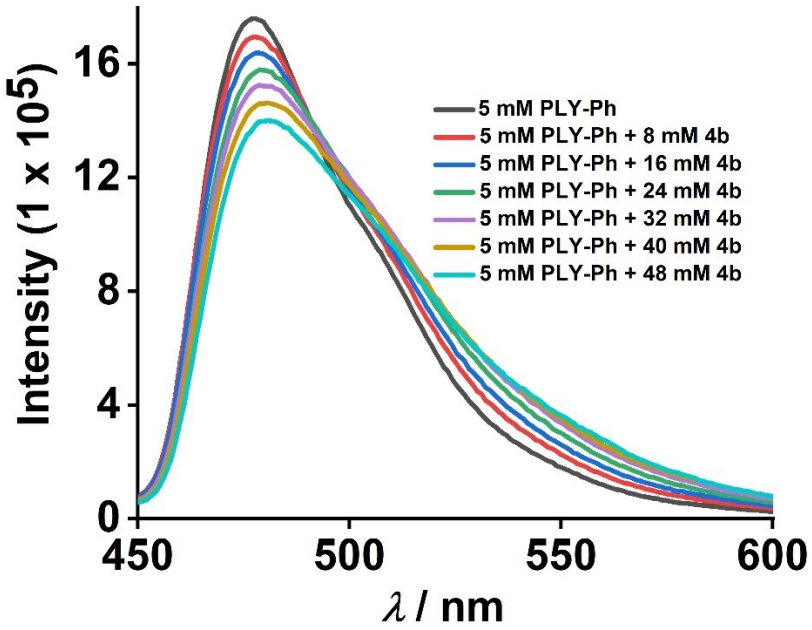

Figure S13: Photoluminescence titration of HO,O-PLY-Ph with chlorobenzene diazonium salt.

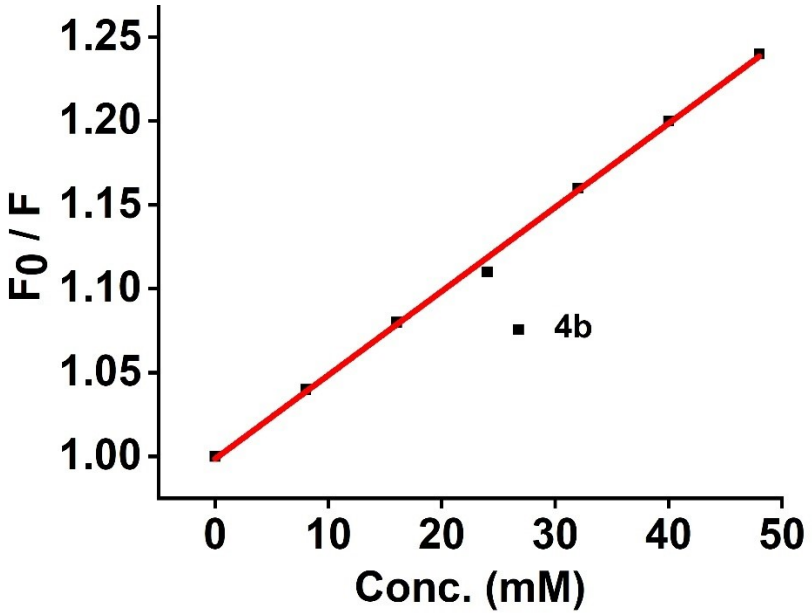

Figure S14: Stern-Volmer plot of the titration of HO,O-PLY-Ph with chlorobenzene diazonium salt.

7.4. UV-Vis-NIR studies for finding the interaction of catalyst 1 with different arenes:

All the UV-VIS experiments have been carried out with 30 µM solution of catalyst **1** in different sets of solutions.

SET 1: 2.45 mL DMSO solution of catalyst **1** + 0.05 mL DMSO.

SET 2: 2.45 mL DMSO solution of catalyst **1** + 0.05 mL thiophene.

SET 3: 2.45 mL DMSO solution of catalyst **1** + 0.05 mL furan.

SET 4: 2.45 mL DMSO solution of catalyst **1** + 0.05 mL benzene.

The spectra are shown in Figure 5c.

7.5. Fluorescence studies for finding the interactions of catalyst 1 with different arenes:

All the fluorescence measurements have been carried out with 2 mM solution of catalyst **1** in different sets of solutions.

SET 1: 2 mL DMSO solution of catalyst **1** + 0.1 mL DMSO.

SET 2: 2 mL DMSO solution of catalyst **1** + 0.1 mL thiophene.

SET 3: 2 mL DMSO solution of catalyst **1** + 0.1 mL furan.

SET 4: 2 mL DMSO solution of catalyst **1** + 0.1 mL benzene.

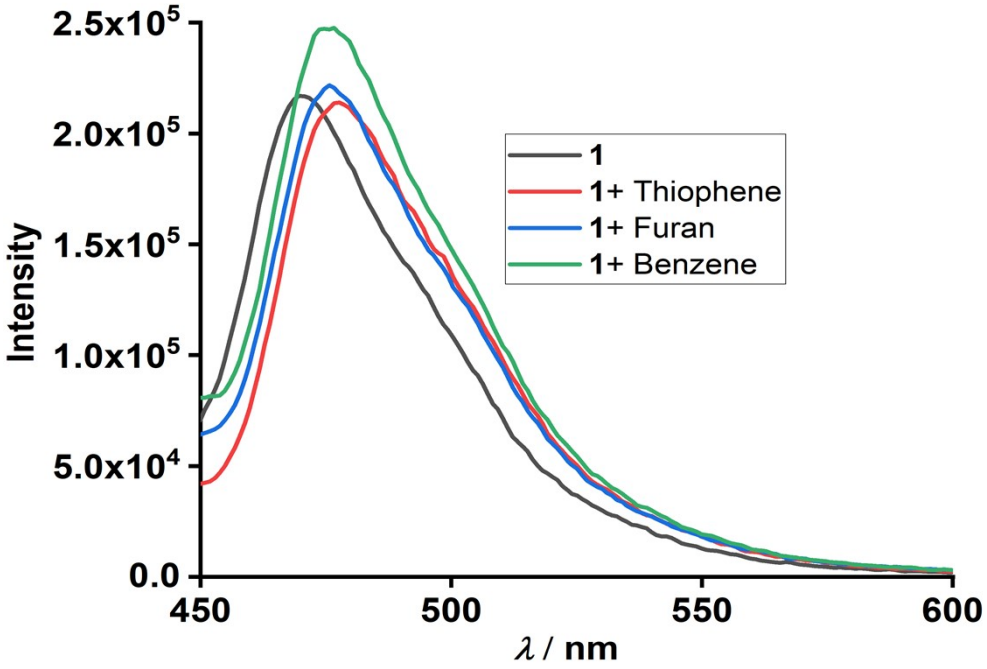

Figure S15. Fluorescence spectra of complex **1** with different arenes used in C–H arylation reaction.

7.6. C-H arylation of mesitylene using catalyst 2:

A mixture of catalyst **2** (5 mol%, 0.016 mmol), mesitylene (1.6 mmol) and aryldiazonium salts (0.32 mmol) in 1 mL of DMSO was placed in a test tube. The reaction mixture was stirred at room temperature with irradiation of 30 W blue LED under air for 24 h. The arylated product was extracted using ethyl acetate (3 x 5 mL) and dried over anhydrous sodium sulphate. The solvent was removed under reduced pressure, and the obtained crude product was purified by column chromatography on silica gel (60-120 mesh) using a hexane/ethyl-acetate mixture to yield the pure desired mono-arylated product.

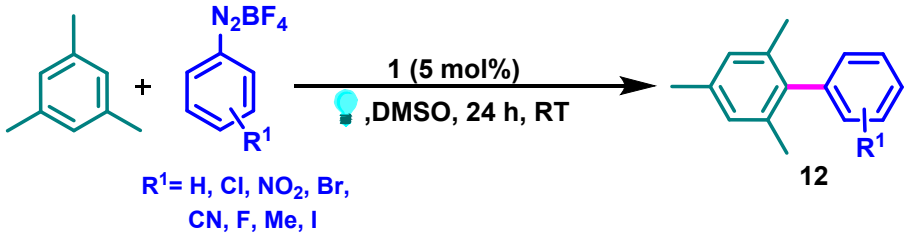

Scheme S7: **2**-catalzed C-H arylation of mesitylene.

7.7. On-Off experiment:

A mixture of catalyst **1** (5 mol%, 0.016 mmol), thiophene (0.96 mmol) and chloro-benzene diazonium salts (0.32 mmol) in 1 mL of DMSO was placed in a test tube. The reaction mixture was stirred at room temperature with irradiation of 30 W blue LED under air for 4 h. After that, the reaction mixture was stirred for another 20 h in dark conditions. The arylated product was extracted using ethyl acetate (3 x 5 mL) and dried over anhydrous sodium sulphate. The solvent was removed under reduced pressure, and the obtained crude product was purified by column chromatography on silica gel (60-120 mesh) using a hexane/ethyl-acetate mixture to yield the pure desired mono-arylated product with 84 % yield.

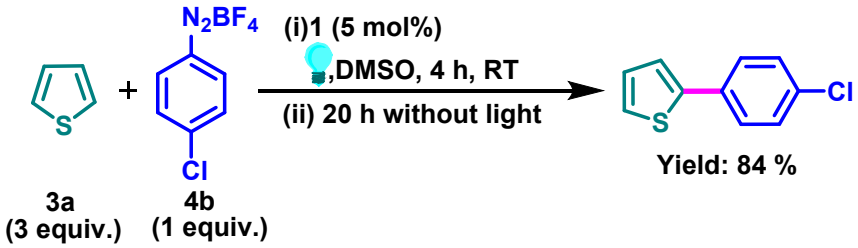

Scheme S8: 1-catalysed C-H arylation of thiophene under light on-off condition.

7.8. Procedure for detection TEMPO trapped biaryl radical using Furan:

A mixture of catalyst (0.16 mmol), furan (0.96 mmol), cyano-benzene diazonium salts (0.32 mmol), and TEMPO (0.32 mmol) in 1 mL of DMSO was placed in a test tube. The reaction mixture was stirred at room temperature with irradiation of 30 W blue LED under air for 24 h. The arylated product was extracted using ethyl acetate (3 x 15 mL) and dried over anhydrous sodium sulphate. The solvent was removed under reduced pressure leads to the crude product. The TEMPO-trapped biaryl radical product (**15**) was detected by mass spectroscopy.

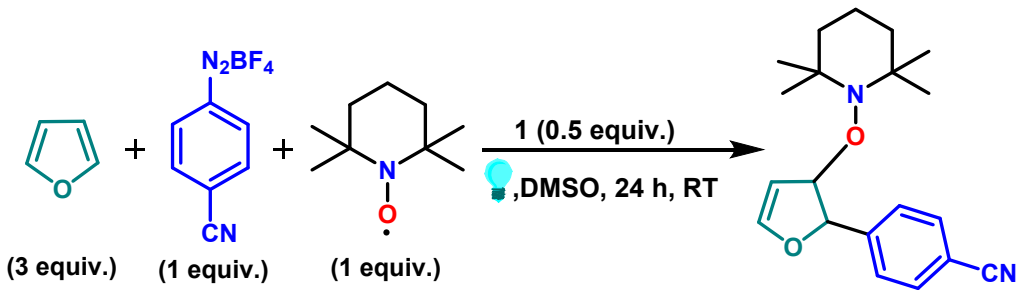

Scheme S9: Trapping of biaryl-radical using TEMPO.

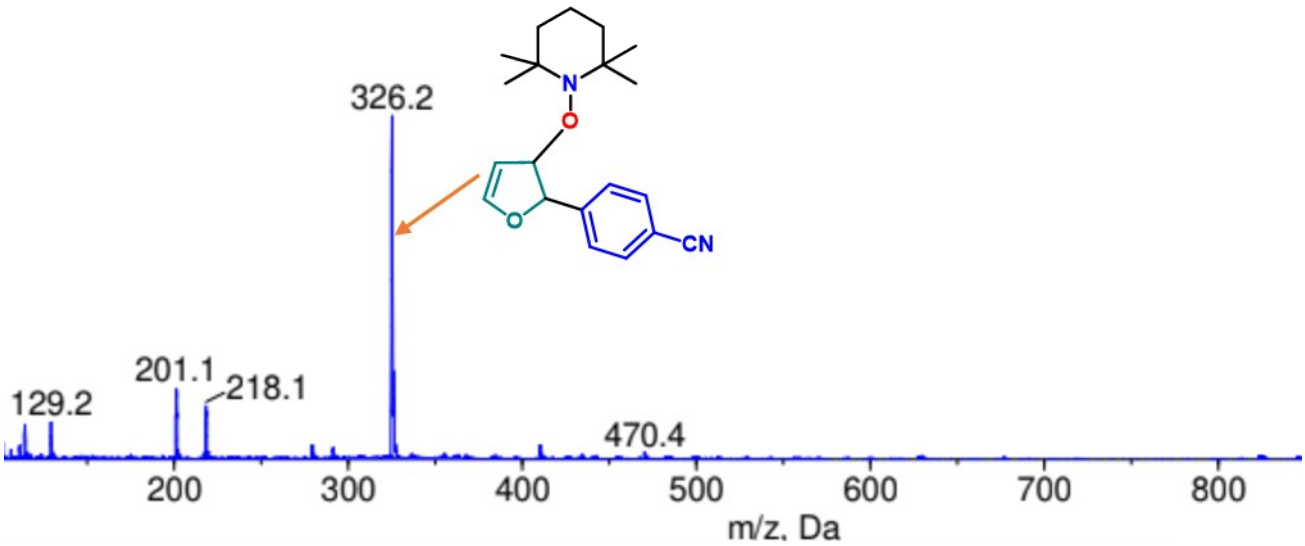

Figure S16: Mass spectrum of compound **15**.

7.9. Kinetic isotope effect:

A mixture of catalyst **1** (116 mg, 5 mol%), benzene diazonium salts (62 mg, 0.32 mmol) and 1:1 mixture of benzene and benzene-d_6 in 1 mL of DMSO was placed in a test tube. The reaction mixture was stirred at room temperature with irradiation of 30 W blue LED under air for 24 h. The arylated product was extracted using ethyl acetate (3 x 25 mL) and dried over anhydrous sodium sulphate. The solvent was removed under reduced pressure, and the obtained crude product was purified by column chromatography on silica gel (60-120 mesh) using a hexane/ethyl-acetate mixture. The GC-MS analysis indicates the formation of 1:1 mixture of phenyl-benzene (**7a**) and deuterated phenyl-benzene (**7a'**).

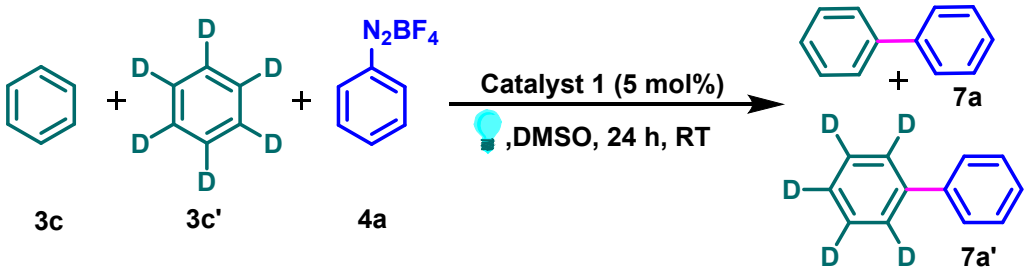

Scheme S10: Kinetic isotope effect experiments

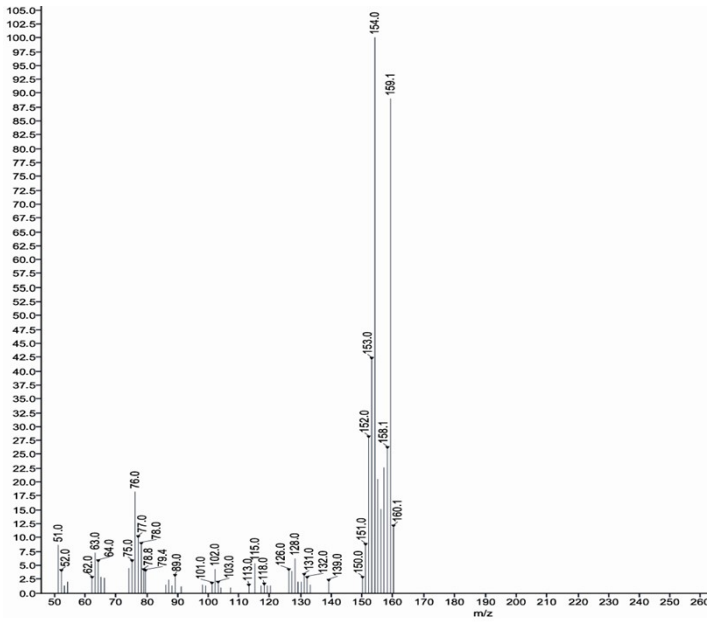

Figure S17: GC-MS spectrum of the mixture of **7a** and **7a'**

8. X-Ray Structure details of 11c and 14:

Single crystals of biaryl product **11c**, and TEMPO-trapped aryl radical **14** were grown by slow evaporation of DCM solutions at RT. The measurement details are given in section 5. Supplementary crystallographic data are available free of charge from The Director, CCDC, 12 Union Road, Cambridge, CB2 1EZ, UK (fax: +44-1223-336033; E-mail: deposit@ccdc.cam.ac.uk or www: http://www.ccdc.cam.ac.uk) upon request, quoting deposition number CCDC 2421684 for TEMPO adduct **14** and CCDC 2311199 for bi-arylated product **11c**.

Table S3: X-ray structural data of compounds **11c** and **14**.

Parameters	**Compound 11c**	**Compound 14**
Empirical formula	$C_{14}H_{13}NO_2$	$C_{16}H_{22}N_2O$
Formula weight	227.25	258.35
T (K)	100	100
Wavelength (Å)	1.54184	1.54184
Crystal system	Monoclinic	Triclinic
Space group	P21/c	P-1 (No. 2)
Unit cell dimensions		
a (Å)	6.6579 (2)	6.6423 (2)
b (Å)	22.1300 (5)	13.8452 (3)
c (Å)	7.8468 (2)	16.6714 (4)
α (°)	90	79.252 (2)
β (°)	101.462 (3)	85.493 (2)
γ (°)	90	83.620 (2)
V (Å^3)	1133.09 (5)	1494.31 (7)
Z	4	4
ρ (gm cm^{-3})	1.332	1.148
Absorption coefficient (mm^{-1})	0.723	0.563
F (000)	480	560
Theta range for data collection	4.0, 78.1	3.3, 77.5
Index ranges (h, k, l)	-8:8, -27:27, -9:9	-8:8, -17:17, -19:20
Reflections collected	9298	23558
Independent reflections	2355	6131
R(int)	0.026	0.038
Final R indices [I>0.0sigma(I)]	2248	5482
Largest diff. peak and hole	-0.33 and 0.28 e. Å^{-3}	-0.22 and 0.19 e. Å^{-3}

9. The analytical and spectroscopic characterization data of the products:

2-phenylthiophene, 5a[8]

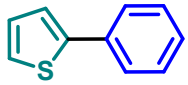

White solid (Yield: 84%). The crude product was purified by column chromatography using silica gel (60-120 mesh) with hexane.

^{1}H NMR (400 MHz, $CDCl_3$) δ (ppm): 7.61-7.58 (m, 2H), 7.38-7.35 (m, 2H), 7.31-7.25 (m, 3H), 7.06 (dd, *J* = 5.1, 3.7 Hz, 1H).

^{13}C NMR (100 MHz, $CDCl_3$) δ (ppm): 144.44, 134.41, 128.89, 128.0, 127.46, 127.17, 125.97, 124.80, 123.08.

2-(4-chlorophenyl)thiophene, 5b[8]

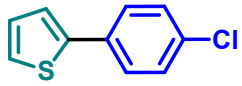

White solid (Yield: 91%). The crude product was purified by column chromatography using silica gel (60-120 mesh) with hexane.

^{1}H NMR (400 MHz, $CDCl_3$) δ (ppm): 7.54 (d, *J* = 8.6 Hz, 2H), 7.35 (d, *J* = 8.7 Hz, 2H), 7.29 (d, *J* = 3.5 Hz, 2H), 7.08 (dd, *J* = 4.9, 3.9 Hz, 1H).

^{13}C NMR (100 MHz, $CDCl_3$) δ (ppm): 143.19, 133.30, 133.03, 129.14, 128.26, 127.22, 125.31, 123.56.

2-(4-methoxyphenyl)thiophene, 5c[8]

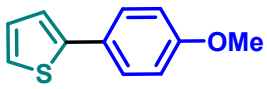

White solid (Yield: 94%). The crude product was purified by column chromatography using silica gel (60-120 mesh) with hexane.

^{1}H NMR (400 MHz, $CDCl_3$) δ (ppm): 7.56-7.52 (m, 2H), 7.20 (d, *J* = 4.0 Hz, 2H), 7.06 (dd, J = 4.9, 3.2 Hz, 1H), 6.92 (d, J = 8.6 Hz, 2H), 3.84 (s, 4H).

^{13}C NMR (100 MHz, $CDCl_3$) δ (ppm): 159.27, 144.54, 132.82, 128.01, 127.32, 123.93, 122.17, 114.80, 114.36, 55.45.

2-(4-ntrophenyl)thiophene, 5d[8]

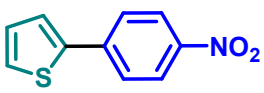

White solid (Yield: 88%). The crude product was purified by column chromatography using silica gel (60-120 mesh) with 1% of EtOAc in hexane.

^{1}H NMR (400 MHz, $CDCl_3$) δ (ppm): 8.24 (d, *J* = 8.9 Hz, 2H), 7.76-7.72 (m, 2H), 7.46 (ddd, *J* = 15.6, 4.4, 0.9 Hz, 2H), 7.15 (dd, *J* = 5.0, 3.7 Hz, 1H).

^{13}C NMR (100 MHz, $CDCl_3$) δ (ppm): 146.73, 141.79, 140.74, 128.81, 127.80, 126.14, 125.82, 124.54.

2-(4-bromophenyl)thiophene, 5e[8]

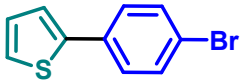

White solid (Yield: 76%). The crude product was purified by column chromatography using silica gel (60-120 mesh) with hexane.

^{1}H NMR (400 MHz, $CDCl_3$) δ (ppm): 7.49 (d, *J* = 3.3 Hz, 4H), 7.30 (d, *J* = 4.3 Hz, 2H), 7.10 – 7.07 (m, 1H).

^{13}C NMR (100 MHz, $CDCl_3$) δ (ppm): 143.04, 133.47, 132.07, 128.29, 127.51, 125.37, 123.60, 121.04.

4-(thiophen-2-yl)benzonitrile, 5f[9]

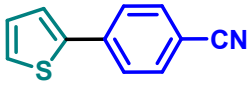

White solid (Yield: 89%). The crude product was purified by column chromatography using silica gel (60-120 mesh) with 1% of EtOAc in hexane.

^{1}H NMR (400 MHz, $CDCl_3$) δ (ppm): 7.68 – 7.61 (m, 4H), 7.39 (dd, *J* = 8.4, 4.6 Hz, 2H), 7.14 – 7.08 (m, 1H).

^{13}C NMR (100 MHz, $CDCl_3$) δ (ppm): 159.29, 142.08, 138.68, 132.76, 128.54, 127.09, 126.10, 125.13, 118.85, 110.56.

2-(4-fluorophenyl)thiophene, 5g[10]

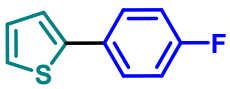

White solid (Yield: 72%). The crude product was purified by column chromatography using silica gel (60-120 mesh) with hexane.

^{1}H NMR (400 MHz, $CDCl_3$) δ (ppm): 7.60 – 7.55 (m, 2H), 7.29 – 7.26 (m, 1H), 7.24 (dd, *J* = 3.7, 1.1 Hz, 1H), 7.10 – 7.05 (m, 3H).

^{13}C NMR (100 MHz, $CDCl_3$) δ (ppm): 163.62, 161.17, 143.42, 133.17, 128.17, 127.75, 127.67, 124.89, 123.19, 116.03, 115.81.

2-(4-methylphenyl)thiophene, 5h[11]

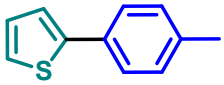

White solid (Yield: 86%). The crude product was purified by column chromatography using silica gel (60-120 mesh) with hexane.

^{1}H NMR (400 MHz, $CDCl_3$) δ (ppm): 7.51 (d, *J* = 8.1 Hz, 2H), 7.31 – 7.25 (m, 2H),7.19 (d, *J* = 8.0 Hz, 2H), 7.07 (dd, *J* = 5.1, 3.7 Hz, 1H), 2.37 (s, 3H).

^{13}C NMR (100 MHz, $CDCl_3$) δ (ppm): 144.88, 137.41, 131.92, 129.63, 128.01, 125.97, 124.35, 122.66, 21.25.

2-(2-iodophenyl)thiophene, 5i[8]

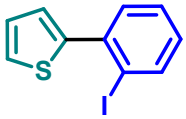

White solid (Yield: 93%). The crude product was purified by column chromatography using silica gel (60-120 mesh) with hexane.

^{1}H NMR (400 MHz, $CDCl_3$) δ (ppm): 7.99 (dd, *J* = 8.0, 0.8 Hz, 1H), 7.45 (dd, *J* = 7.7, 1.7 Hz, 1H), 7.40 (ddd, *J* = 5.9, 3.7, 0.8 Hz, 2H), 7.20 (dd, *J* = 3.5, 0.9 Hz, 1H), 7.12 (dd, *J* = 5.0, 3.6 Hz, 1H), 7.07 – 7.03 (m, 1H).

^{13}C NMR (100 MHz, $CDCl_3$) δ (ppm): 146.14, 141.27, 139.13, 137.38, 135.58, 129.84, 128.59, 128.50, 128.17, 100.93.

2-(3-chlorophenyl)thiophene, 5j[12]

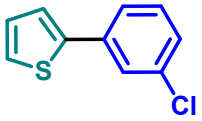

White solid (Yield: 84%). The crude product was purified by column chromatography using silica gel (60-120 mesh) with hexane.

^{1}H NMR (400 MHz, $CDCl_3$) δ (ppm): 7.58 (t, *J* = 1.7 Hz, 1H), 7.48 – 7.45 (m, 1H),7.32 – 7.28 (m, 3H), 7.07 (dd, *J* = 5.0, 3.8 Hz, 1H).

^{13}C NMR (100 MHz, $CDCl_3$) δ (ppm): 142.76, 136.16, 134.79, 130.11, 128.15, 127.37, 125.90, 125.59, 124.08, 123.87.

2-(4-chlorophenyl)furan, 6a[8]

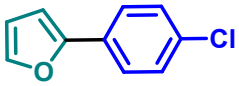

White solid (Yield: 92%). The crude product was purified by column chromatography using silica gel (60-120 mesh) with hexane.

^{1}H NMR (400 MHz, $CDCl_3$) δ (ppm): 7.63 – 7.59 (m, 2H), 7.49 (d, *J* = 1.4 Hz, 1H), 7.39 – 7.35 (m, 2H), 6.66 (d, *J* = 3.3 Hz, 1H), 6.49 (dd, *J* = 3.3, 1.8 Hz, 1H).

^{13}C NMR (100 MHz, $CDCl_3$) δ (ppm): 153.04, 142.44, 133.05, 129.47, 128.97, 125.11, 111.88, 105.51.

2-(4-methoxyphenyl)furan, 6b[8]

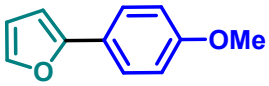

White solid (Yield: 89%). The crude product was purified by column chromatography using silica gel (60-120 mesh) with 1% of EtOAc in hexane.

^{1}H NMR (400 MHz, $CDCl_3$) δ (ppm): 7.61 (d, *J* = 8.9 Hz, 2H), 7.43 (d, *J* = 1.9 Hz, 1H), 6.92 (d, *J* = 8.8 Hz, 2H), 6.52 (d, *J* = 3.6 Hz, 1H), 6.45 (dd, *J* = 3.3, 1.8 Hz, 1H), 3.84 (s, 3H).

^{13}C NMR (100 MHz, $CDCl_3$) δ (ppm): 159.12, 154.22, 141.48, 125.33, 124.15, 114.22, 111.62, 103.46, 55.42.

2-(4-nitrophenyl)furan, 6c[8]

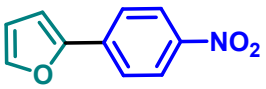

White solid (Yield: 93%). The crude product was purified by column chromatography using silica gel (60-120 mesh) with 1% of EtOAc in hexane.

^{1}H NMR (400 MHz, $CDCl_3$) δ (ppm): 8.27 – 8.23 (m, 2H), 7.82 – 7.78 (m, 2H), 7.58 (d, *J* = 2.0 Hz, 1H), 6.88 (d, *J* = 3.4 Hz, 1H),6.56 (dd, *J* = 3.5, 1.9 Hz, 1H).

^{13}C NMR (100 MHz, $CDCl_3$) δ (ppm): 151.84, 146.52, 144.27, 136.55, 124.44, 124.04, 112.55, 109.08.

2-(4-bromophenyl)furan, 6d[8]

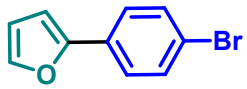

White solid (Yield: 78%). The crude product was purified by column chromatography using silica gel (60-120 mesh) with hexane.

^{1}H NMR (400 MHz, $CDCl_3$) δ (ppm): 7.59 – 7.51 (m, 4H), 7.49 (d, *J* = 2.0 Hz, 1H), 6.67 (d, *J* = 3.5 Hz, 1H), 6.49 (dd, *J* = 3.6, 1.9 Hz, 1H).

^{13}C NMR (100 MHz, $CDCl_3$) δ (ppm): 153.04, 142.50, 132.00, 131.90, 129.89, 125.39, 121.17, 111.91, 108.02, 105.65.

4-(furan-2-yl)benzonitrile, 6e[13]

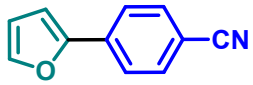

White solid (Yield: 80%). The crude product was purified by column chromatography using silica gel (60-120 mesh) with hexane.

^{1}H NMR (400 MHz, $CDCl_3$) δ (ppm): 7.77 – 7.72 (m, 2H), 7.68 – 7.63 (m, 2H), 7.57 – 7.51 (m, 1H), 6.81 (d, *J* = 3.1 Hz, 1H), 6.55 – 6.50 (m, 1H).

^{13}C NMR (100 MHz, $CDCl_3$) δ (ppm): 152.07, 143.80, 134.74, 132.69, 124.04, 119.07, 112.35, 110.37, 108.27.

2-(4-fluorophenyl)furan, 6f[12]

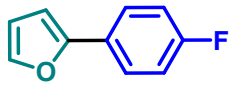

White solid (Yield: 68%). The crude product was purified by column chromatography using silica gel (60-120 mesh) with hexane.

^{1}H NMR (400 MHz, $CDCl_3$) δ (ppm): 7.65 – 7.60 (m, 2H), 7.44 (d, *J* = 1.9 Hz, 1H), 7.07 (d, *J* = 9.0 Hz, 2H), 6.56 (d, *J* = 3.4 Hz, 1H), 6.44 (dd, *J* = 3.4, 1.7 Hz, 1H).

^{13}C NMR (100 MHz, $CDCl_3$) δ (ppm): 163.36, 160.91, 153.18, 142.03, 127.29, 125.58, 125.50, 115.89, 115.78, 115.67, 115.56, 111.67, 106.88, 104.61.

2-(4-methylphenyl)furan, 6g[8]

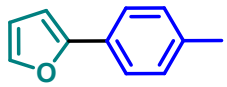

White solid (Yield: 71%). The crude product was purified by column chromatography using silica gel (60-120 mesh) with hexane.

^{1}H NMR (400 MHz, $CDCl_3$) δ (ppm): 7.56 (d, *J* = 8.2 Hz, 2H), 7.46 – 7.43 (m, 1H), 7.19 (d, *J* = 8.0 Hz, 2H), 6.59 (d, *J* = 3.3 Hz, 1H), 6.45 (dd, *J* = 3.3, 1.8 Hz, 1H), 2.36 (s, 3H).

^{13}C NMR (100 MHz, $CDCl_3$) δ (ppm): 154.26, 141.75, 131.93, 129.43, 128.33, 123.85, 111.62, 104.29, 21.24.

Phenylbenzene, 7a[8]

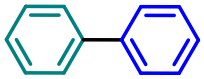

White solid (Yield: 78%). The crude product was purified by column chromatography using silica gel (60-120 mesh) with hexane.

^{1}H NMR (400 MHz, $CDCl_3$) δ (ppm): 7.59 (d, *J* = 7.1 Hz, 4H), 7.44 (t, *J* = 7.6 Hz, 4H), 7.34 (t, *J* = 7.3 Hz, 2H).

^{13}C NMR (100 MHz, $CDCl_3$) δ (ppm): 141.27, 128.77, 127.27, 127.19.

4-chlorophenylbenzene, 7b[8]

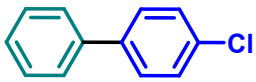

White solid (Yield: 85%). The crude product was purified by column chromatography using silica gel (60-120 mesh) with hexane.

^{1}H NMR (400 MHz, $CDCl_3$) δ (ppm): 7.54 (dd, *J* = 13.7, 8.0 Hz, 4H), 7.47 – 7.35 (m, 5H).

^{13}C NMR (100 MHz, $CDCl_3$) δ (ppm): 140.10, 139.78, 133.48, 129.00, 128.98, 128.49, 128.37, 127.68, 127.09.

4-methoxyphenylbenzene, 7c[8]

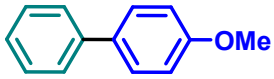

White solid (Yield: 89%). The crude product was purified by column chromatography using silica gel (60-120 mesh) with 1% of EtOAc in hexane.

^{1}H NMR (400 MHz, $CDCl_3$) δ (ppm): 7.59 – 7.50 (m, 4H), 7.42 (t, *J* = 7.7 Hz, 2H), 7.33 – 7.29 (m, 1H), 6.99 (d, *J* = 8.8 Hz, 2H), 3.86 (s, 3H).

^{13}C NMR (100 MHz, $CDCl_3$) δ (ppm): 159.39, 140.93, 132.84, 128.83, 128.27, 126.85, 126.77, 114.86, 114.30, 55.45.

4-nitrophenylbenzene, 7d[8]

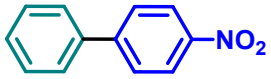

White solid (Yield: 87%). The crude product was purified by column chromatography using silica gel (60-120 mesh) with hexane.

^{1}H NMR (400 MHz, $CDCl_3$) δ (ppm): 8.30 (d, *J* = 8.9 Hz, 2H), 7.77 – 7.71 (m, 2H), 7.63 (dd, *J* = 8.2, 1.2 Hz, 2H), 7.53 – 7.43 (m, 3H).

^{13}C NMR (100 MHz, $CDCl_3$) δ (ppm): 147.46, 147.21, 138.93, 129.26, 129.02, 127.91, 127.49, 124.21.

4-bromophenylbenzene, 7e[14]

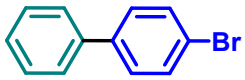

White solid (Yield: 73%). The crude product was purified by column chromatography using silica gel (60-120 mesh) with hexane.

^{1}H NMR (400 MHz, $CDCl_3$) δ (ppm): 7.60 – 7.52 (m, 4H), 7.49 – 7.41 (m, 4H), 7.40 – 7.34 (m, 1H).

^{13}C NMR (100 MHz, $CDCl_3$) δ (ppm): 140.24, 140.11, 132.68, 132.54, 131.97, 129.01, 128.85, 127.75, 127.05, 121.64.

4-cyanophenylbenzene, 7f[9]

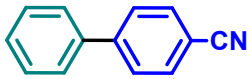

White solid (Yield: 75%). The crude product was purified by column chromatography using silica gel (60-120 mesh) with hexane.

^{1}H NMR (400 MHz, $CDCl_3$) δ (ppm): 7.75 – 7.71 (m, 2H), 7.70 – 7.67 (m, 2H), 7.59 (dd, *J* = 8.2, 1.1 Hz, 2H), 7.52 – 7.46 (m, 2H), 7.45 – 7.40 (m, 1H).

^{13}C NMR (100 MHz, $CDCl_3$) δ (ppm): 145.79, 139.29, 132.71, 129.77, 128.77, 127.84, 127.34, 119.05, 111.01.

4-fluorophenylbenzene, 7g[15]

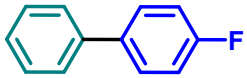

White solid (Yield: 66%). The crude product was purified by column chromatography using silica gel (60-120 mesh) with hexane.

^{1}H NMR (400 MHz, $CDCl_3$) δ (ppm): 7.57 (dd, *J* = 7.9, 4.3 Hz, 4H), 7.46 (t, *J* = 7.6 Hz, 2H), 7.36 (dd, *J* = 8.4, 6.4 Hz, 1H), 7.15 (t, *J* = 8.7 Hz, 2H).

^{13}C NMR (100 MHz, $CDCl_3$) δ (ppm): 163.79, 161.45, 140.37, 137.44, 128.91, 128.82, 128.74, 127.35, 127.12, 115.80, 115.59.

4-methylphenylbenzene, 7h[14]

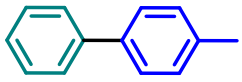

White solid (Yield: 71%). The crude product was purified by column chromatography using silica gel (60-120 mesh) with hexane.

^{1}H NMR (400 MHz, $CDCl_3$) δ (ppm):7.63 – 7.59 (m, 2H), 7.52 (d, *J* = 8.1 Hz, 2H), 7.45 (t, *J* = 7.7 Hz, 2H), 7.36 (d, *J* = 7.4 Hz, 1H), 7.28 – 7.24 (m, 2H), 2.42 (s, 3H).

^{13}C NMR (100 MHz, $CDCl_3$) δ (ppm): 141.18, 138.42, 136.90, 131.07, 129.91, 129.48, 128.71, 126.99, 21.10.

2-iodophenylbenzene, 7i[16]

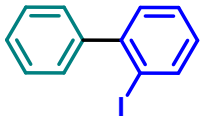

White solid (Yield: 72%). The crude product was purified by column chromatography using silica gel (60-120 mesh) with 1% of EtOAc in hexane.

^{1}H NMR (400 MHz, $CDCl_3$) δ (ppm): 7.98 (dd, *J* = 8.0, 0.8 Hz, 1H), 7.48 – 7.31 (m, 7H), 7.05 (td, *J* = 7.8, 1.8 Hz, 1H).

^{13}C NMR (100 MHz, $CDCl_3$) δ (ppm): 146.75, 144.41, 139.58, 130.16, 129.36, 128.85, 128.19,128.03, 127.72, 98.69.

n-(4-chlorophenyl)toluene, 8a[15]

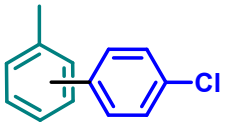

After completion of the reaction, product was extracted in 25 mL ethyl acetate and dried over anhydrous sodium sulphate. The solvent was removed under reduced pressure. All isomeric products (ortho, meta and para) were collected together from other reaction impurities by column chromatography over silica gel (100-200 mesh) using 3% EtOAc in hexane mixture. Total yield was calculated by taking weight of obtained mixture of products. This mixture of products was subjected to ^{1}H NMR spectroscopic characterization. The percentage of different regio-isomers was calculated by relative integration of the protons arising from the respective isomers.

n-(4-bromophenyl)toluene, 8b

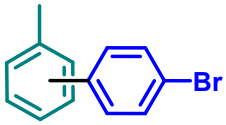

After completion of the reaction, product was extracted in 25 mL ethyl acetate and dried over anhydrous sodium sulphate. The solvent was removed under reduced pressure. All isomeric products (ortho, meta and para) were collected together from other reaction impurities by column chromatography over silica gel (100-200 mesh) using 5% EtOAc in hexane mixture. Total yield was calculated by taking weight of obtained mixture of products. This mixture of products was subjected to ^{1}H NMR spectroscopic characterization. The percentage of different regio-isomers was calculated by relative integration of the protons arising from the respective isomers.

n-(4-nitrophenyl)toluene, 8c[15]

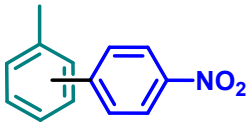

After completion of the reaction, product was extracted in 25 mL ethyl acetate and dried over anhydrous sodium sulphate. The solvent was removed under reduced pressure. All isomeric products (ortho, meta and para) were collected together from other reaction impurities by column chromatography over silica gel (100-200 mesh) using 2% EtOAc in hexane mixture. Total yield was calculated by taking weight of obtained mixture of products. This mixture of products was subjected to ^{1}H NMR spectroscopic characterization. The percentage of different regio-isomers was calculated by relative integration of the protons arising from the respective isomers.

n-(4-methoxyphenyl)toluene, 8d[15]

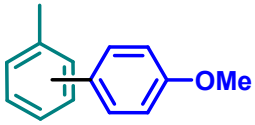

After completion of the reaction, product was extracted in 25 mL ethyl acetate and dried over anhydrous sodium sulphate. The solvent was removed under reduced pressure. All isomeric products (ortho, meta and para) were collected together from other reaction impurities by column chromatography over silica gel (100-200 mesh) using 3% EtOAc in hexane mixture. Total yield was calculated by taking weight of obtained mixture of products. This mixture of products was subjected to ^{1}H NMR spectroscopic characterization.

The percentage of different regio-isomers was calculated by the relative integration of the protons arising from the respective isomers.

3,4-dimethyl-1,1'-biphenyl, 9a[17,18]

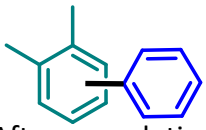

After completion of the reaction, the product was extracted in 25 mL ethyl acetate and dried over anhydrous sodium sulphate. The solvent was removed under reduced pressure. All isomeric products (ortho and meta) were collected from other reaction impurities using column chromatography over silica gel (100-200 mesh) using 1% EtOAc in a hexane mixture. The total yield was calculated by taking the weight of the obtained product mixture. This mixture of products was subjected to ^{1}H NMR spectroscopic characterization. The percentage of different regio-isomers was calculated by the relative integration of the protons arising from the respective isomers.

4'-Nitro-3,4-dimethyl-1,1'-biphenyl, 9b[19]

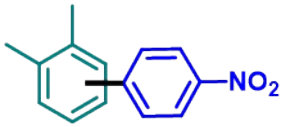

After completion of the reaction, the product was extracted in 25 mL ethyl acetate and dried over anhydrous sodium sulphate. The solvent was removed under reduced pressure. All isomeric products (ortho and meta) were collected from other reaction impurities using column chromatography over silica gel (100-200 mesh) using 1% EtOAc in hexane mixture. The total yield was calculated by taking the weight of the obtained mixture of products. This mixture of products was subjected to ^{1}H NMR spectroscopic characterization. The percentage of different regio-isomers was calculated by the relative integration of the protons arising from the respective isomers.

4'-Bromo-3,4-dimethyl-1,1'-biphenyl, 9c[20]

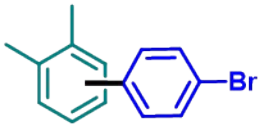

After completion of the reaction, the product was extracted in 25 mL ethyl acetate and dried over anhydrous sodium sulphate. The solvent was removed under reduced pressure. All isomeric products (ortho and meta) were collected from other reaction impurities using column chromatography over silica gel (100-200 mesh) using 2% EtOAc in hexane mixture. The total yield was calculated by taking the weight of the obtained mixture of products. This mixture of products was subjected to ^{1}H NMR spectroscopic characterization. The percentage of different regio-isomers was calculated by the relative integration of the protons arising from the respective isomers.

4'-Fluoro-3,4-dimethyl-1,1'-biphenyl, 9d[21]

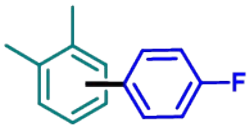

After completion of the reaction, the product was extracted in 25 mL ethyl acetate and dried over anhydrous sodium sulphate. The solvent was removed under reduced pressure. All isomeric products (ortho and meta) were collected from other reaction impurities using column chromatography over silica gel (100-200 mesh) using 1% EtOAc in hexane mixture. The total yield was calculated by taking the weight of the obtained mixture of products. This mixture of products was subjected to ^{1}H NMR spectroscopic characterization. The percentage of different regio-isomers was calculated by the relative integration of the protons arising from the respective isomers.

4'-Nitro-3,5-dimethyl-1,1'-biphenyl, 10a[22,23]

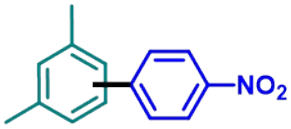

After completion of the reaction, the product was extracted in 25 mL ethyl acetate and dried over anhydrous sodium sulphate. The solvent was removed under reduced pressure. All isomeric products (ortho and meta) were collected from other reaction impurities using column chromatography over silica gel (100-200 mesh) using 3% EtOAc in hexane mixture. The total yield was calculated by taking the obtained product mixture's weight. This mixture of products was subjected to ^{1}H NMR spectroscopic characterization. The percentage of

different regio-isomers was calculated by the relative integration of the protons arising from the respective isomers.

4'-Bromo-3,5-dimethyl-1,1'-biphenyl, 10b[24]

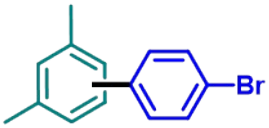

After completion of the reaction, the product was extracted in 25 mL ethyl acetate and dried over anhydrous sodium sulphate. The solvent was removed under reduced pressure. All isomeric products (ortho and meta) were collected from other reaction impurities using column chromatography over silica gel (100-200 mesh) using 1% EtOAc in hexane mixture. The total yield was calculated by taking the obtained product mixture's weight. This mixture of products was subjected to ^{1}H NMR spectroscopic characterization. The percentage of different regio-isomers was calculated by the relative integration of the protons arising from the respective isomers.

4-chloro-2',5'-dimethylbiphenyl, 11a[25]

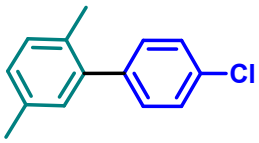

White solid (Yield: 78%). The crude product was purified by column chromatography using silica gel (60-120 mesh) with hexane.

^{1}H NMR (400 MHz, $CDCl_3$) δ (ppm): 7.43 – 7.37 (m, 2H), 7.29 – 7.25 (m, 2H), 7.18 (d, *J* = 7.7 Hz, 1H), 7.11 (d, *J* = 7.8 Hz, 1H), 7.04 (s, 1H), 2.37 (s, 3H), 2.23 (s, 3H).

^{13}C NMR (100 MHz, $CDCl_3$) δ (ppm): 140.60, 135.43, 132.81, 132.18, 130.59, 130.45, 129.58, 128.31, 20.96, 19.95.

4-bromo-2',5'-dimethylbiphenyl, 11b[25]

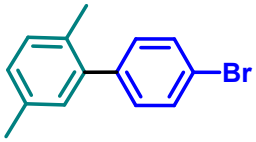

White solid (Yield: 66%). The crude product was purified by column chromatography using silica gel (60-120 mesh) with hexane.

^{1}H NMR (400 MHz, $CDCl_3$) δ (ppm): 7.51 (dd, *J* = 8.4, 2.0 Hz, 2H), 7.20 – 7.11 (m, 3H), 7.08 (d, *J* = 1.9 Hz, 1H), 7.00 (d, *J* = 2.0 Hz, 1H), 2.33 (s, 3H), 2.19 (s, 3H).

^{13}C NMR (100 MHz, $CDCl_3$) δ (ppm): 140.99, 140.49, 135.37, 132.04, 131.18, 130.88, 130.39, 130.31, 128.30, 20.90, 19.89.

4-nitro-2',5'-dimethylbiphenyl, 11c[26]

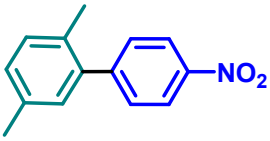

White solid (Yield: 70%). The crude product was purified by column chromatography using silica gel (60-120 mesh) with hexane.

^{1}H NMR (400 MHz, $CDCl_3$) δ (ppm): 8.29 (d, *J* = 8.5 Hz, 2H), 7.50 (d, *J* = 8.9 Hz, 2H), 7.22 (d, *J* = 7.7 Hz, 1H), 7.16 (dd, *J* = 7.6, 1.9 Hz, 1H), 7.06 (d, *J* = 1.9 Hz, 1H), 2.39 (s, 3H), 2.24 (s, 3H).

^{13}C NMR (100 MHz, $CDCl_3$) δ (ppm): 149.11, 139.54, 135.77, 132.12, 131.62, 130.76, 130.18, 129.26, 123.48, 20.98, 19.92.

4-methoxy-2',5'-dimethylbiphenyl, 11d[27]

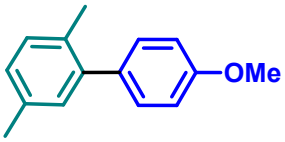

White solid (Yield: 74%). The crude product was purified by column chromatography using silica gel (60-120 mesh) with hexane.

^{1}H NMR (400 MHz, $CDCl_3$) δ (ppm): 7.27 (d, *J* = 8.4 Hz, 2H), 7.17 (d, *J* = 7.8 Hz, 1H), 7.12 – 7.07 (m, 2H), 6.97 (d, *J* = 8.4 Hz, 2H), 3.88 (s, 3H), 2.37 (s, 3H), 2.26 (s, 3H).

^{13}C NMR (100 MHz, $CDCl_3$) δ (ppm): 158.55, 141.46, 135.24, 134.63, 132.39, 130.74, 129.09, 128.29, 127.75, 114.27, 113.55, 55.37, 20.99, 20.10.

2-phenylmesitylene, 12a[8]

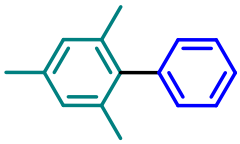

White solid (Yield: 76%). The crude product was purified by column chromatography using silica gel (60-120 mesh) with hexane.

^{1}H NMR (400 MHz, $CDCl_3$) δ (ppm): 7.43 (t, *J* = 7.3 Hz, 2H), 7.35 (d, *J* = 7.0 Hz, 1H), 7.20 – 7.11 (m, 2H), 6.96 (s, 2H), 2.35 (s, 3H), 2.02 (s, 6H).

^{13}C NMR (100 MHz, $CDCl_3$) δ (ppm): 143.61, 141.27, 139.29, 136.06, 131.13, 129.38, 128.44, 128.12, 127.13, 126.58, 21.10, 20.81.

1-chloro-4-mesitylbenzene, 12b[8]

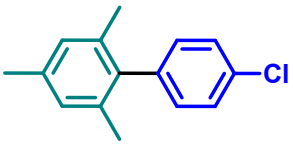

White solid (Yield: 82%). The crude product was purified by column chromatography using silica gel (60-120 mesh) with hexane.

^{1}H NMR (400 MHz, $CDCl_3$) δ (ppm): 7.40 (d, *J* = 8.4 Hz, 2H), 7.08 (d, *J* = 8.4 Hz, 2H), 6.95 (s, 2H), 2.34 (s, 3H), 2.00 (s, 6H).

^{13}C NMR (100 MHz, $CDCl_3$) δ (ppm): 139.60, 137.85, 137.04, 136.00, 132.58, 130.84, 128.75, 128.26, 21.12, 20.80.

1-nitro-4-mesitylbenzene, 12c[8]

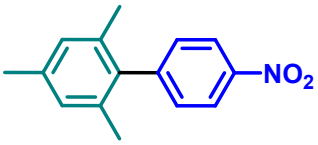

White solid (Yield: 77%). The crude product was purified by column chromatography using silica gel (60-120 mesh) with hexane.

^{1}H NMR (400 MHz, $CDCl_3$) δ (ppm): 8.30 (d, *J* = 8.8 Hz, 2H), 7.33 (d, *J* = 8.8 Hz, 2H), 6.97 (s, 2H), 2.34 (s, 3H), 1.99 (s, 6H).

^{13}C NMR (100 MHz, $CDCl_3$) δ (ppm): 148.66, 146.94, 137.82, 136.86, 135.36, 130.57, 128.49, 123.86, 21.13, 20.71.

1-bromo-4-mesitylbenzene, 12d[8]

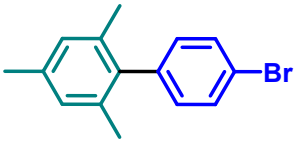

White solid (Yield: 67%). The crude product was purified by column chromatography using silica gel (60-120 mesh) with hexane.

^{1}H NMR (400 MHz, $CDCl_3$) δ (ppm): 7.55 (d, *J* = 8.4 Hz, 2H), 7.02 (d, *J* = 8.3 Hz, 2H), 6.94 (s, 2H), 2.33 (s, 3H), 1.99 (s, 6H).

^{13}C NMR (100 MHz, $CDCl_3$) δ (ppm): 140.08, 137.88, 137.07, 135.92, 131.70, 131.22, 128.26, 120.72, 21.12, 20.81.

1-cyano-4-mesitylbenzene, 12e[28]

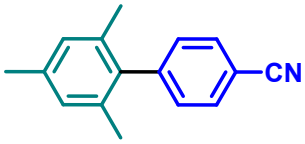

White solid (Yield: 66%). The crude product was purified by column chromatography using silica gel (60-120 mesh) with hexane.

^{1}H NMR (400 MHz, $CDCl_3$) δ (ppm): 7.72 (d, *J* = 8.2 Hz, 2H), 7.27 (d, *J* = 8.3 Hz, 2H), 6.96 (s, 2H), 2.34 (s, 3H), 1.97 (s, 6H).

^{13}C NMR (100 MHz, $CDCl_3$) δ (ppm): 146.53, 137.68, 137.24, 135.42, 132.42, 130.45, 128.45, 119.13, 110.72, 21.13, 20.71.

1-fluoro-4-mesitylbenzene, 12f[29]

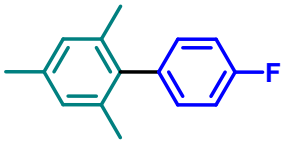

White solid (Yield: 71%). The crude product was purified by column chromatography using silica gel (60-120 mesh) with hexane.

^{1}H NMR (400 MHz, $CDCl_3$) δ (ppm): 7.14 – 7.07 (m, 4H), 6.94 (s, 2H), 2.33 (s, 3H), 1.99 (s, 6H).

^{13}C NMR (100 MHz, $CDCl_3$) δ (ppm): 163.00, 160.67, 138.07, 136.24, 130.96, 130.88, 128.20, 115.50, 115.29, 21.10, 20.82.

1-methyl-4-mesitylbenzene, 12g[8]

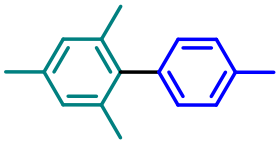

White solid (Yield: 67%). The crude product was purified by column chromatography using silica gel (60-120 mesh) with hexane.

^{1}H NMR (400 MHz, $CDCl_3$) δ (ppm): 7.23 (d, *J* = 7.6 Hz, 2H),7.03 (d, *J* = 8.0 Hz, 2H), 6.94 (s, 2H), 2.41 (s, 3H), 2.33 (s, 3H), 2.01 (s, 6H).

^{13}C NMR (100 MHz, $CDCl_3$) δ (ppm): 139.01, 138.00, 136.40, 136.14, 135.95, 129.42, 129.15, 129.06, 128.01, 127.72, 127.01, 21.23, 21.00, 20.77.

1-iodo-2-mesitylbenzene, 12h[8]

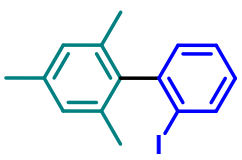

White solid (Yield: 62%). The crude product was purified by column chromatography using silica gel (60-120 mesh) with hexane.

^{1}H NMR (400 MHz, $CDCl_3$) δ (ppm): 7.96 (dd, *J* = 8.0, 0.8 Hz, 1H), 7.42 (dd, *J* = 7.5, 1.0 Hz, 1H), 7.15 (dd, *J* = 7.6, 1.6 Hz, 1H), 7.08 – 7.04 (m, 1H), 6.97 (s, 2H), 2.37 (s, 3H), 1.95 (s, 6H).

^{13}C NMR (100 MHz, $CDCl_3$) δ (ppm): 146.14, 141.27, 139.13, 137.39, 135.58, 129.85, 128.59, 128.51, 128.17, 100.94, 21.28, 20.35.

4'-Chloro-2-nitro-1,1'-biphenyl, 13a[15]

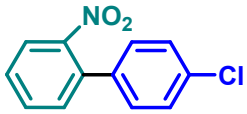

White solid (Yield: 82%). The crude product was purified by column chromatography using silica gel (60-120 mesh) with 1% of EtOAc in hexane.

^{1}H NMR (400 MHz, $CDCl_3$) δ (ppm): 7.93 – 7.86 (m, 1H), 7.76 – 7.69 (m, 1H), 7.47 – 7.38 (m, 3H), 7.32 – 7.22 (m, 2H).

^{13}C NMR (100 MHz, $CDCl_3$) δ (ppm): 149.18, 135.32, 132.57, 131.94, 129.48, 129.37, 129.01, 128.73, 128.66, 127.78, 124.36, 124.31.

4'-methoxy-n-nitro-1,1'-biphenyl, 13b[15]

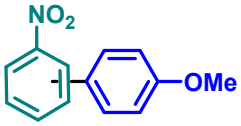

After completion of the reaction, product was extracted in 25 mL ethyl acetate and dried over anhydrous sodium sulphate. The solvent was removed under reduced pressure. All isomeric products (ortho, meta and para) were collected together from other reaction impurities by column chromatography over silica gel (100-200 mesh) using 3% EtOAc in hexane mixture. Total yield was calculated by taking weight of obtained mixture of products. This mixture of products was subjected to ^{1}H NMR spectroscopic characterization. The percentage of different regio-isomers was calculated by relative integration of the protons arising from the respective isomers.

10. ^{1}H NMR and ^{13}C NMR spectra of the products:

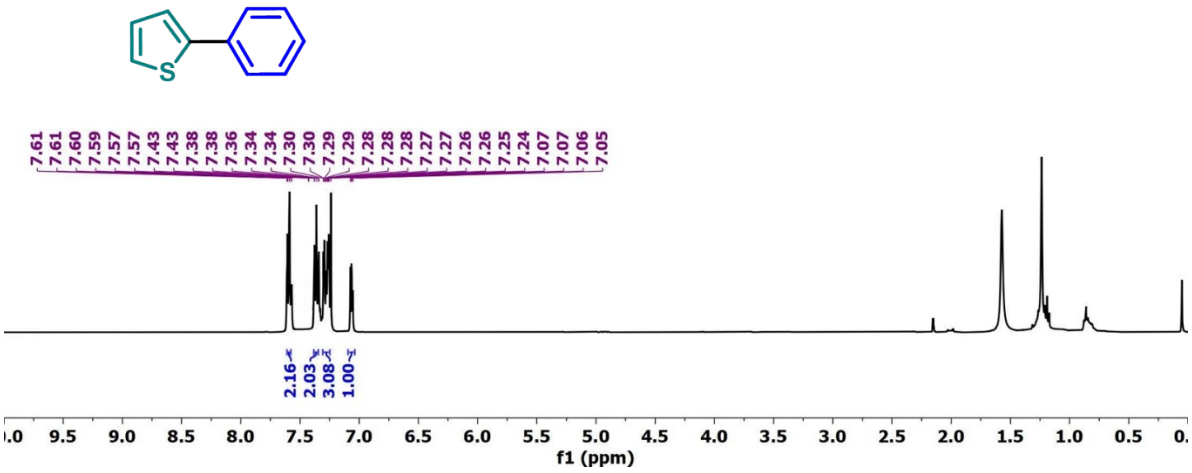

Figure S18: ^{1}H NMR spectrum of **5a**.

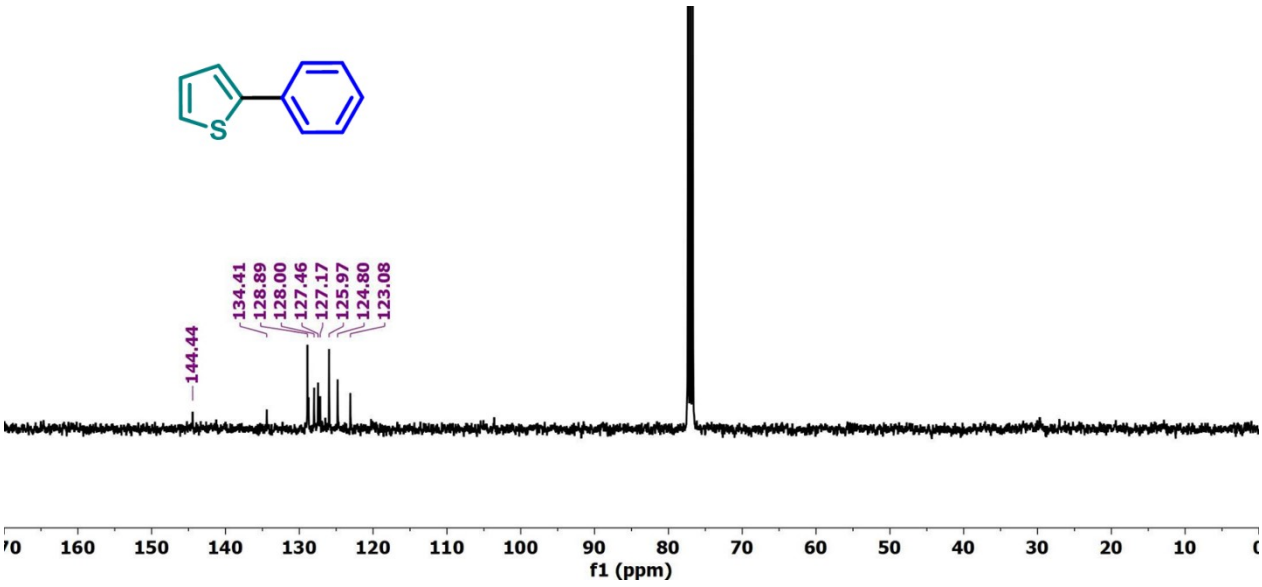

Figure S19: ^{13}C {^{1}H} NMR spectrum of **5a**.

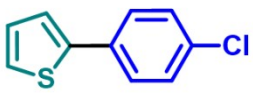

Figure S20: ^{1}H NMR spectrum of **5b**.

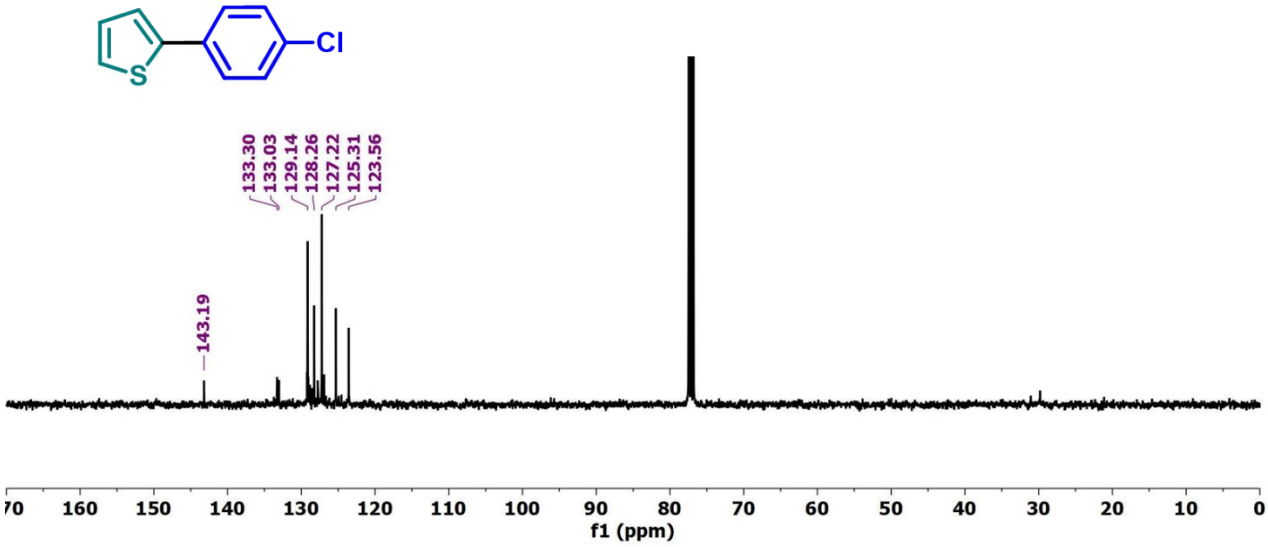

Figure S21: ^{13}C {^{1}H} NMR spectrum of **5b**.

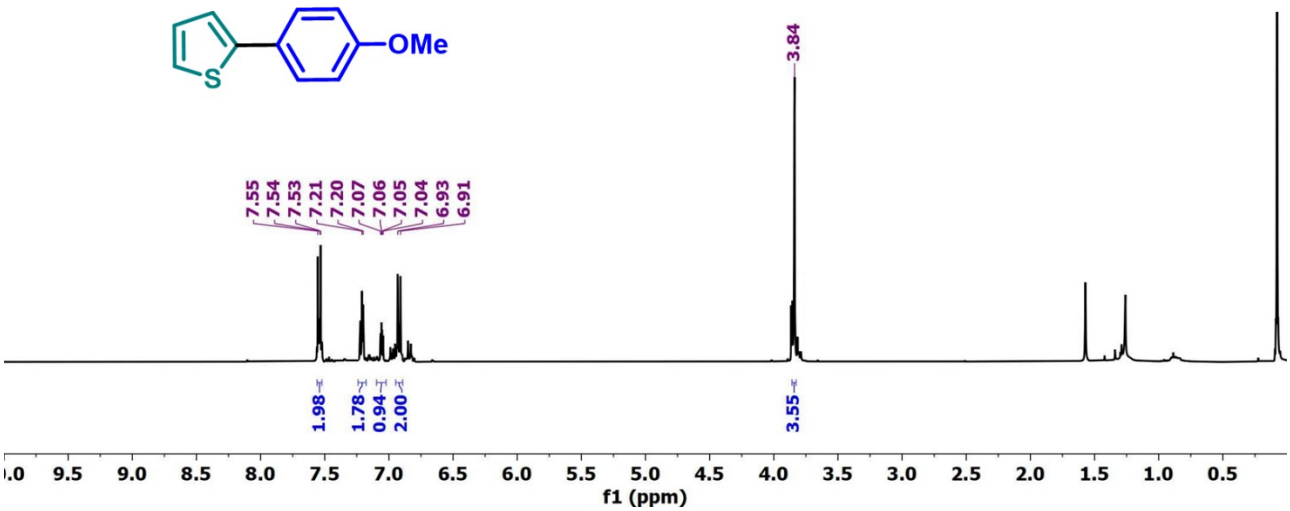

Figure S22: ^{1}H NMR spectrum of **5c**.

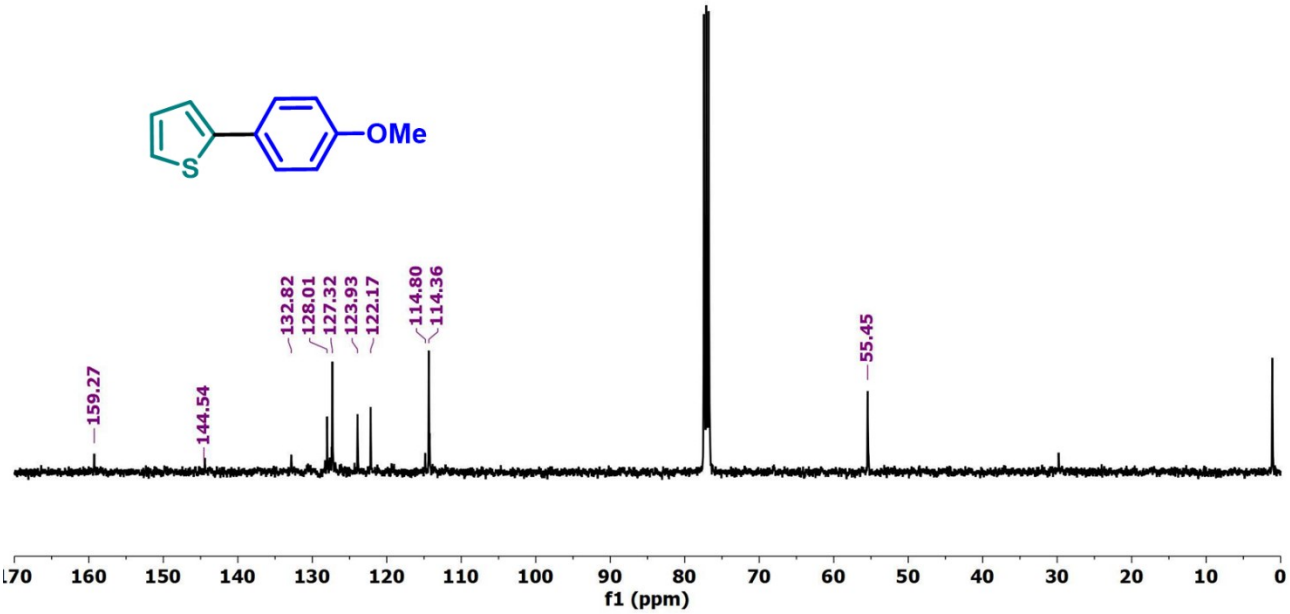

Figure S23: ^{13}C {^{1}H} NMR spectrum of **5c**.

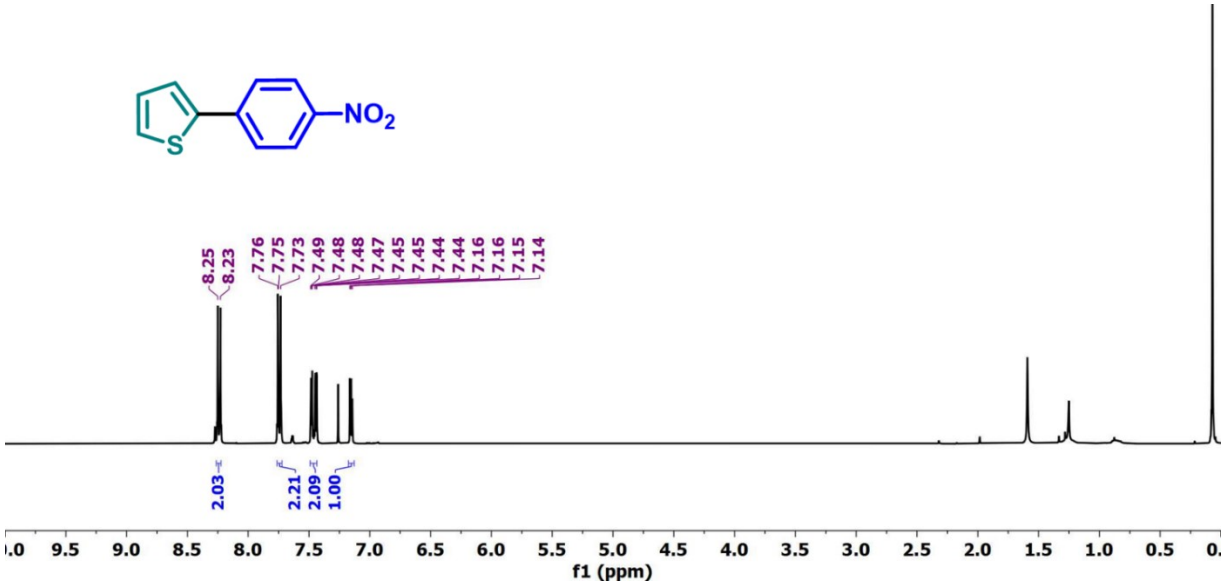

Figure S24: ^{1}H NMR spectrum of **5d**.

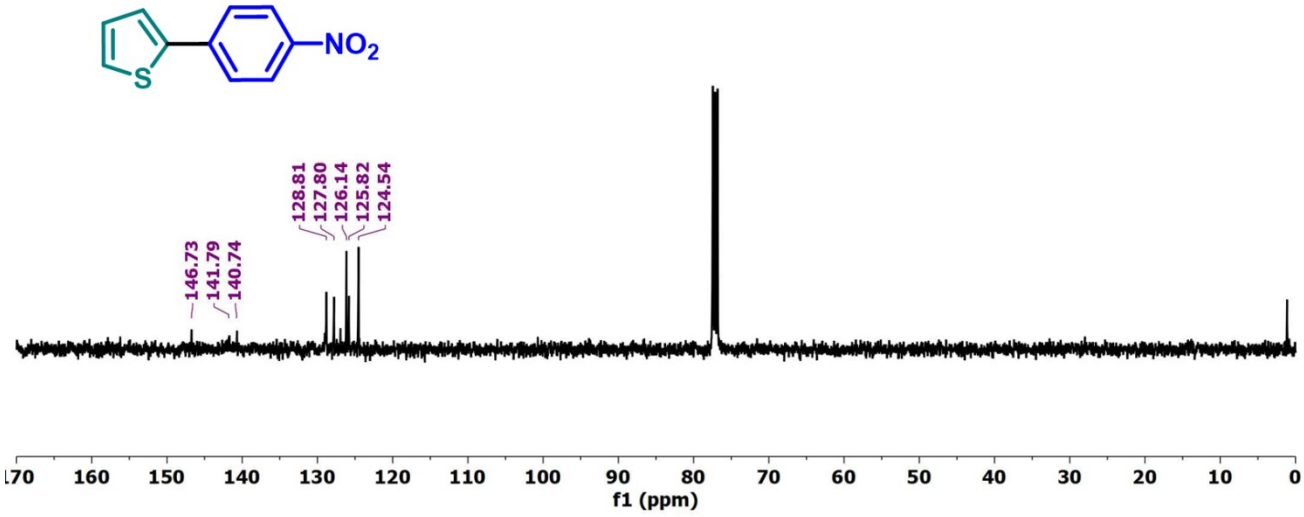

Figure S25: ^{13}C {^{1}H} NMR spectrum of **5d**.

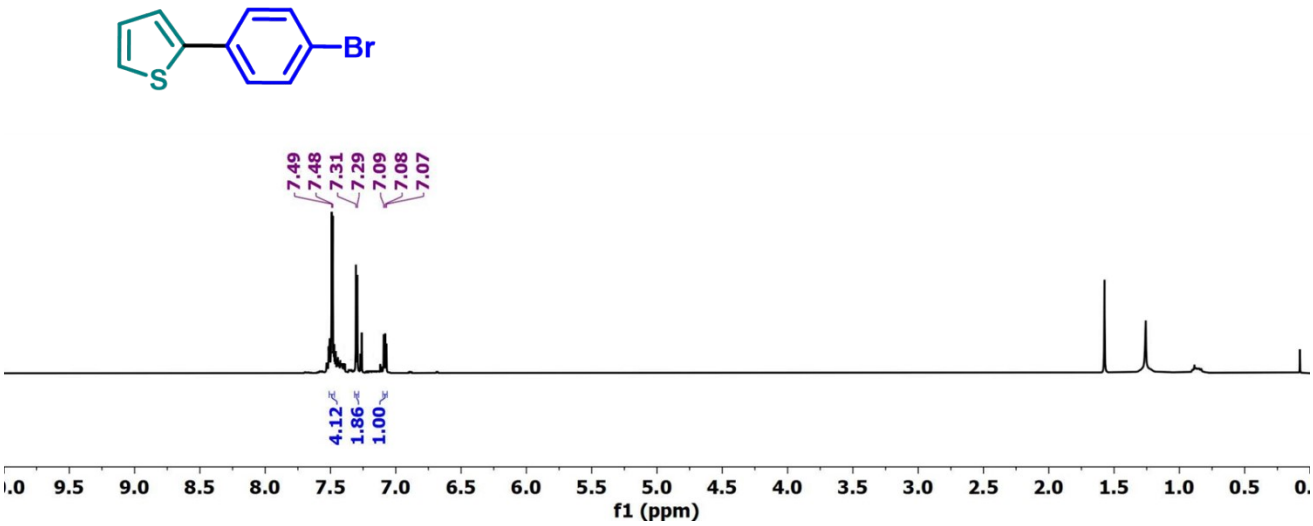

Figure S26: ^{1}H NMR spectrum of **5e**.

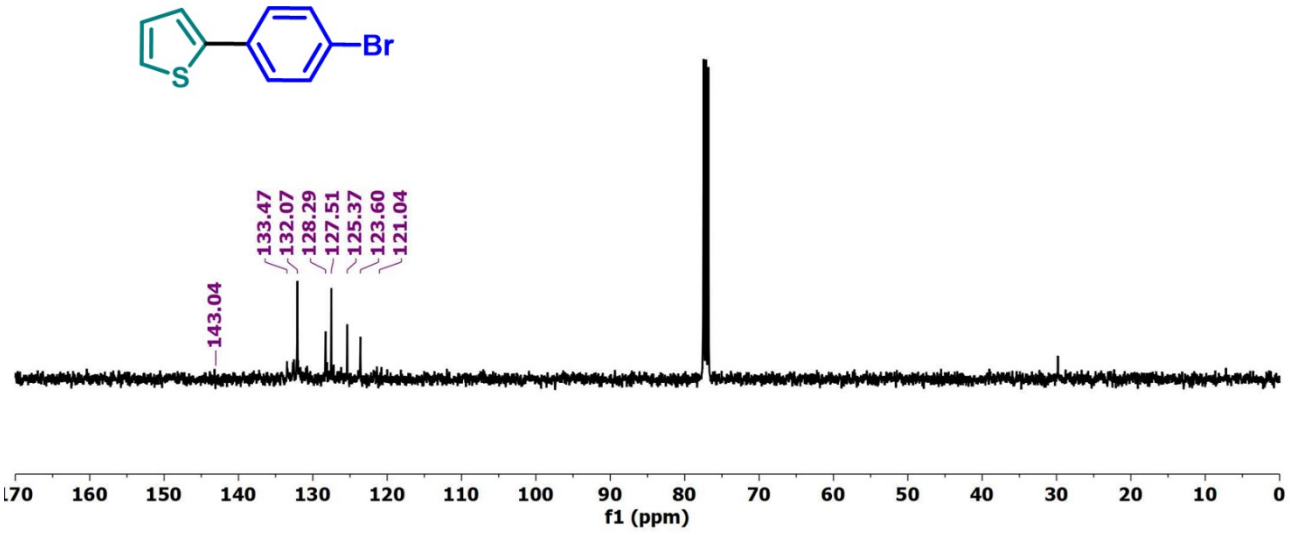

Figure S27: ^{13}C {^{1}H} NMR spectrum of **5e**.

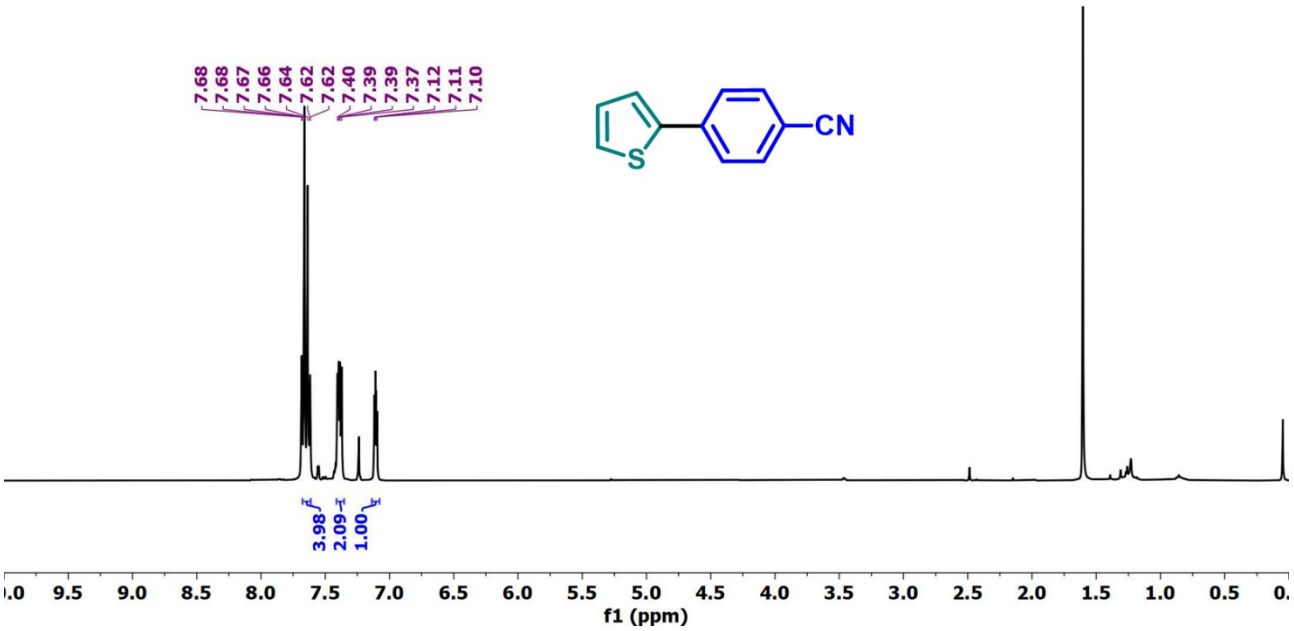

Figure S28: ^{1}H NMR spectrum of **5f**.

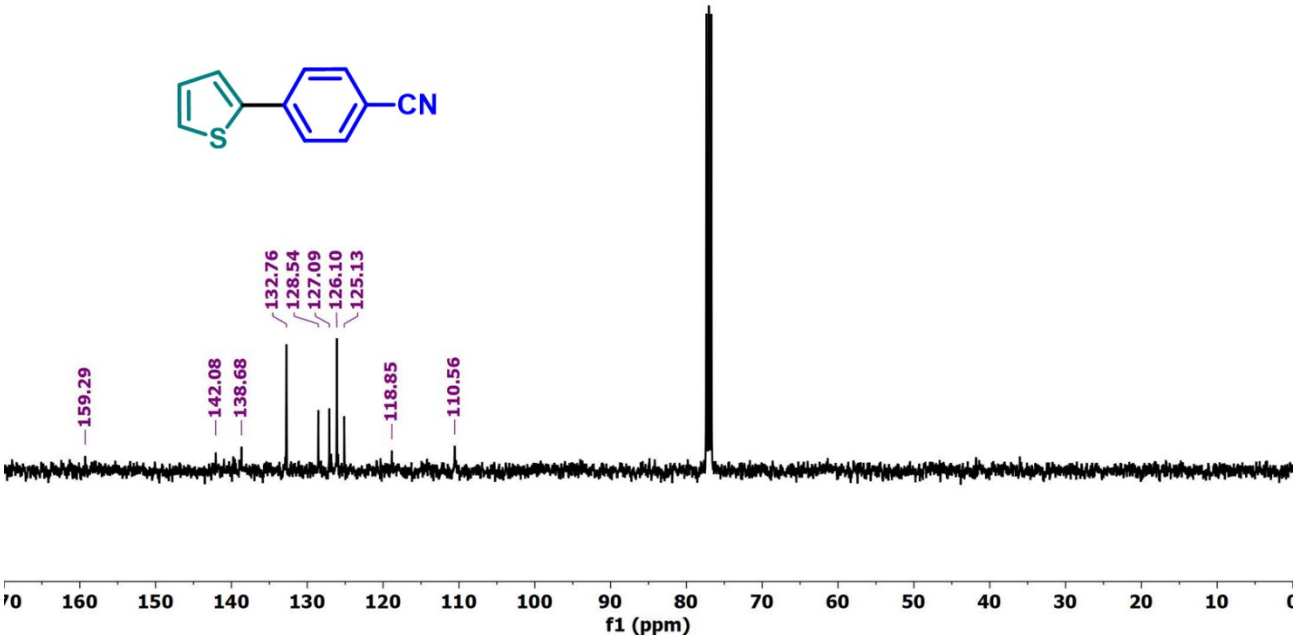

Figure S29: ^{13}C {^{1}H} NMR spectrum of **5f**.

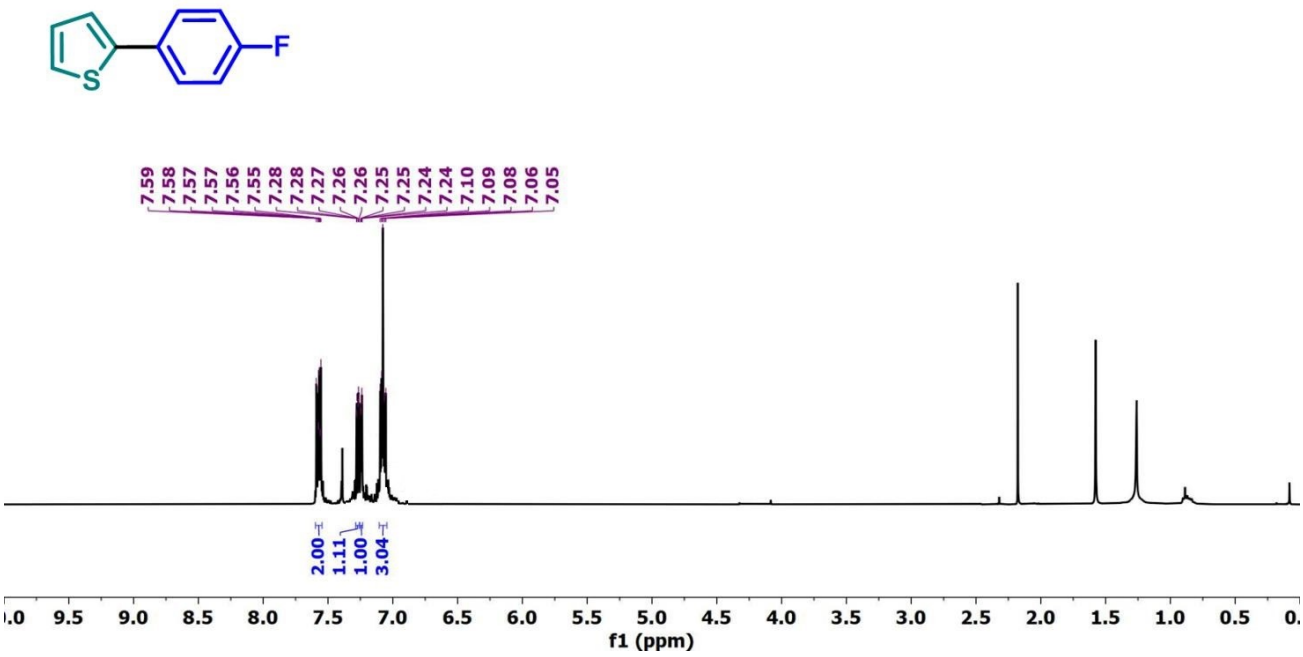

Figure S30: ^{1}H NMR spectrum of **5g**.

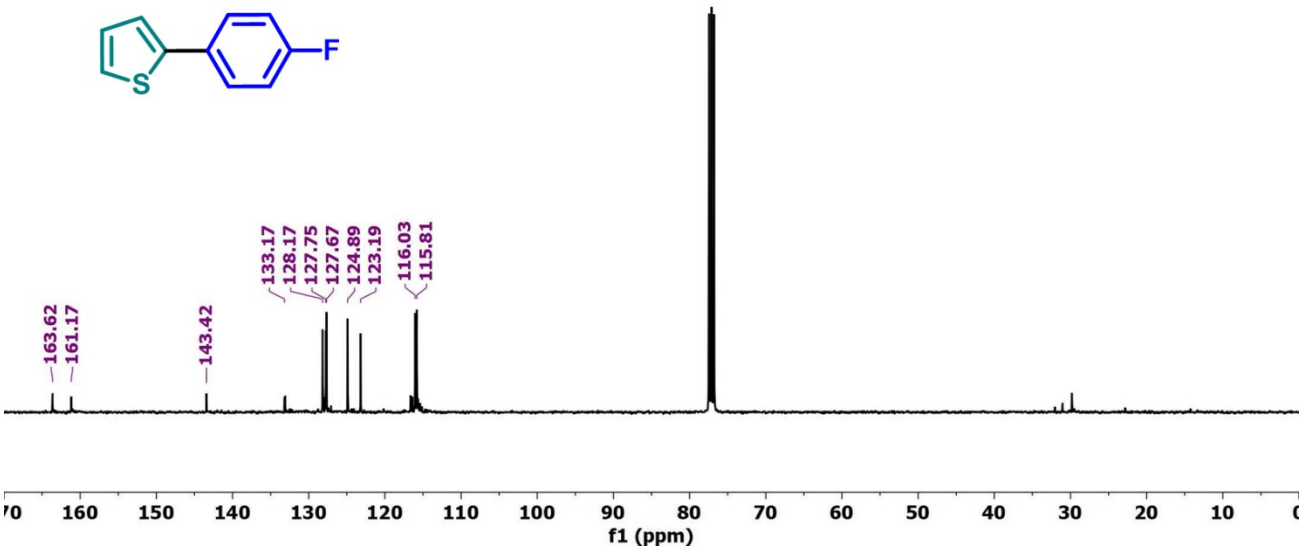

Figure S31: ^{13}C {^{1}H} NMR spectrum of **5g**.

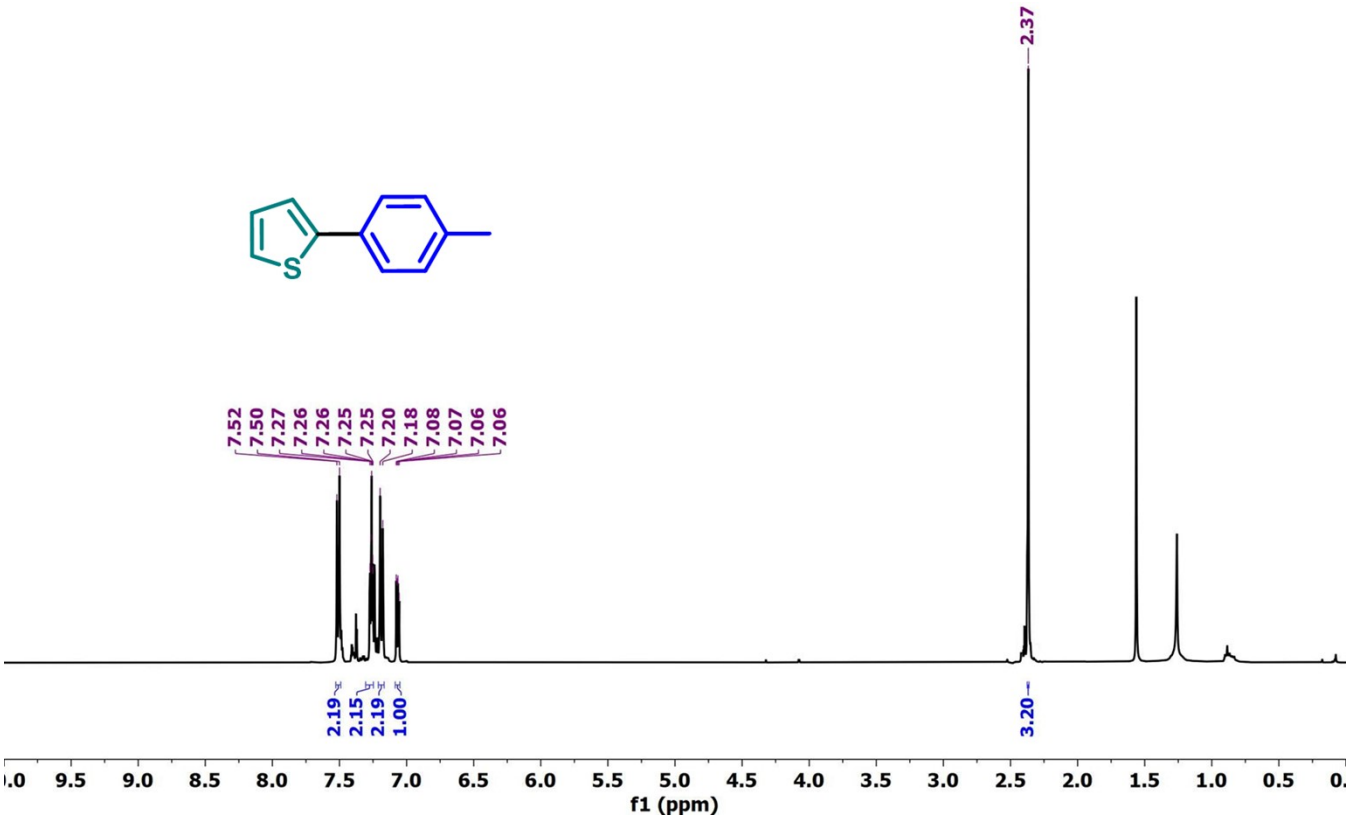

Figure S32: ^{1}H NMR spectrum of **5h**.

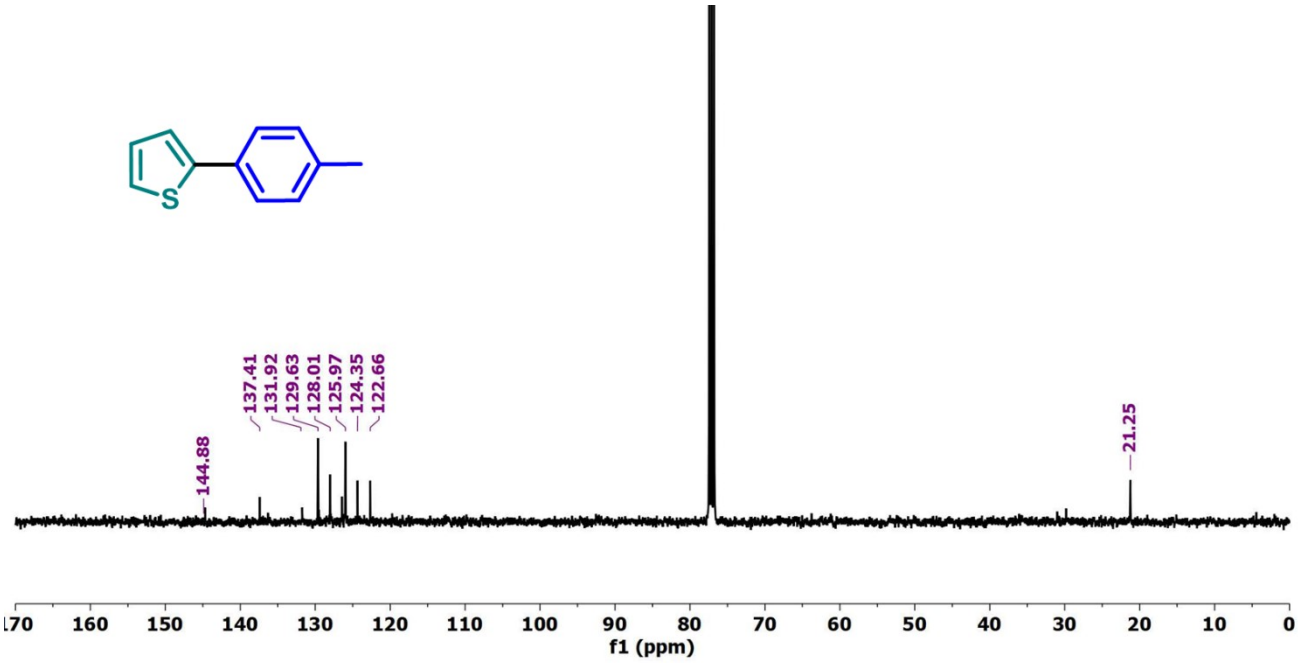

Figure S33: ^{13}C {^{1}H} NMR spectrum of **5h**.

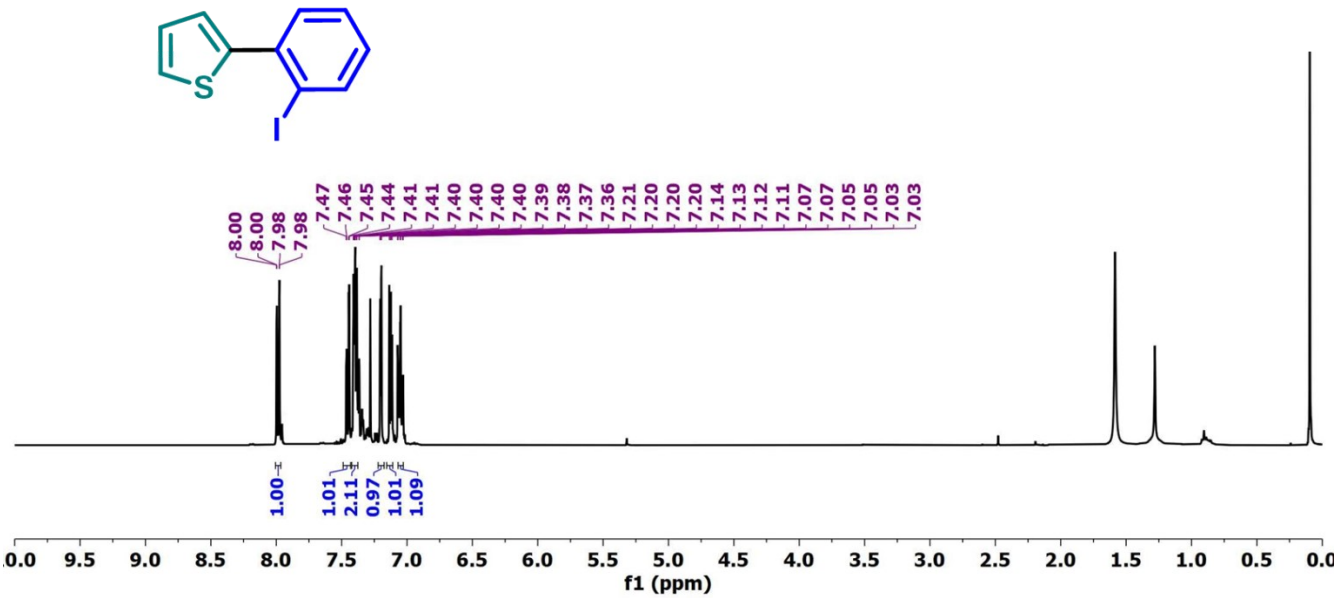

Figure S34: ^{1}H NMR spectrum of **5i**.

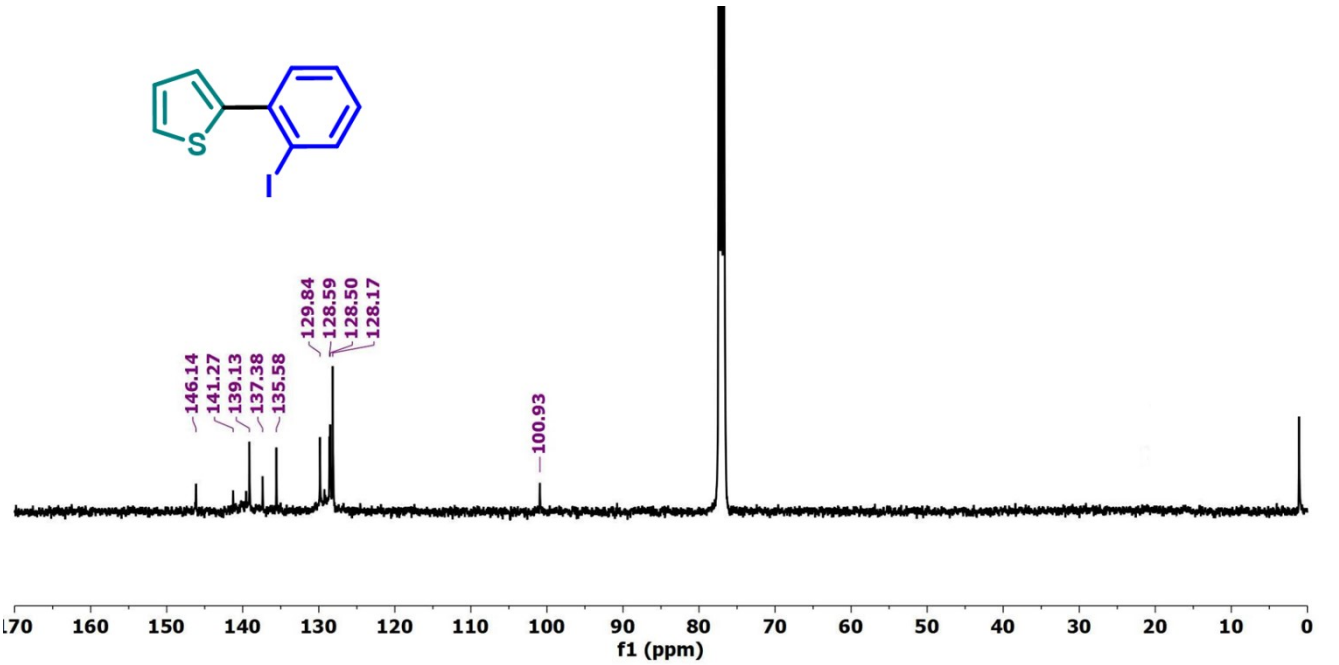

Figure S35: ^{13}C {^{1}H} NMR spectrum of **5i**.

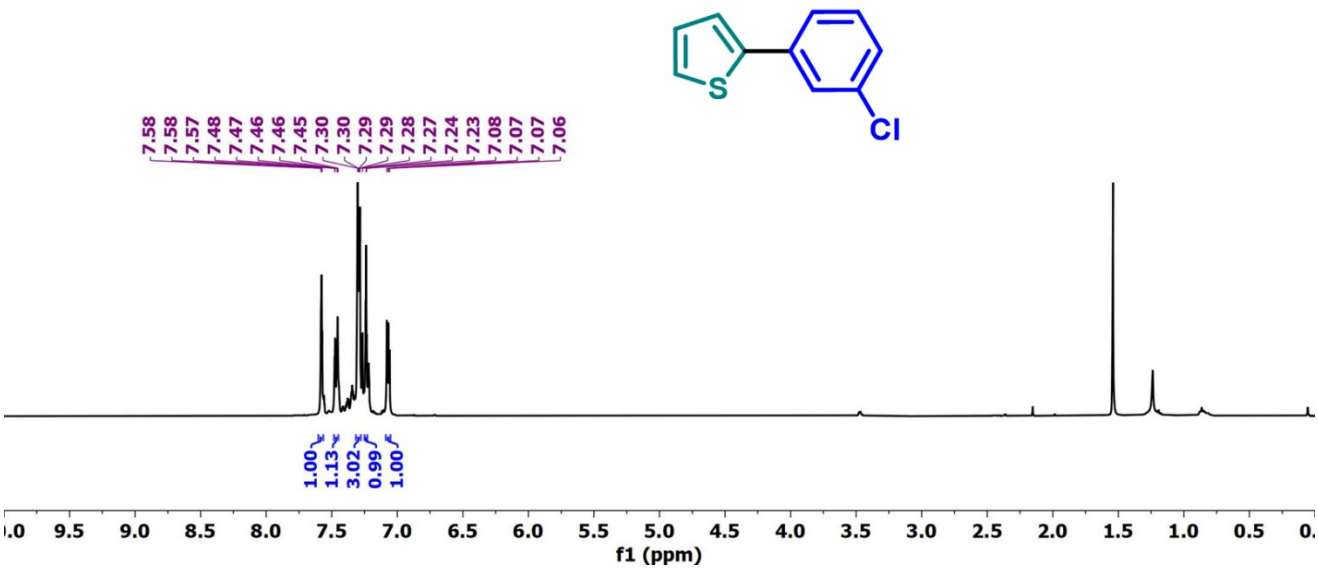

Figure S36: ^{1}H NMR spectrum of **5j**.

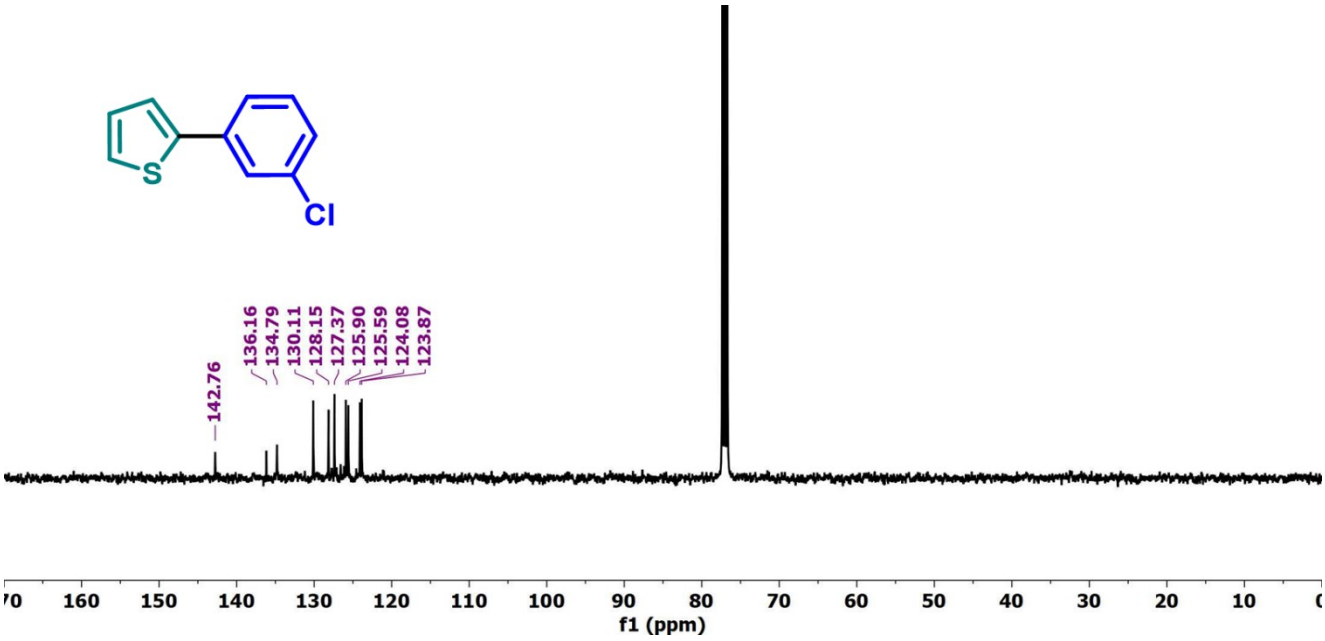

Figure S37: ^{13}C {^{1}H} NMR spectrum of **5j**.

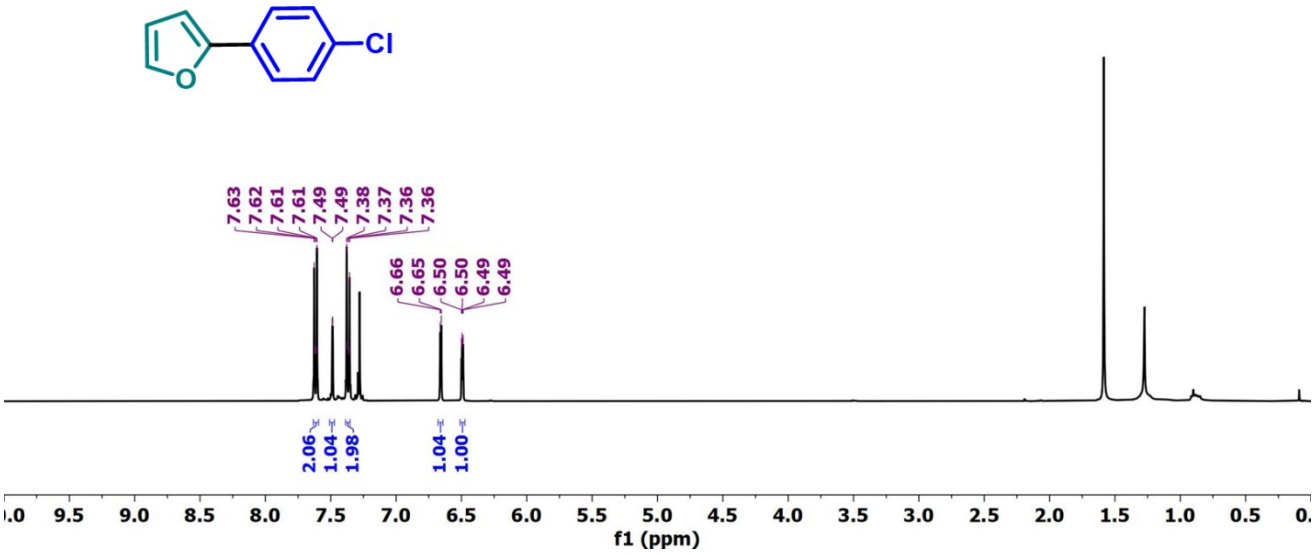

Figure S38: ^{1}H NMR spectrum of **6a**.

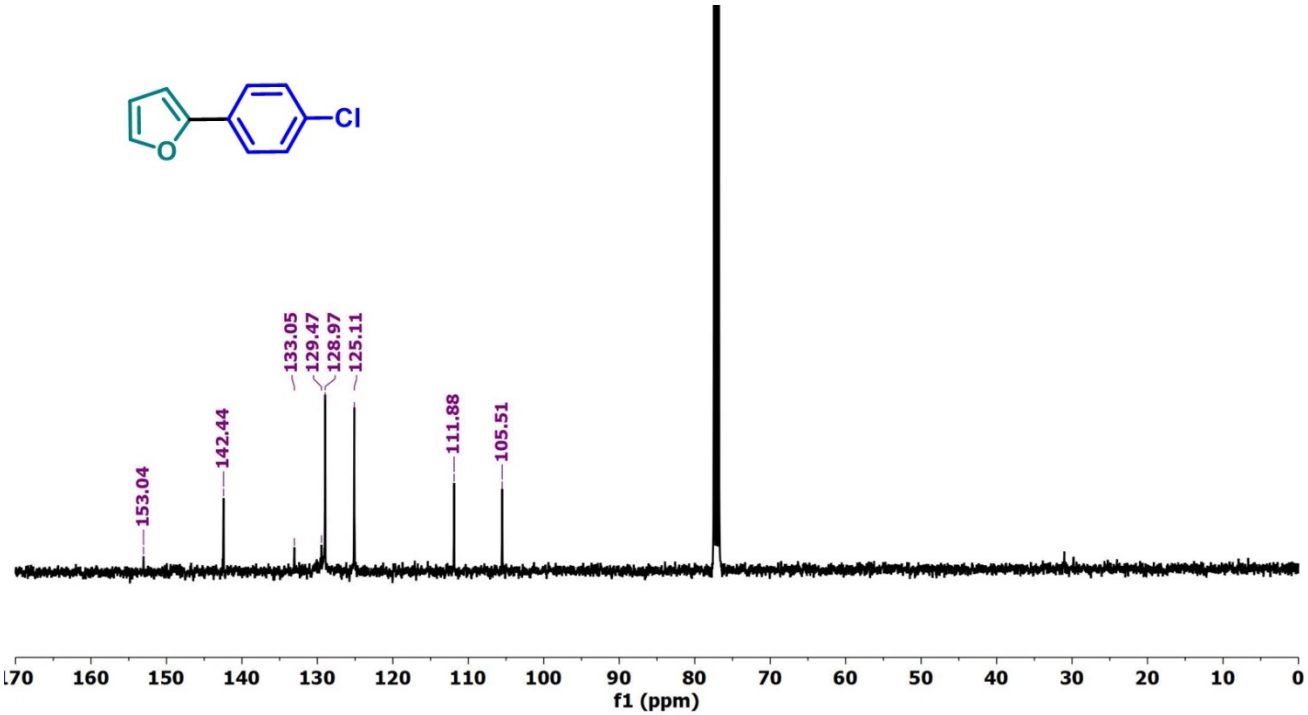

Figure S39: ^{13}C {^{1}H} NMR spectrum of **6a**.

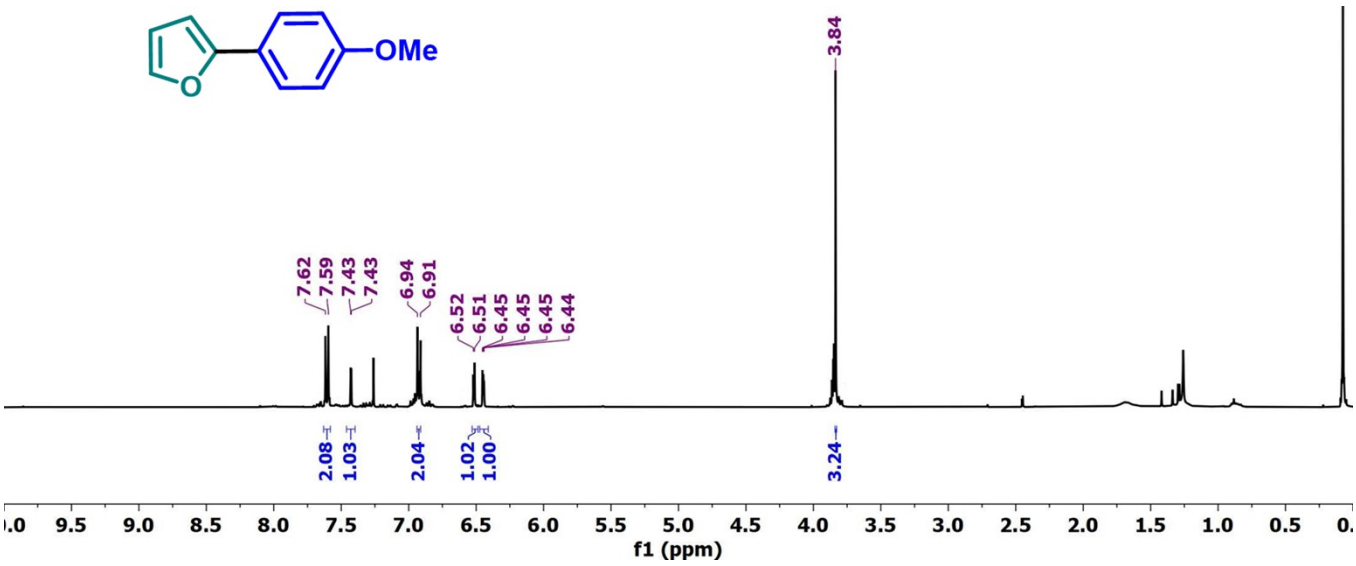

Figure S40: ^{1}H NMR spectrum of **6b**.

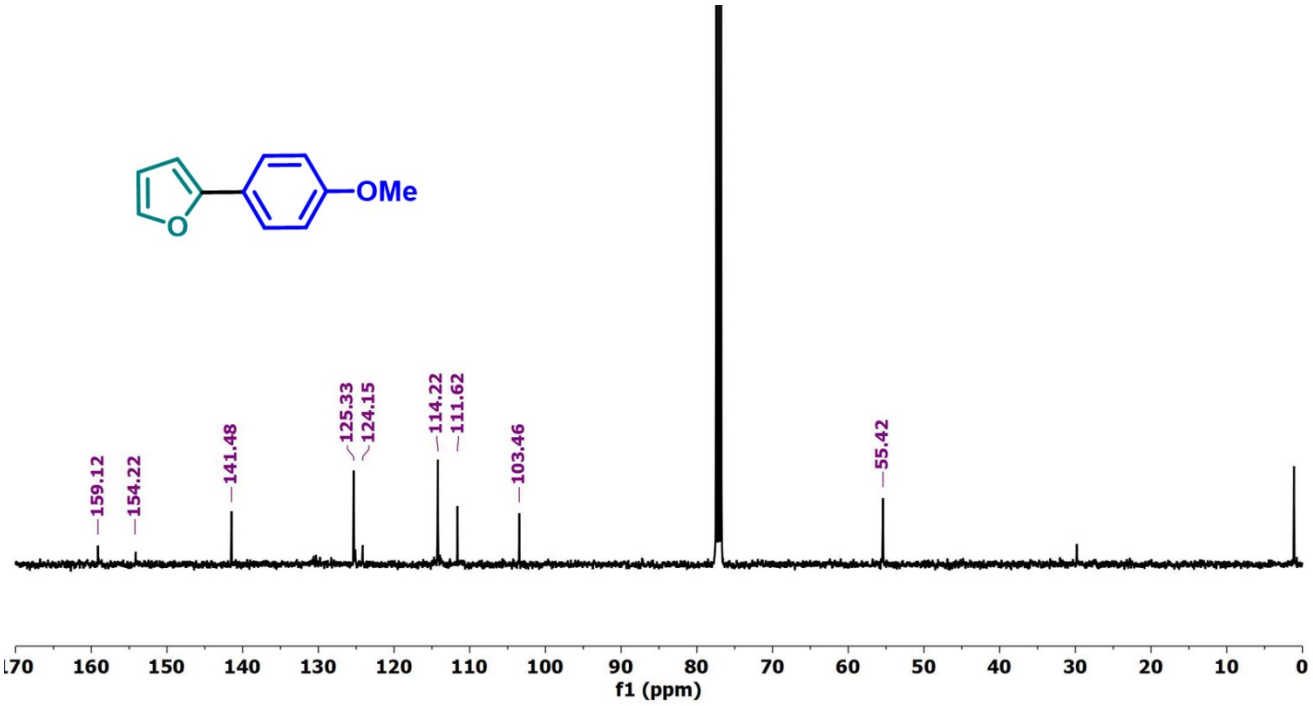

Figure S41: ^{13}C {^{1}H} NMR spectrum of **6b**.

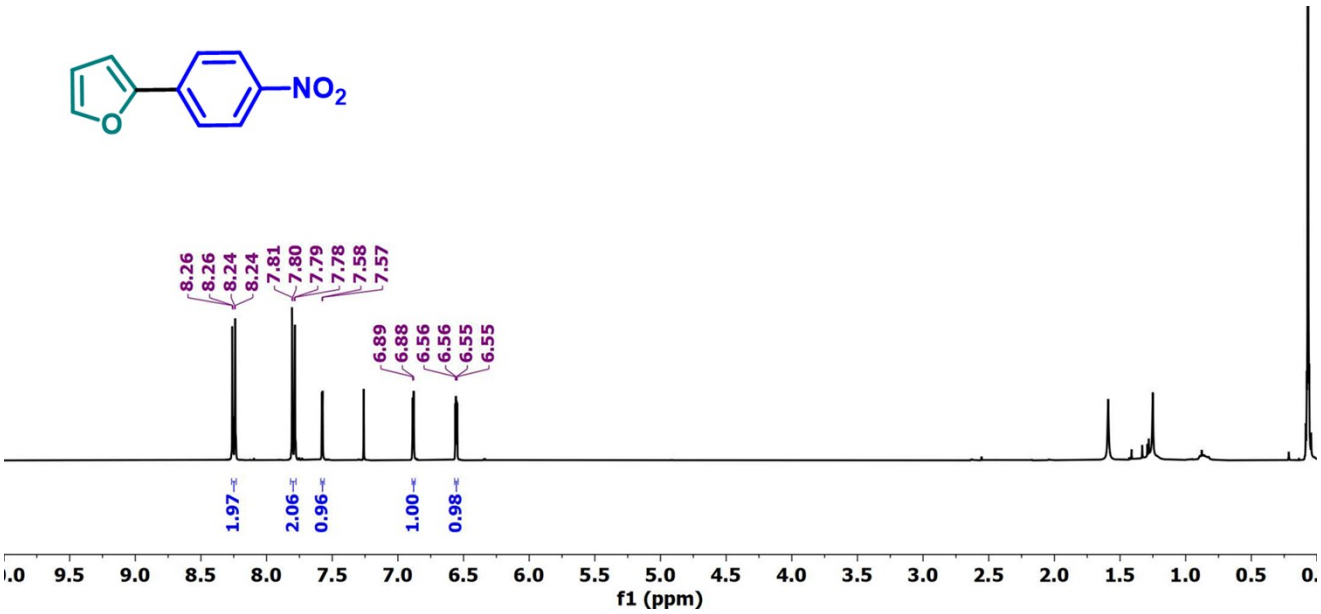

Figure S42: ^{1}H NMR spectrum of **6c**.

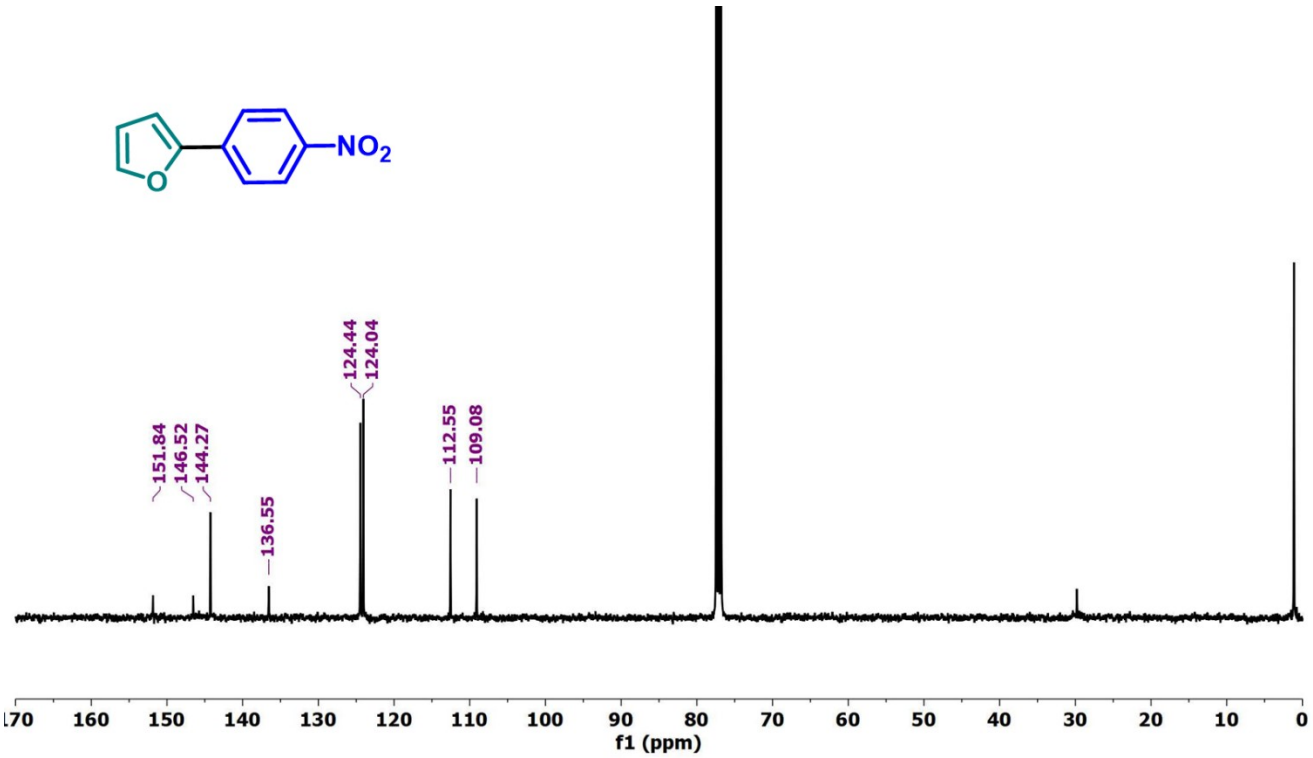

Figure S43: ^{13}C {^{1}H} NMR spectrum of **6c**.

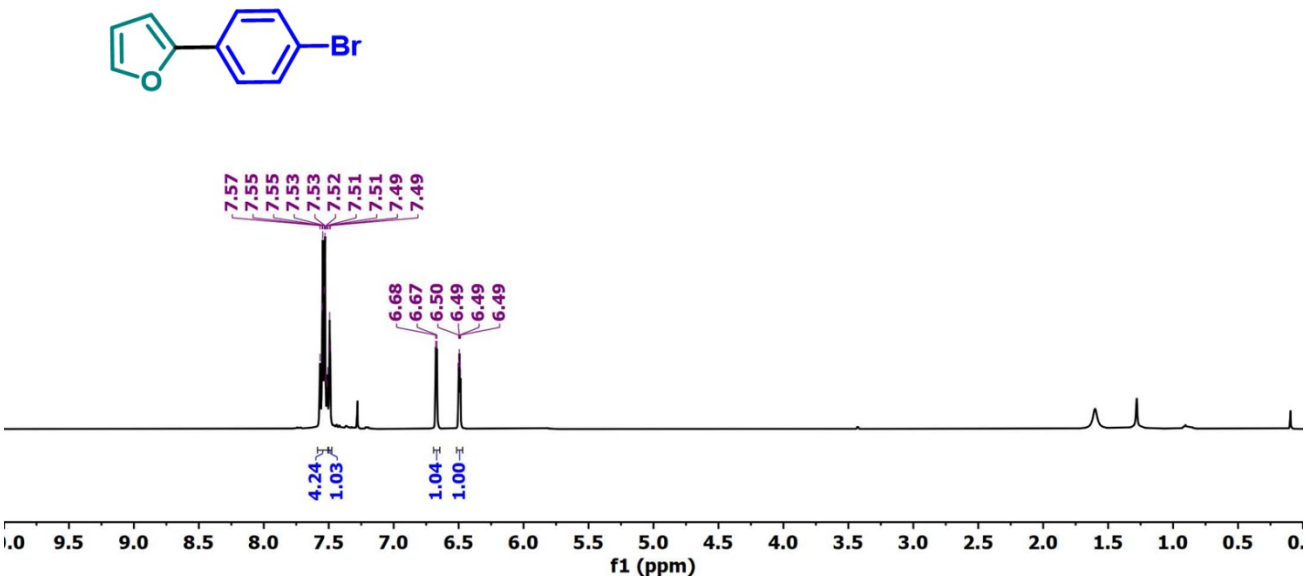

Figure S44: ^{1}H NMR spectrum of **6d**.

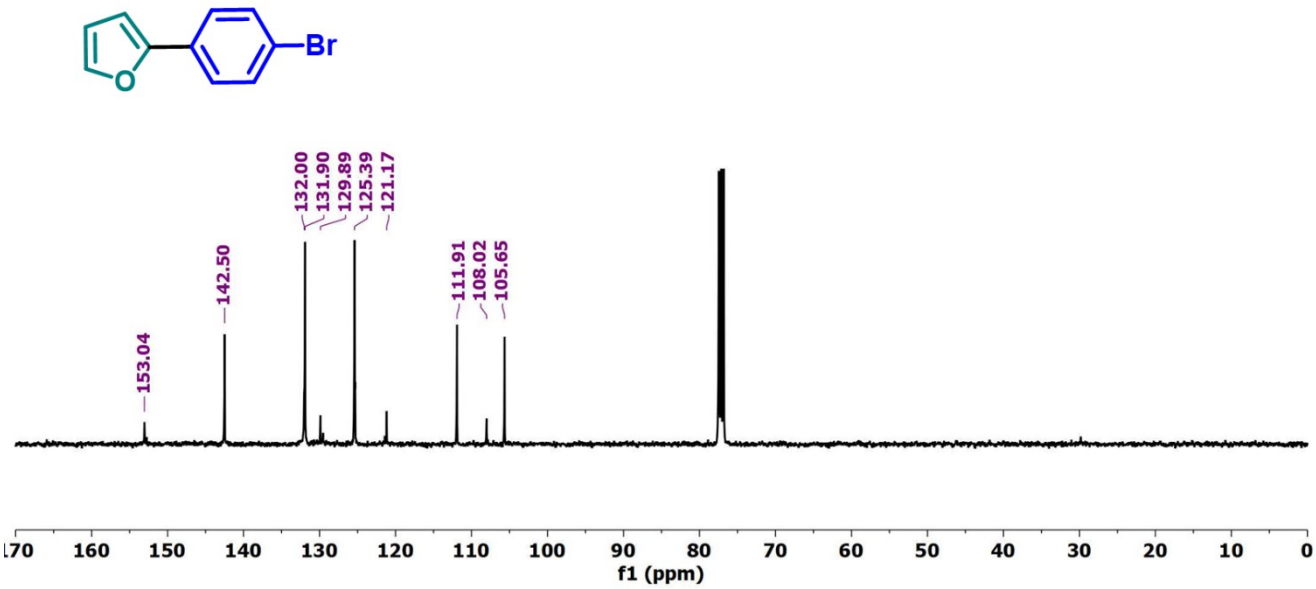

Figure S45: ^{13}C {^{1}H} NMR spectrum of **6d**.

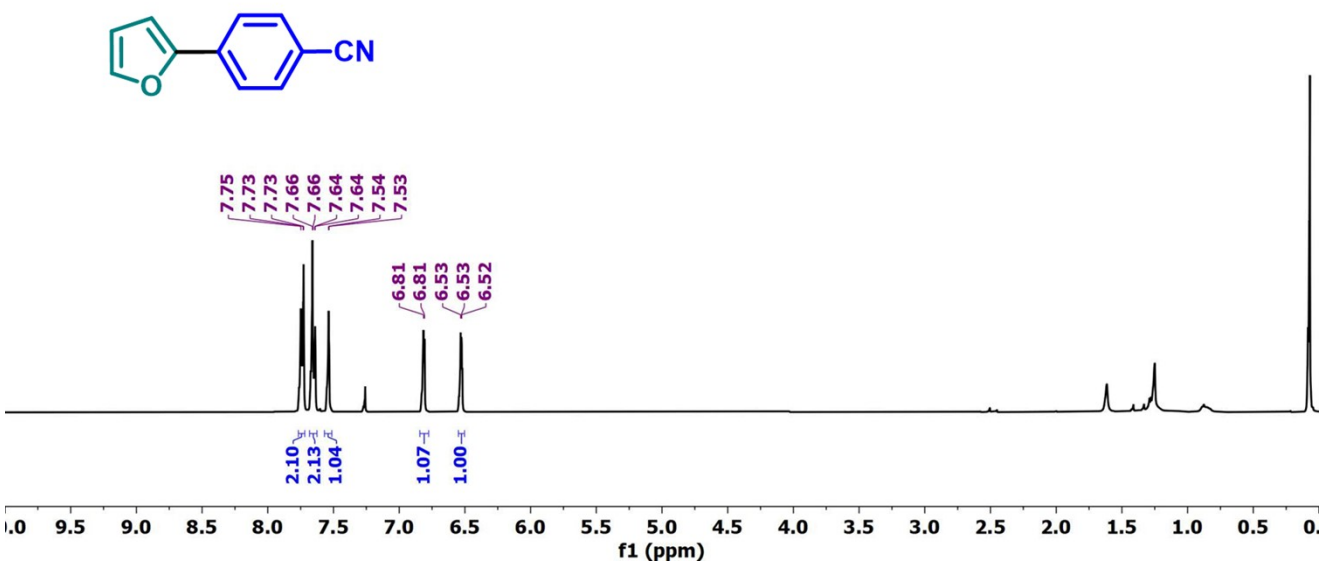

Figure S46: ^{1}H NMR spectrum of **6e**.

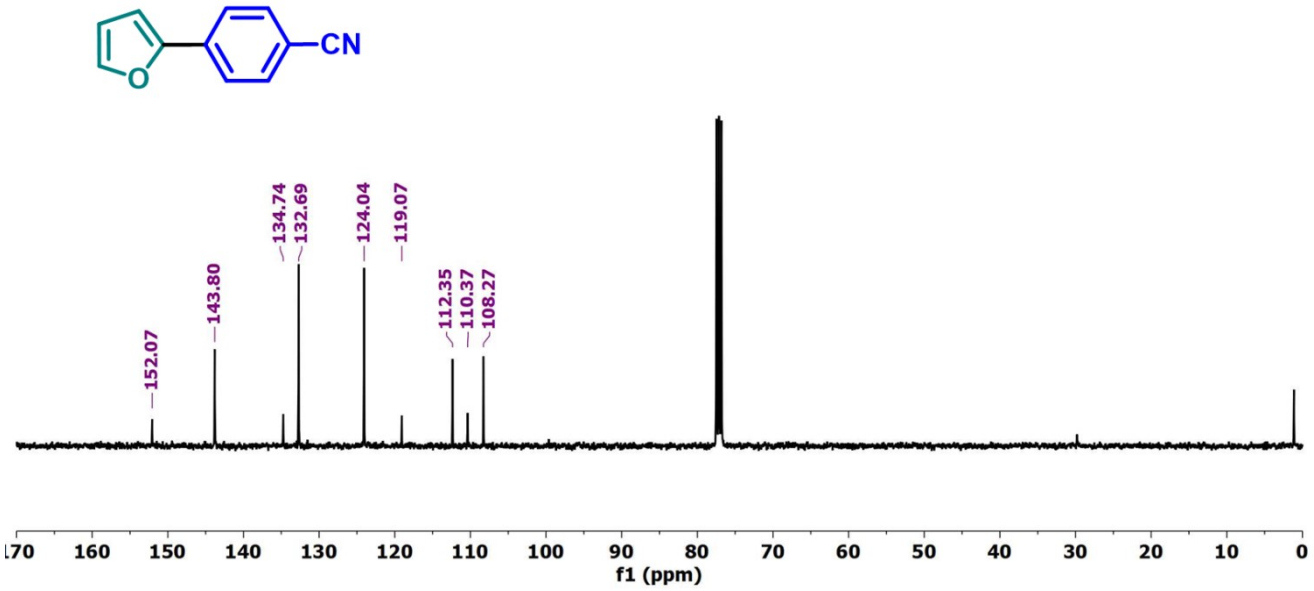

Figure S47: ^{13}C {^{1}H} NMR spectrum of **6e**.

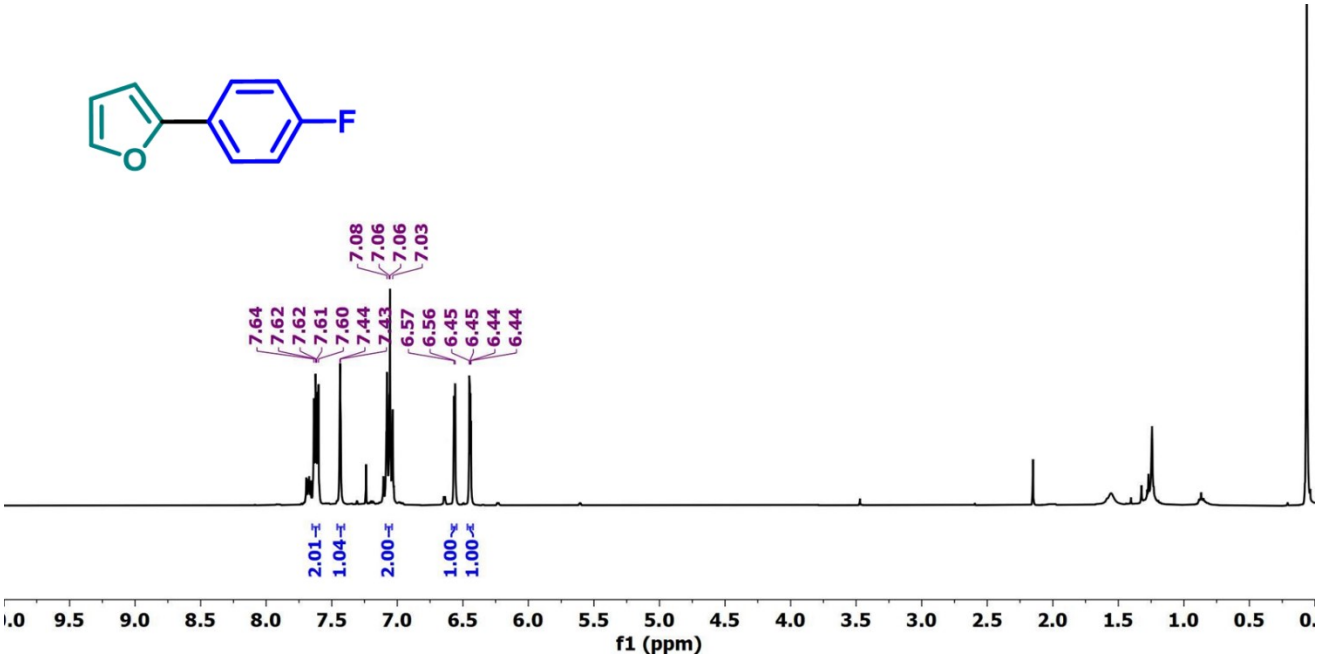

Figure S48: ^{1}H NMR spectrum of **6f**.

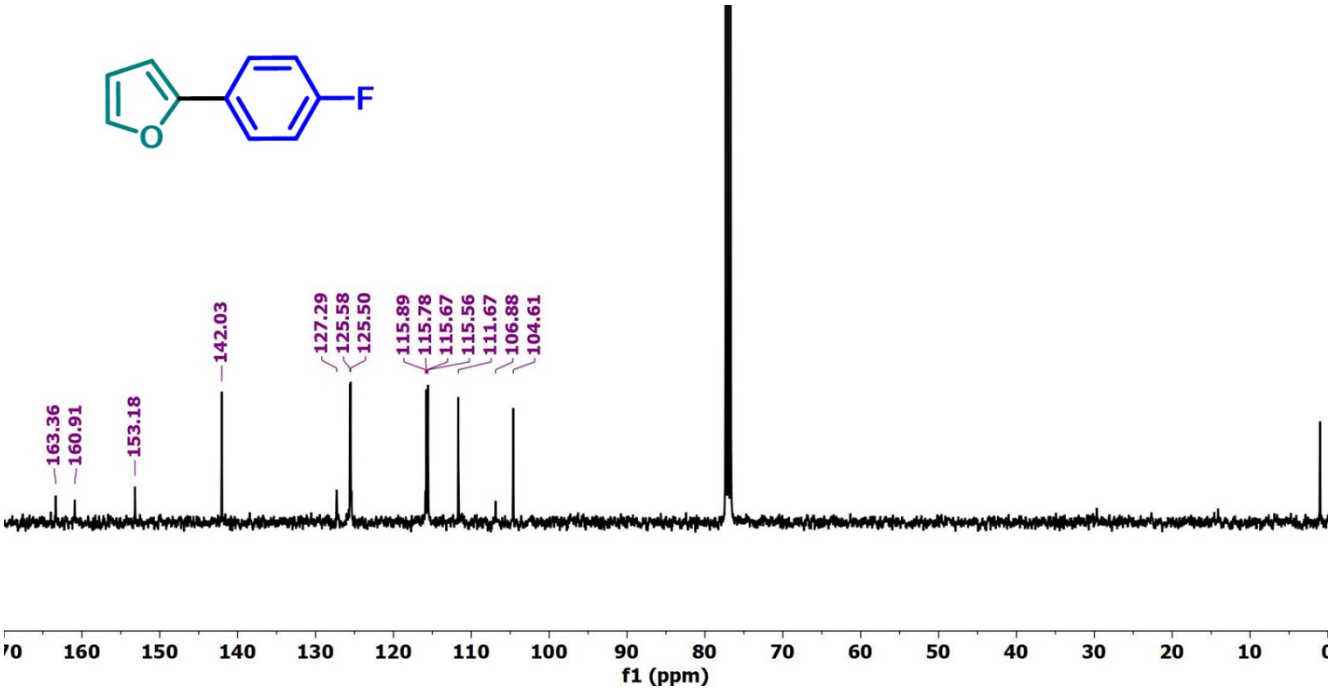

Figure S49: ^{13}C {^{1}H} NMR spectrum of **6f**.

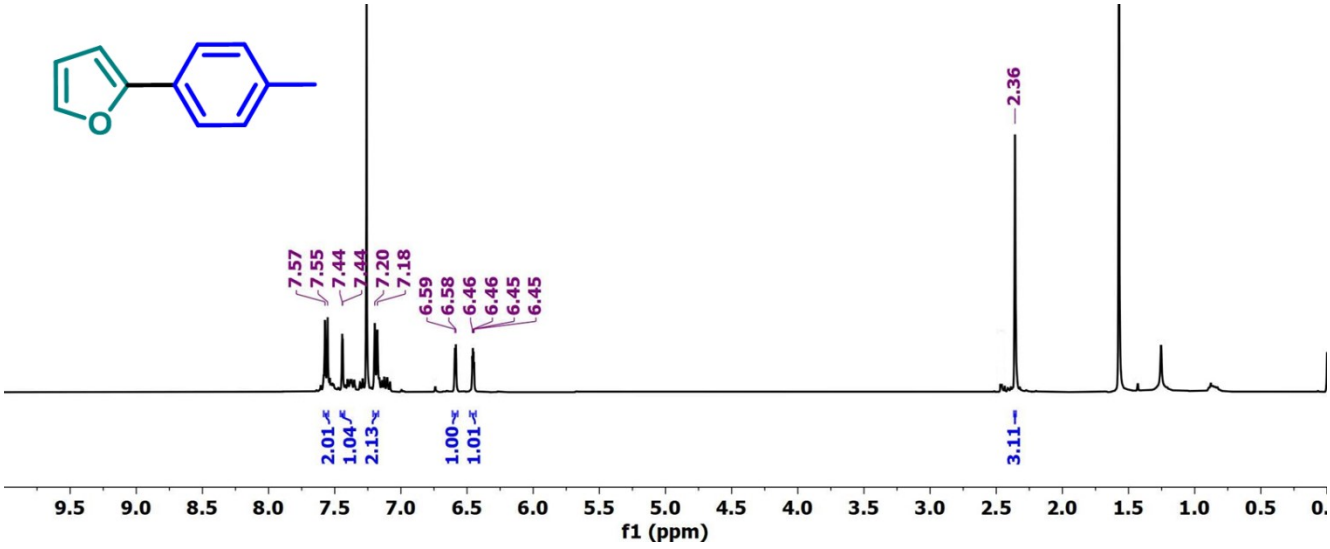

Figure S50: ^{1}H NMR spectrum of **6g**.

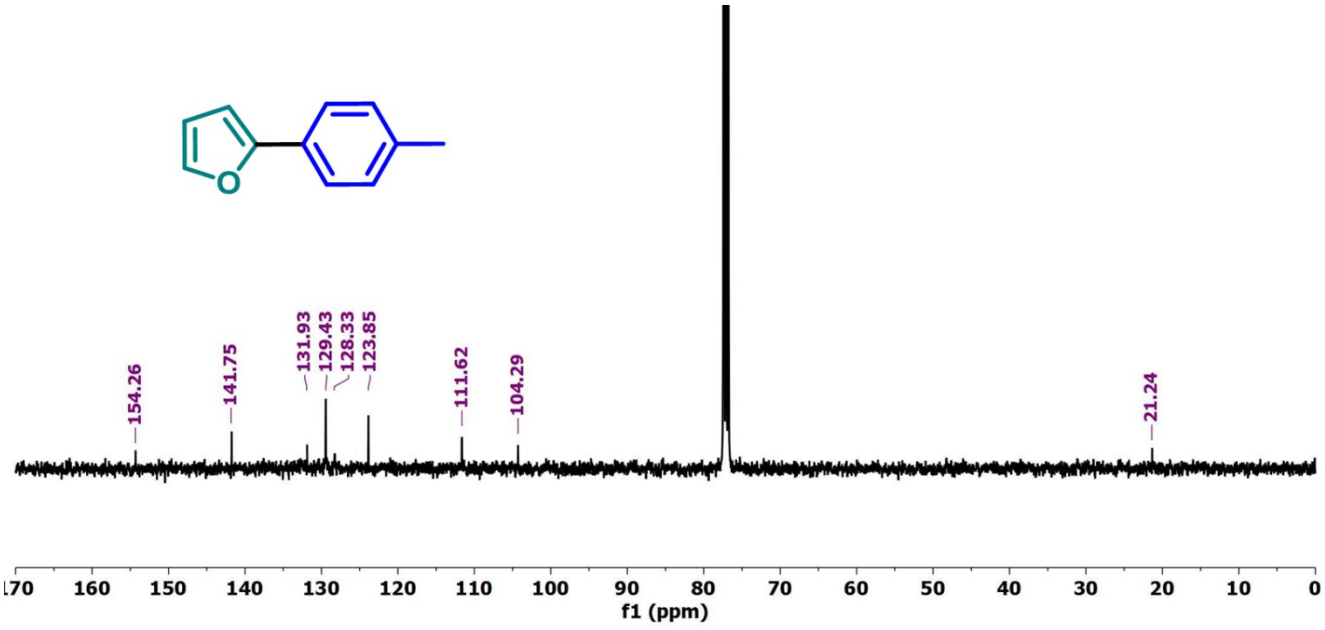

Figure S51: ^{13}C {^{1}H} NMR spectrum of **6g**.

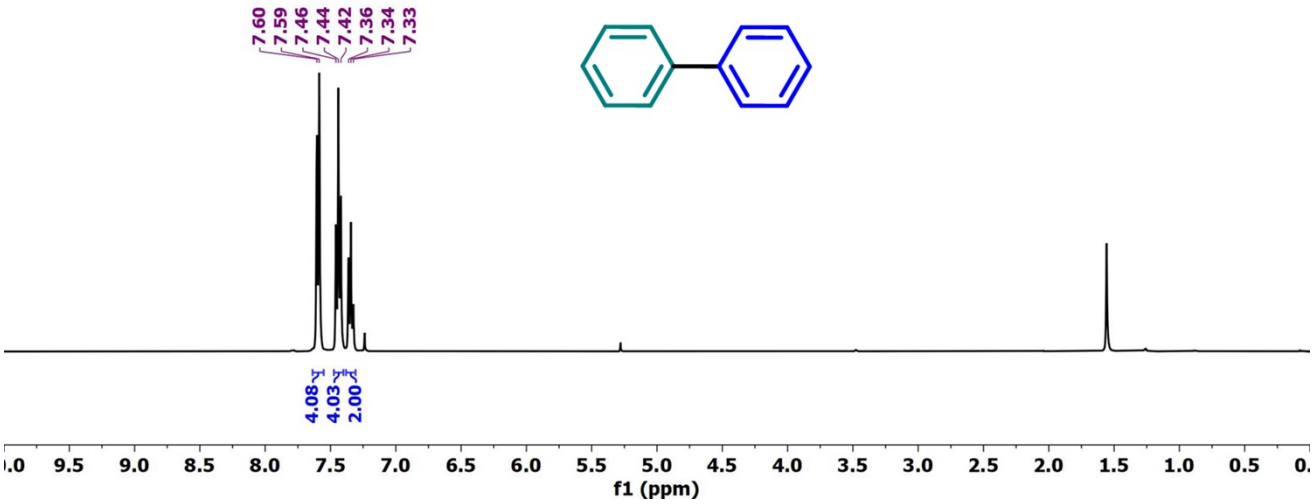

Figure S52: ^{1}H NMR spectrum of **7a**.

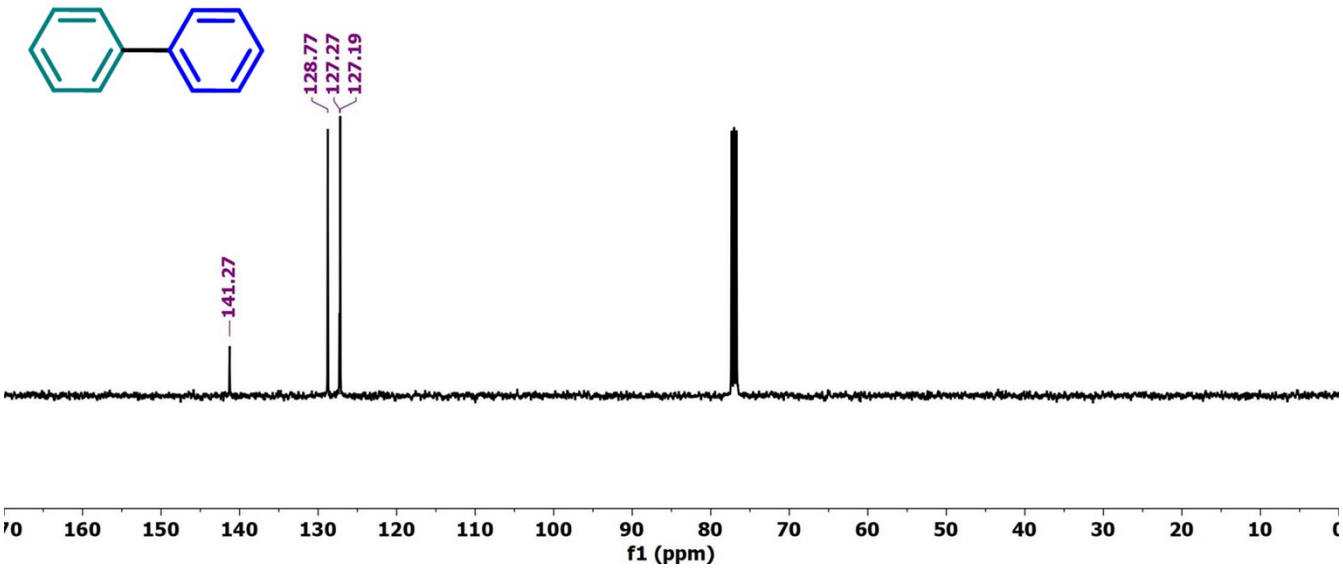

Figure S53: ^{13}C {^{1}H} NMR spectrum of **7a**.

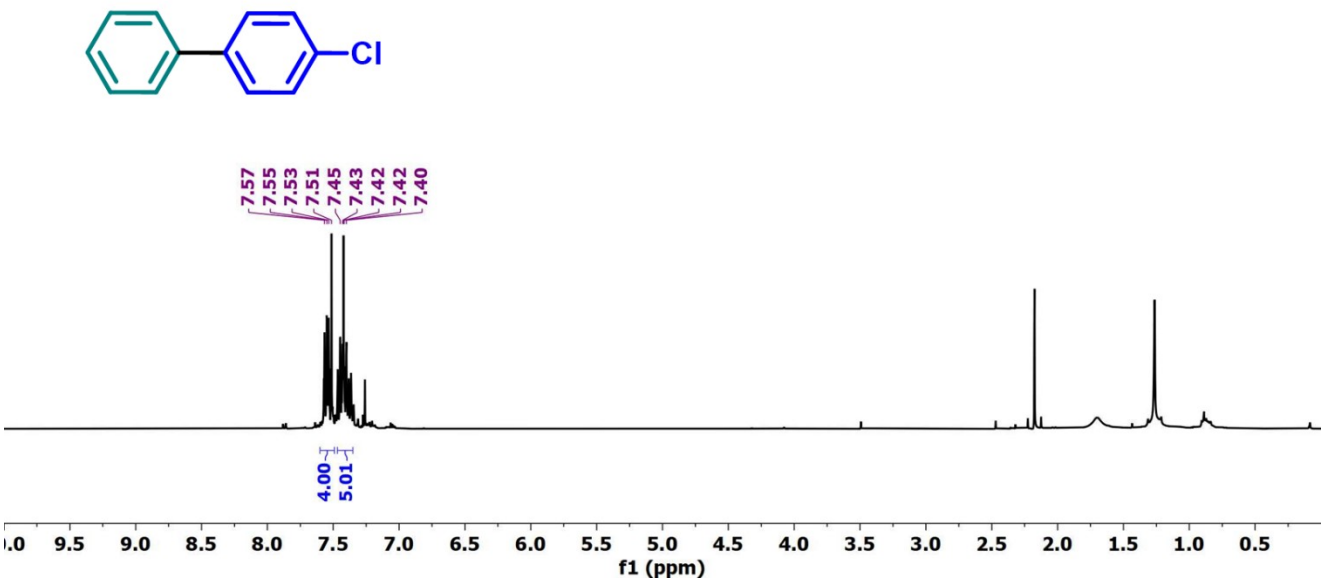

Figure S54: ^{1}H NMR spectrum of **7b**.

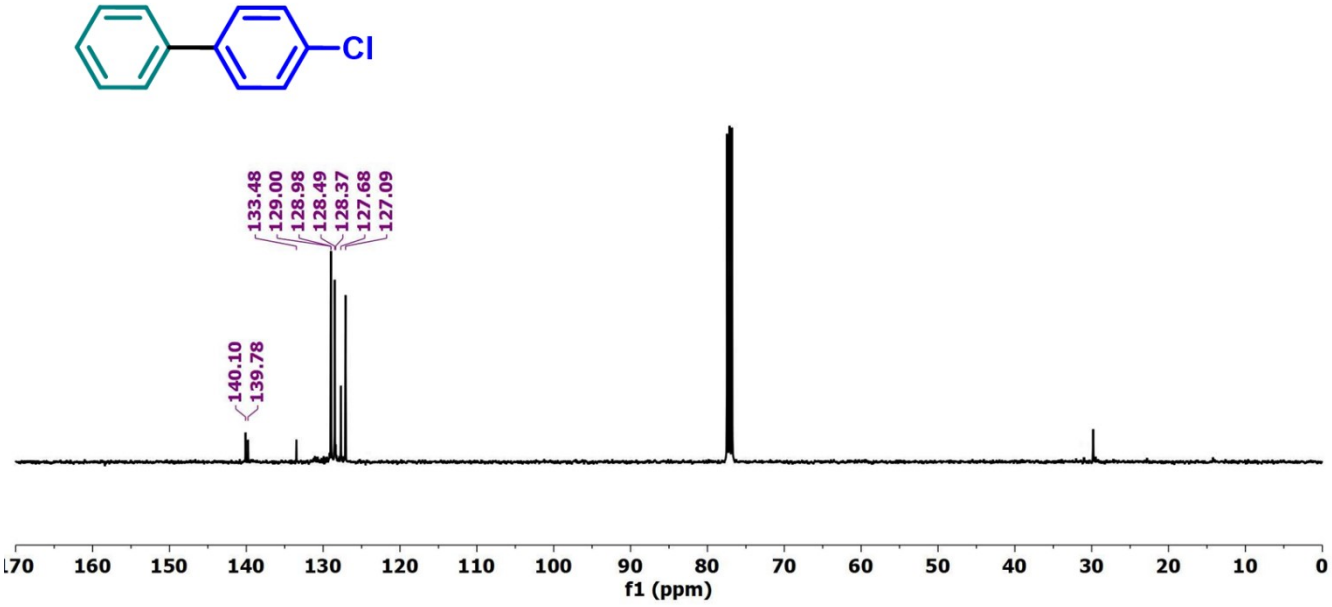

Figure S55: ^{13}C {^{1}H} NMR spectrum of **7b**.

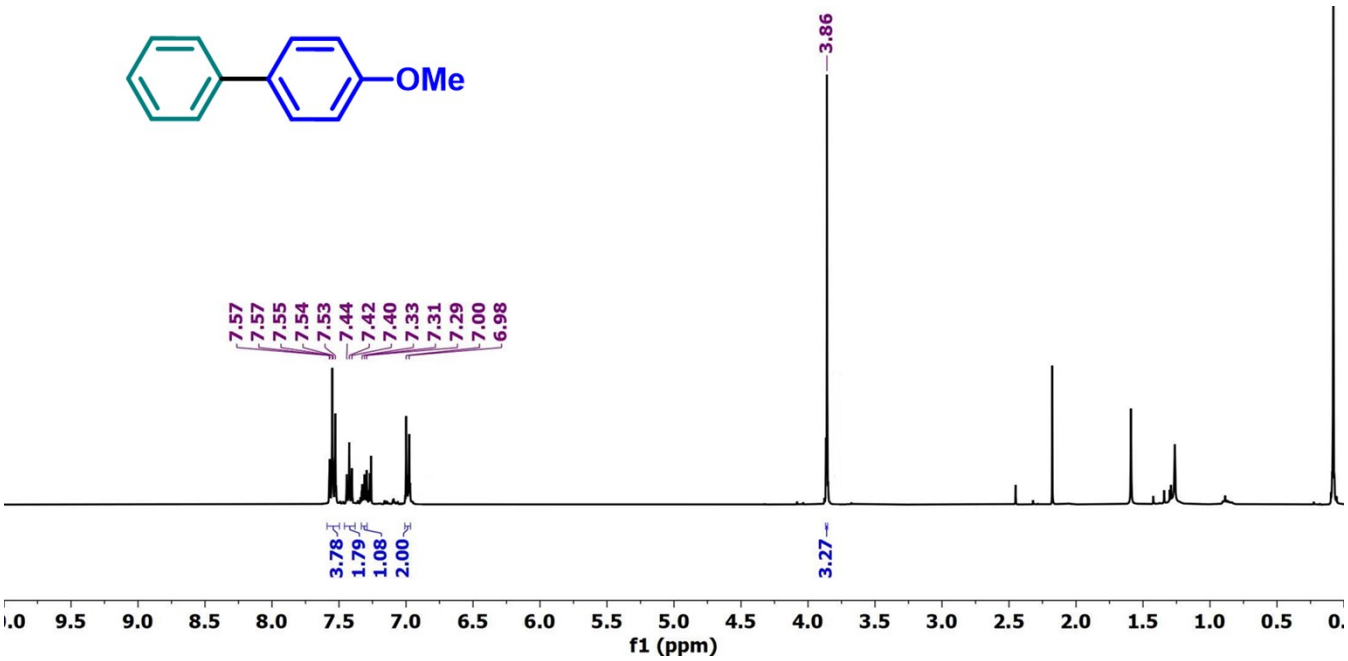

Figure S56: ^{1}H NMR spectrum of **7c**.

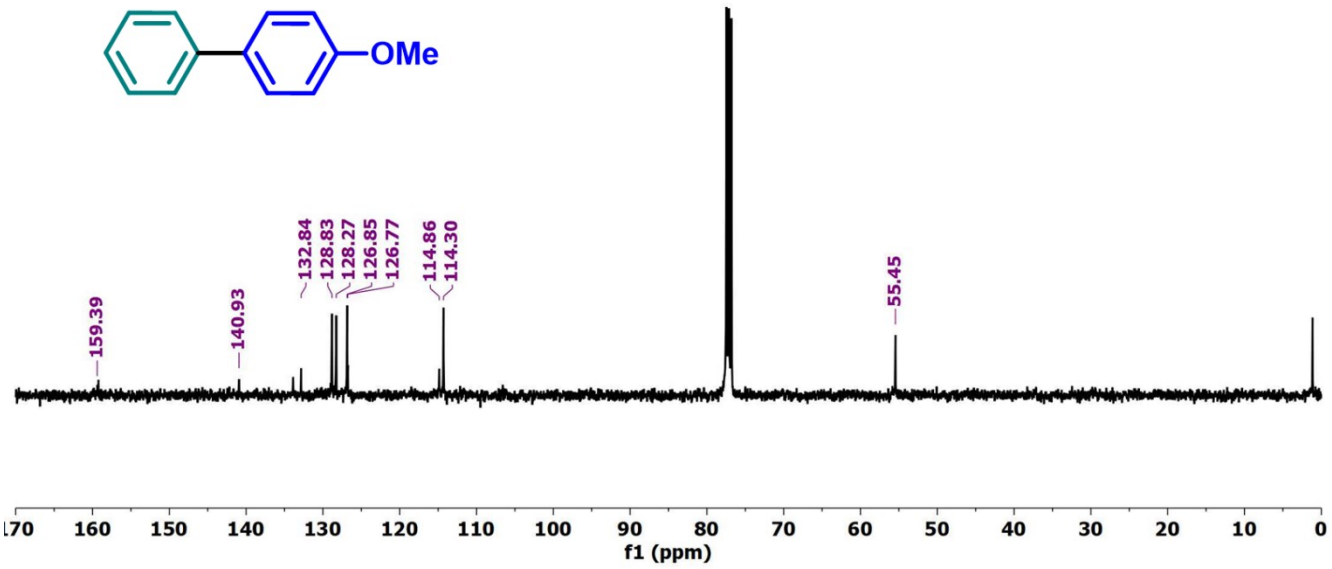

Figure S57: ^{13}C {^{1}H} NMR spectrum of **7c**.

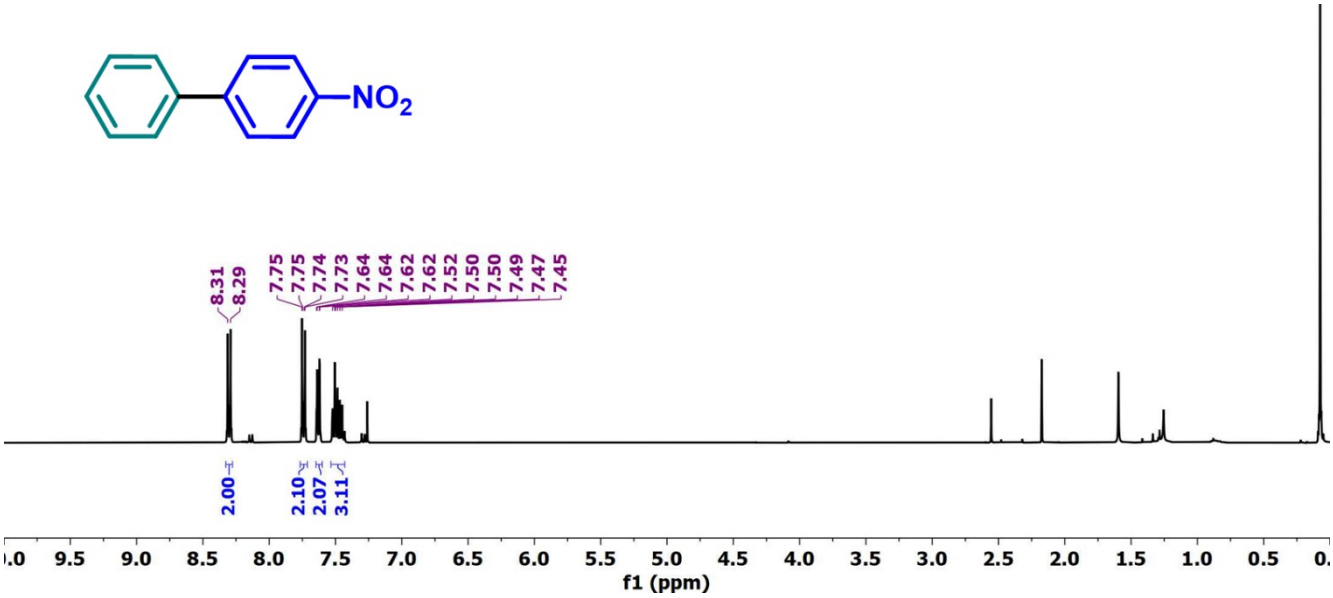

Figure S58: ^{1}H NMR spectrum of **7d**.

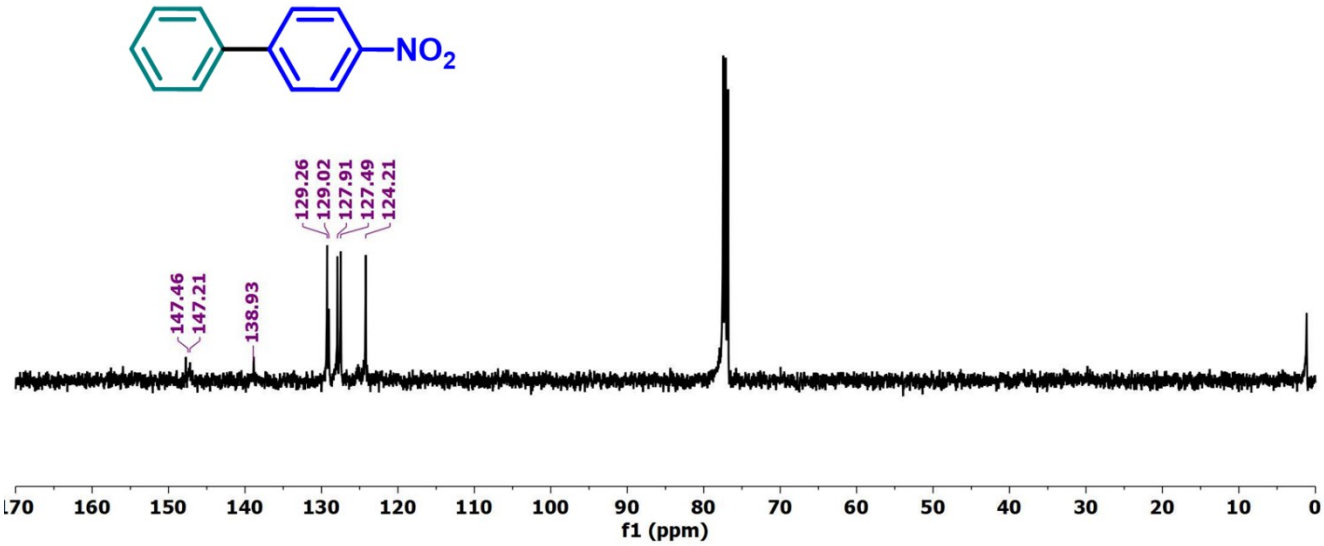

Figure S59: ^{13}C {^{1}H} NMR spectrum of **7d**.

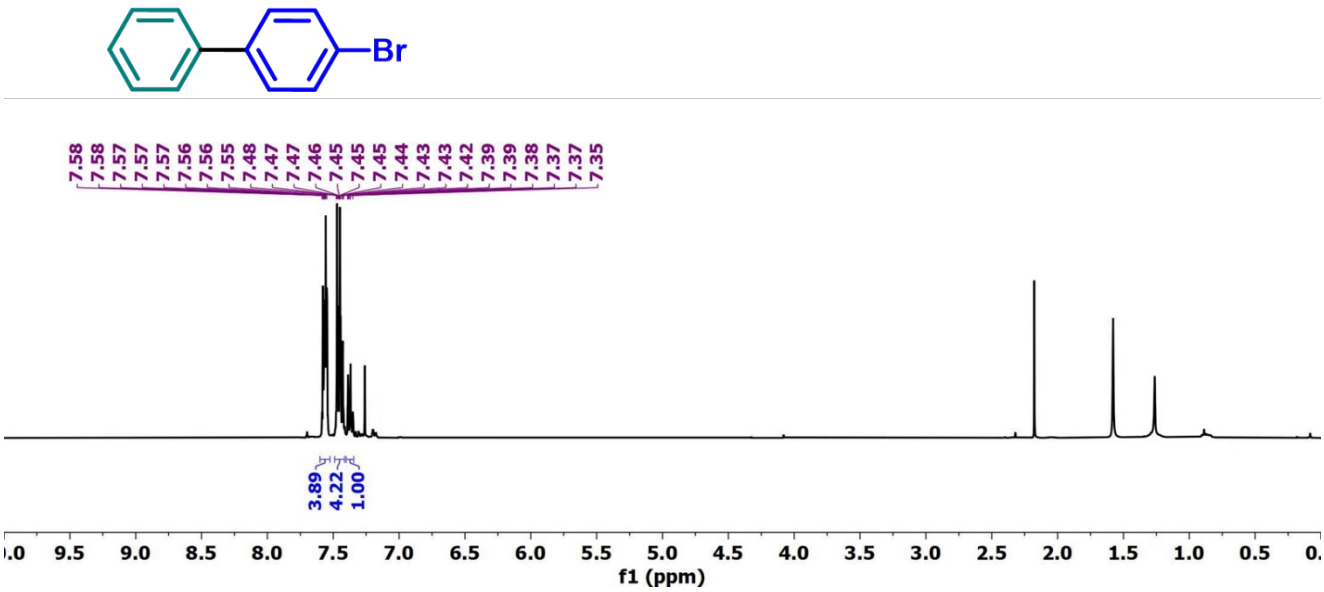

Figure S60: ^{1}H NMR spectrum of **7e**.

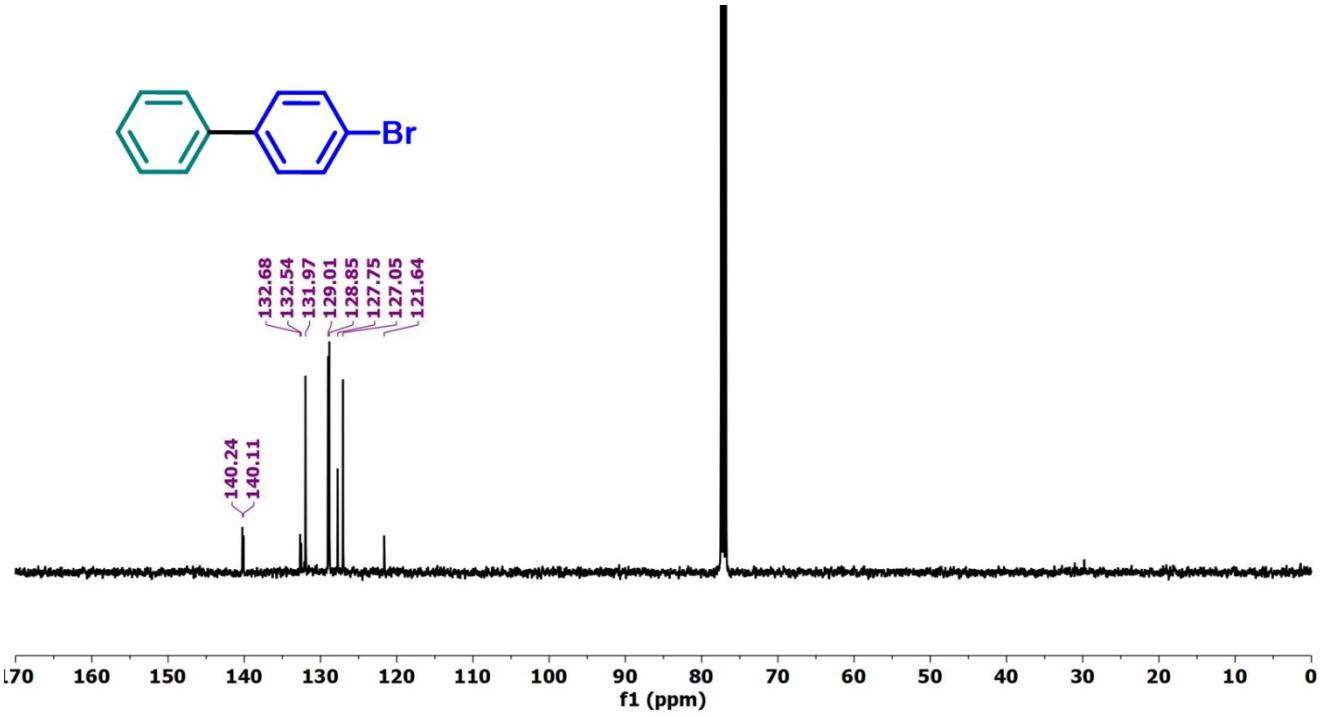

Figure S61: ^{13}C {^{1}H} NMR spectrum of **7e**.

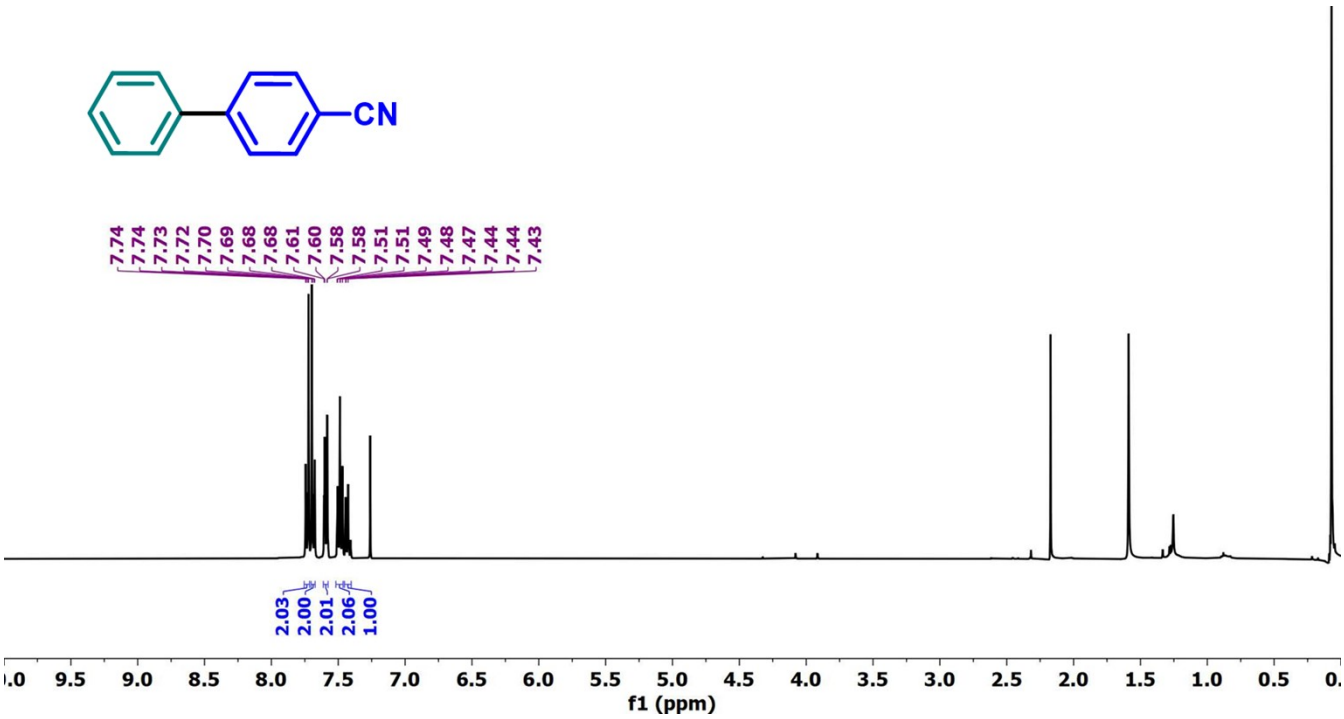

Figure S62: ^{1}H NMR spectrum of **7f**.

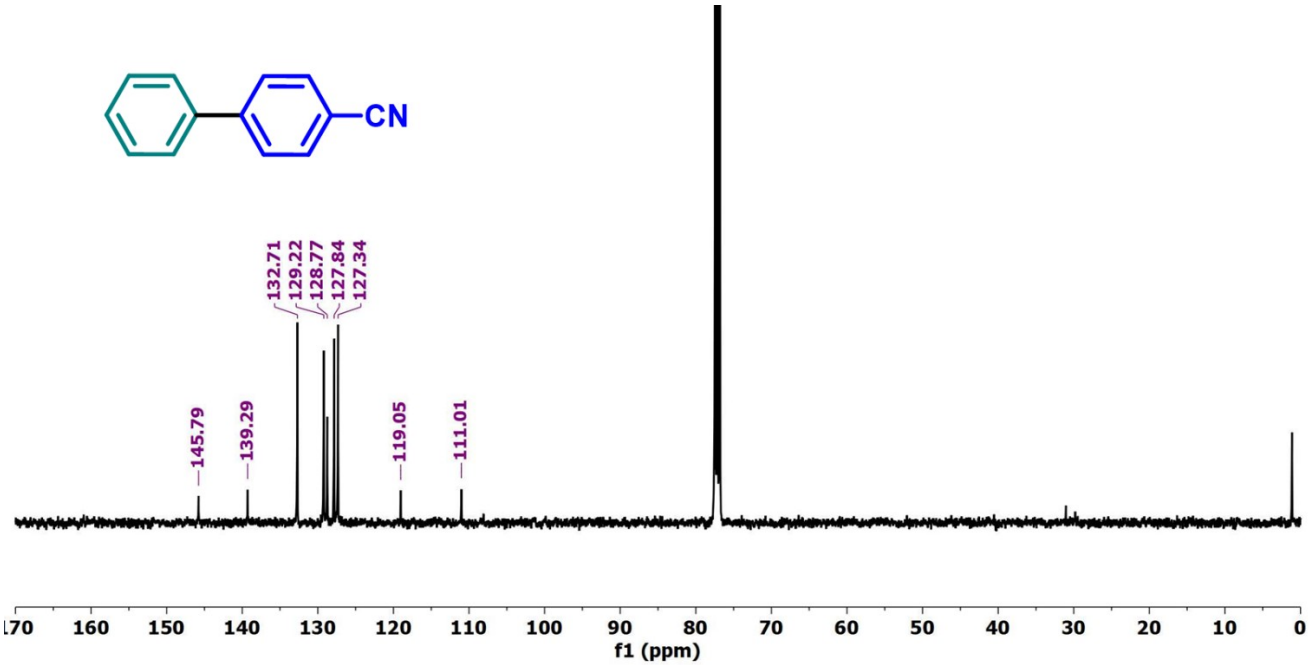

Figure S63: ^{13}C {^{1}H} NMR spectrum of **7f**.

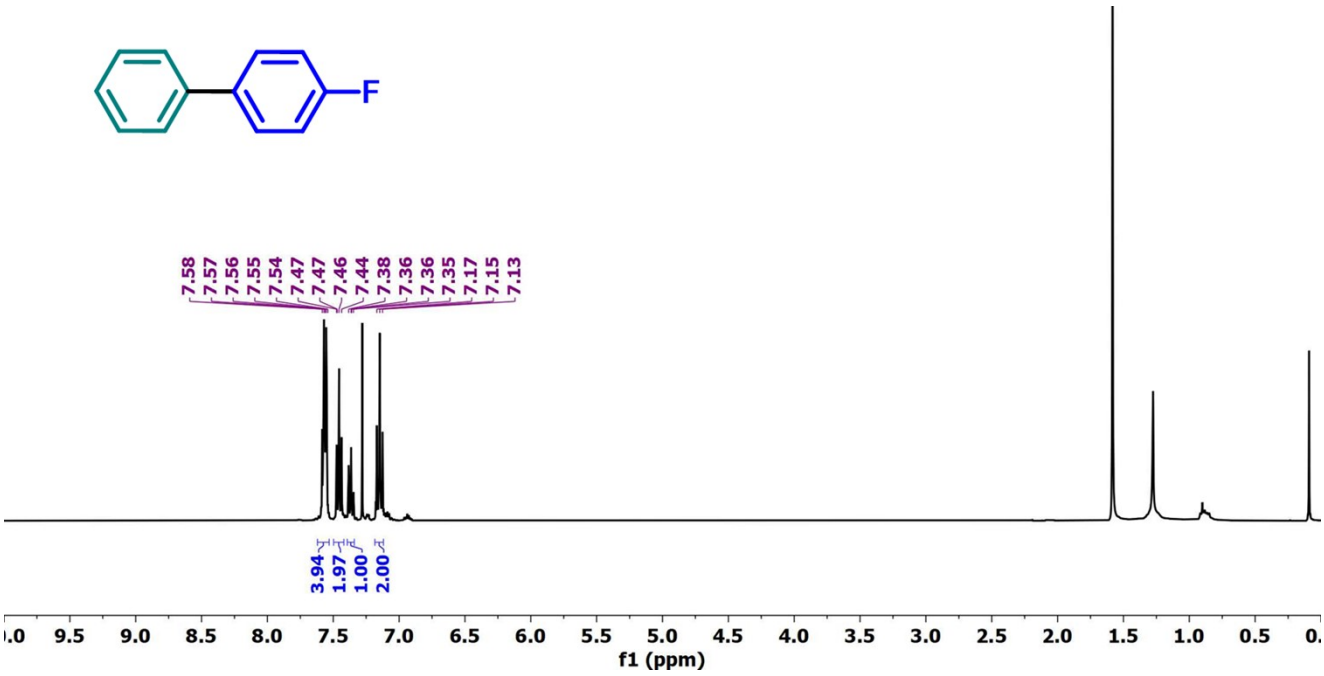

Figure S64: ^{1}H NMR spectrum of **7g**.

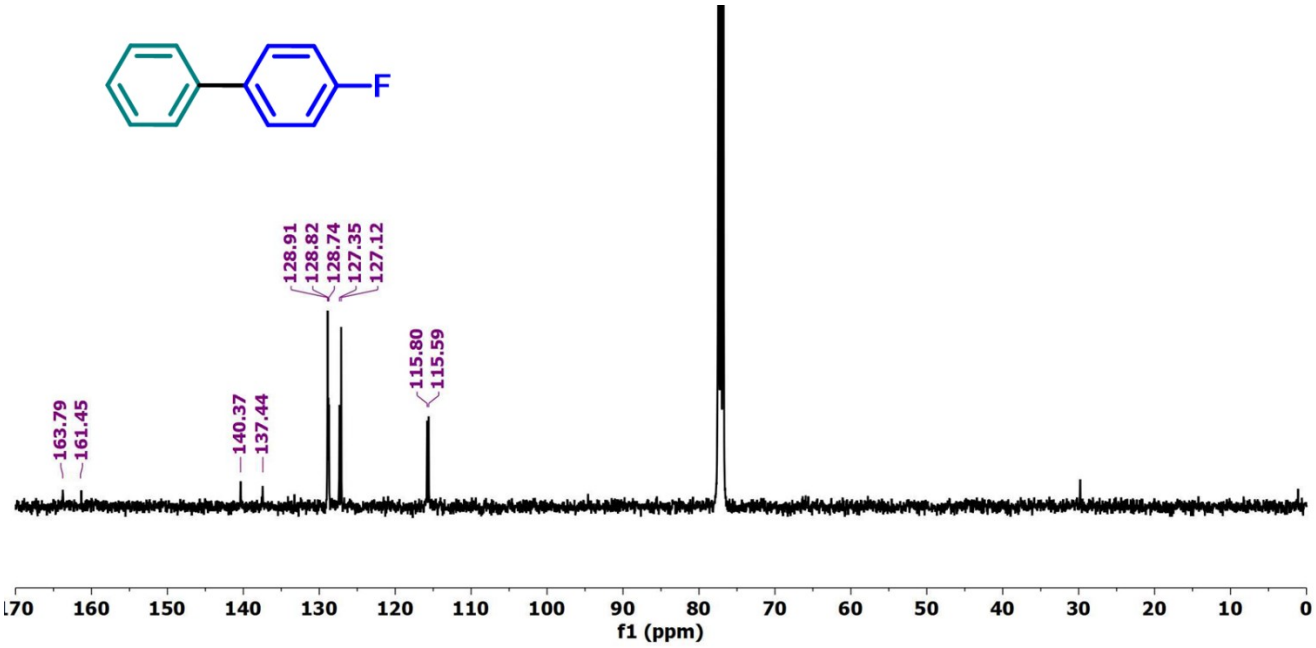

Figure S65: ^{13}C {^{1}H} NMR spectrum of **7g**.

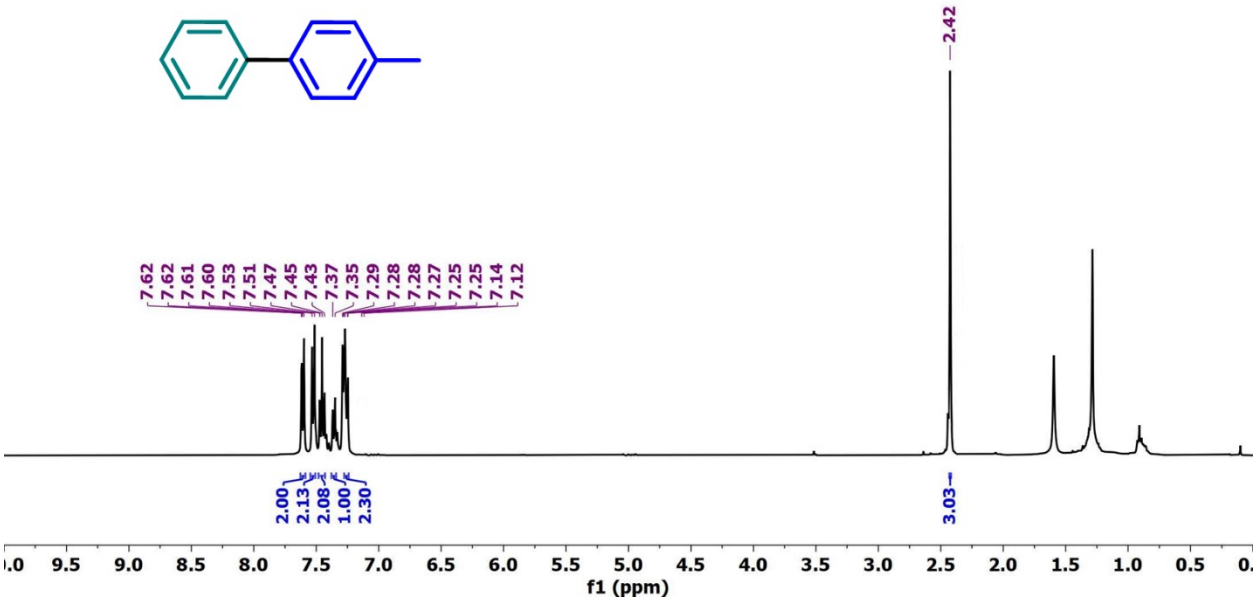

Figure S66: ^{1}H NMR spectrum of **7h**.

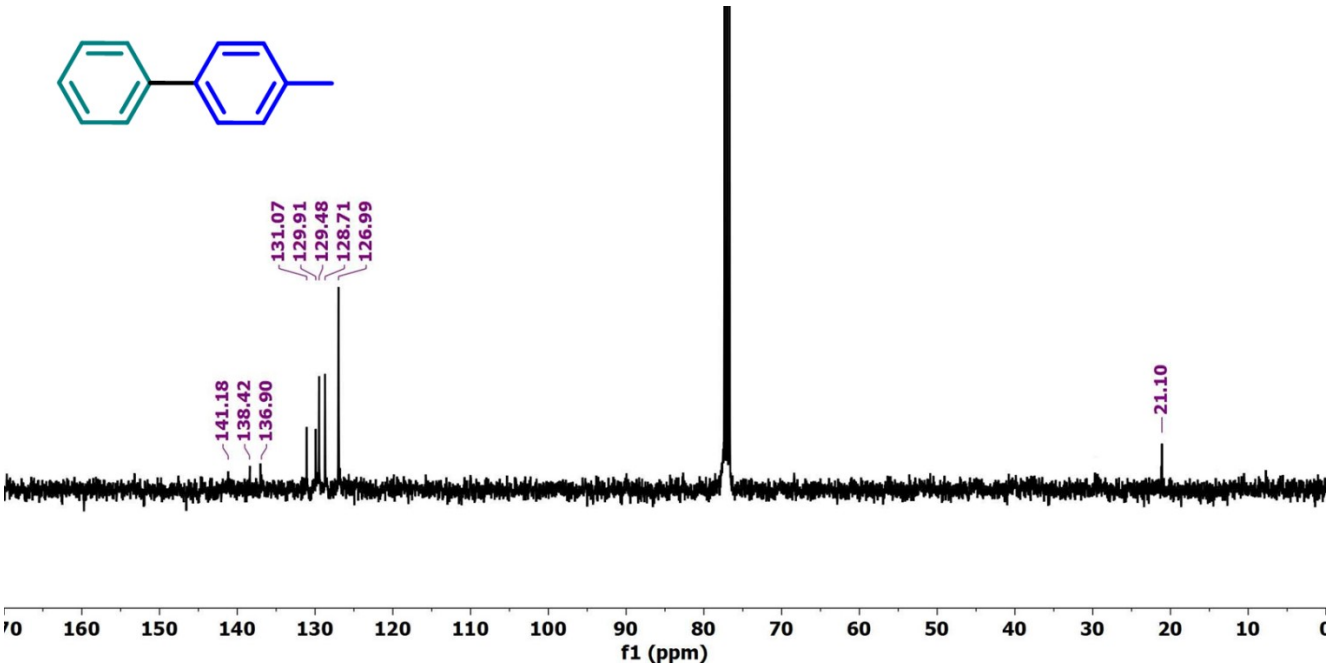

Figure S67: ^{13}C {^{1}H} NMR spectrum of **7h**.

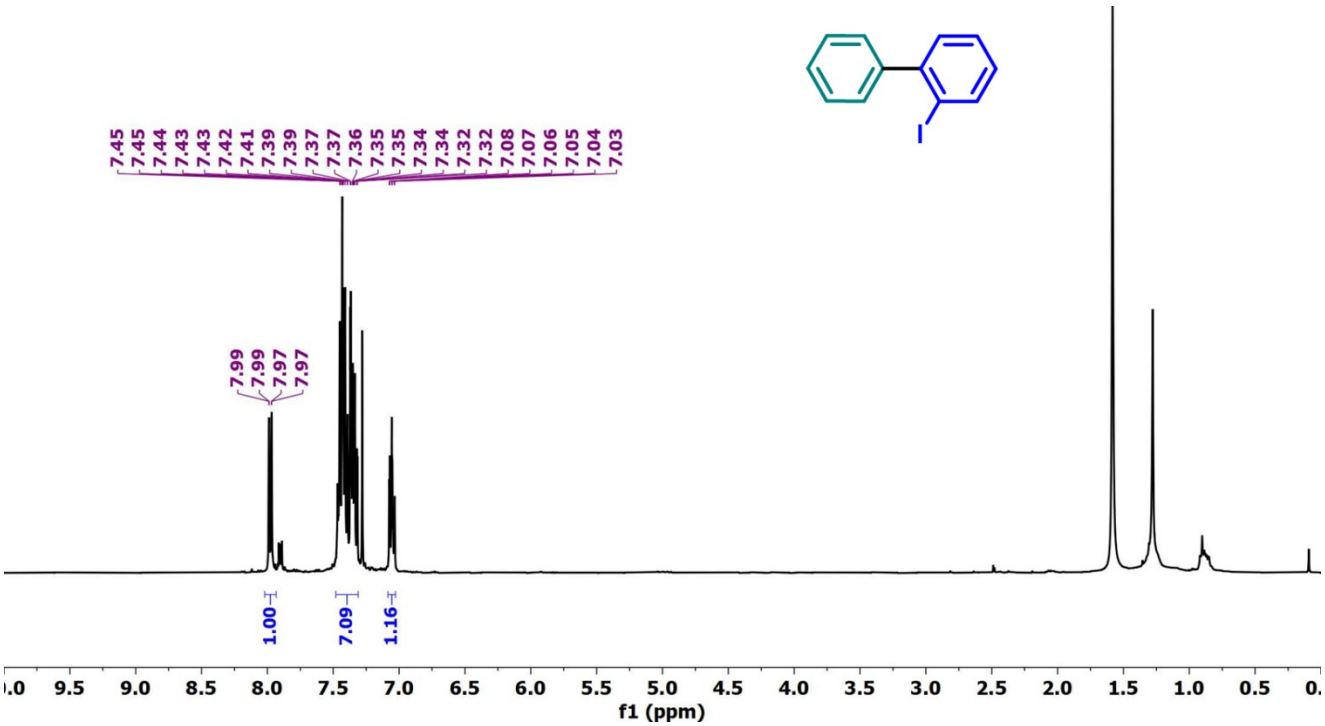

Figure S68: ^{1}H NMR spectrum of **7i**.

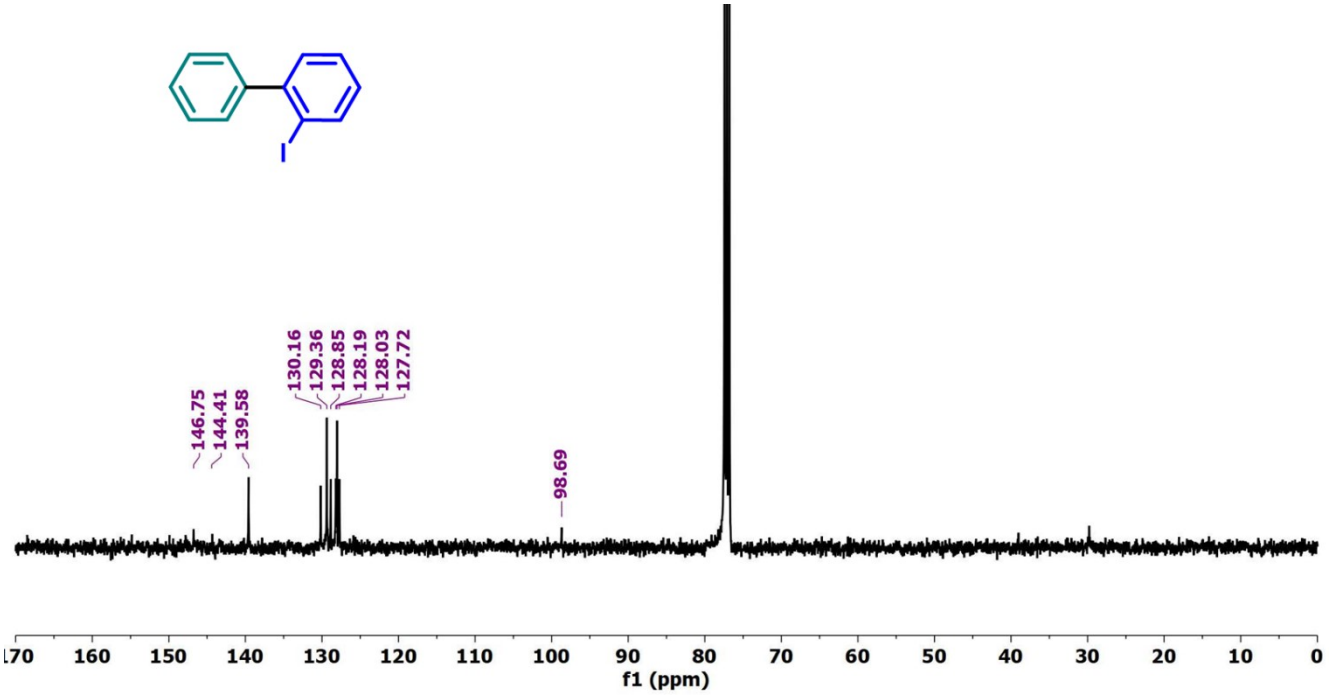

Figure S69: ^{13}C {^{1}H} NMR spectrum of **7i**.

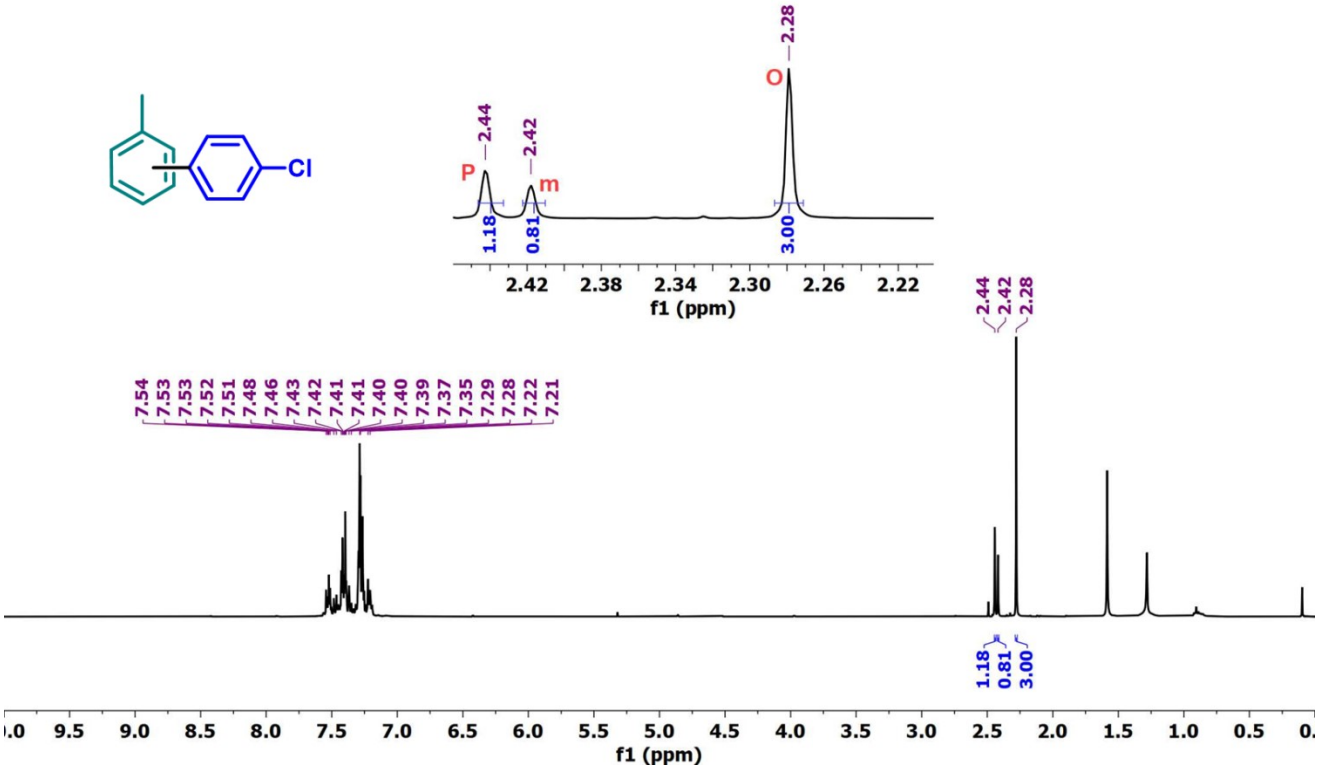

Figure S70: ^{1}H NMR spectrum of **8a**.

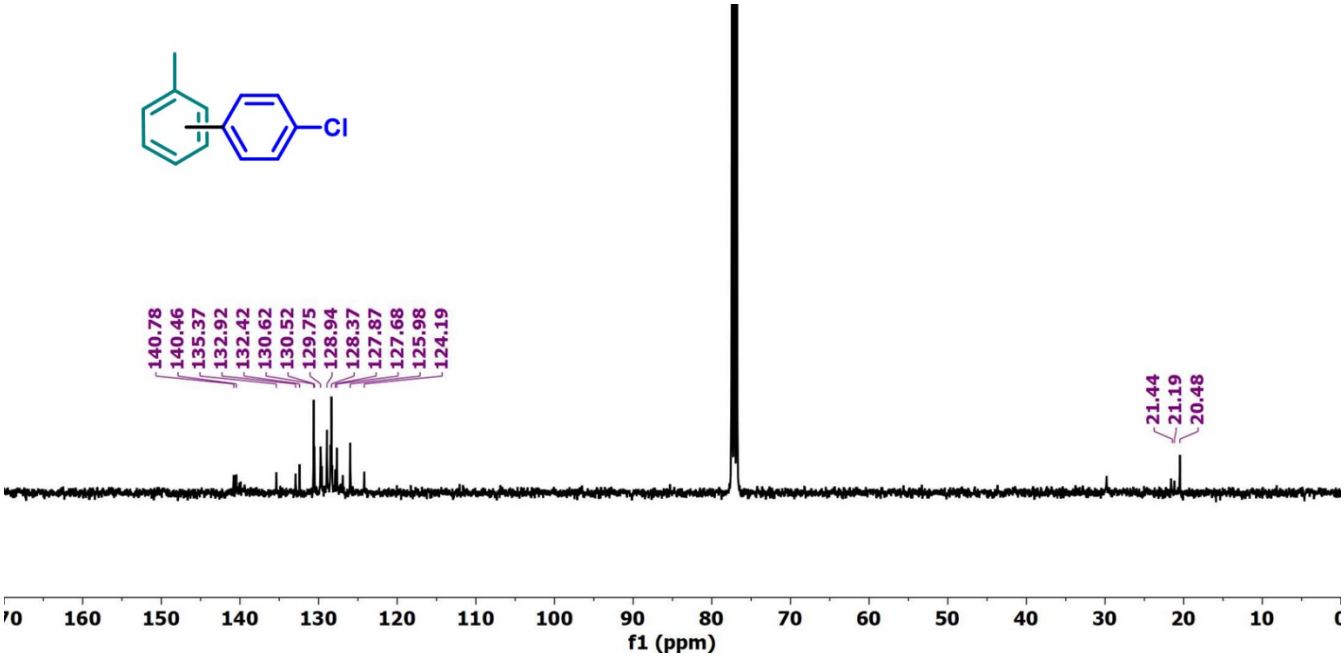

Figure S71: ^{13}C {^{1}H} NMR spectrum of **8a**.

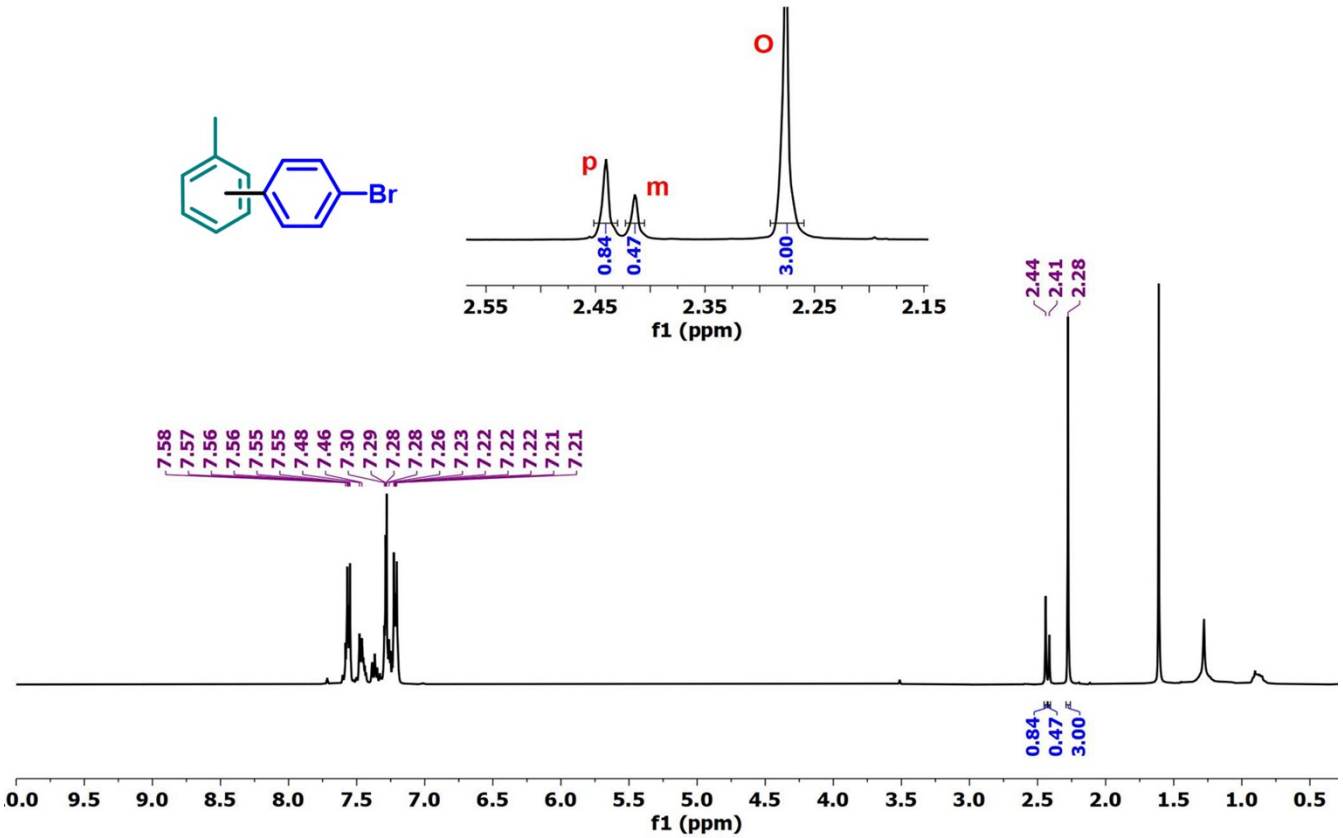

Figure S72: ^{1}H NMR spectrum of **8b**.

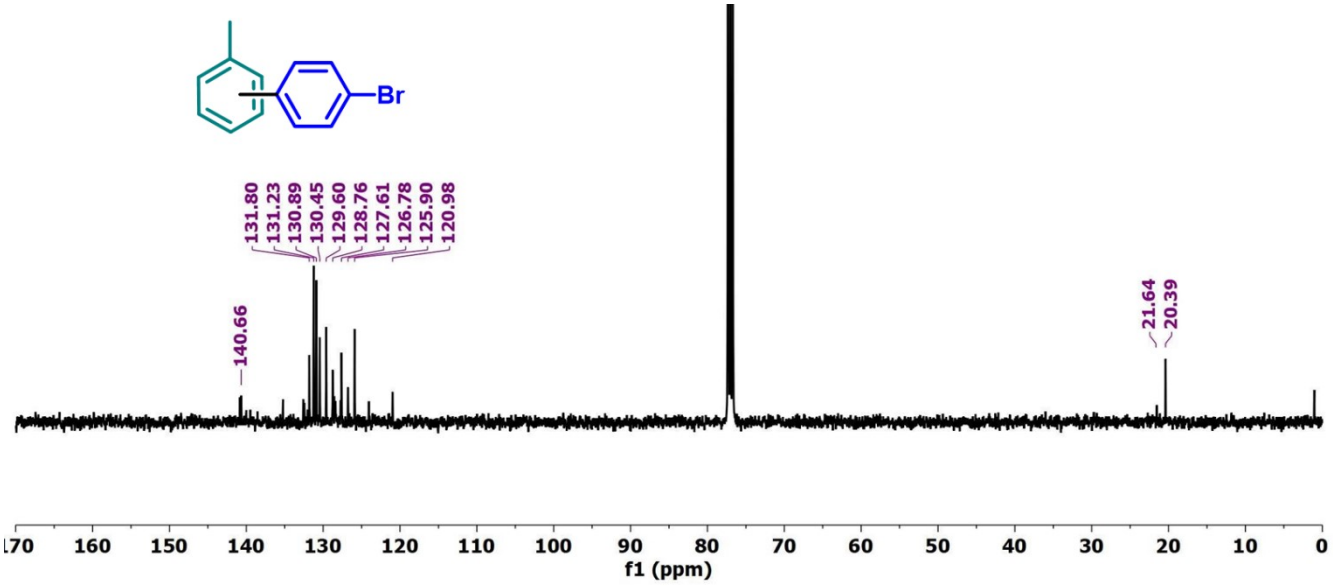

Figure S73: ^{13}C {^{1}H} NMR spectrum of **8b**.

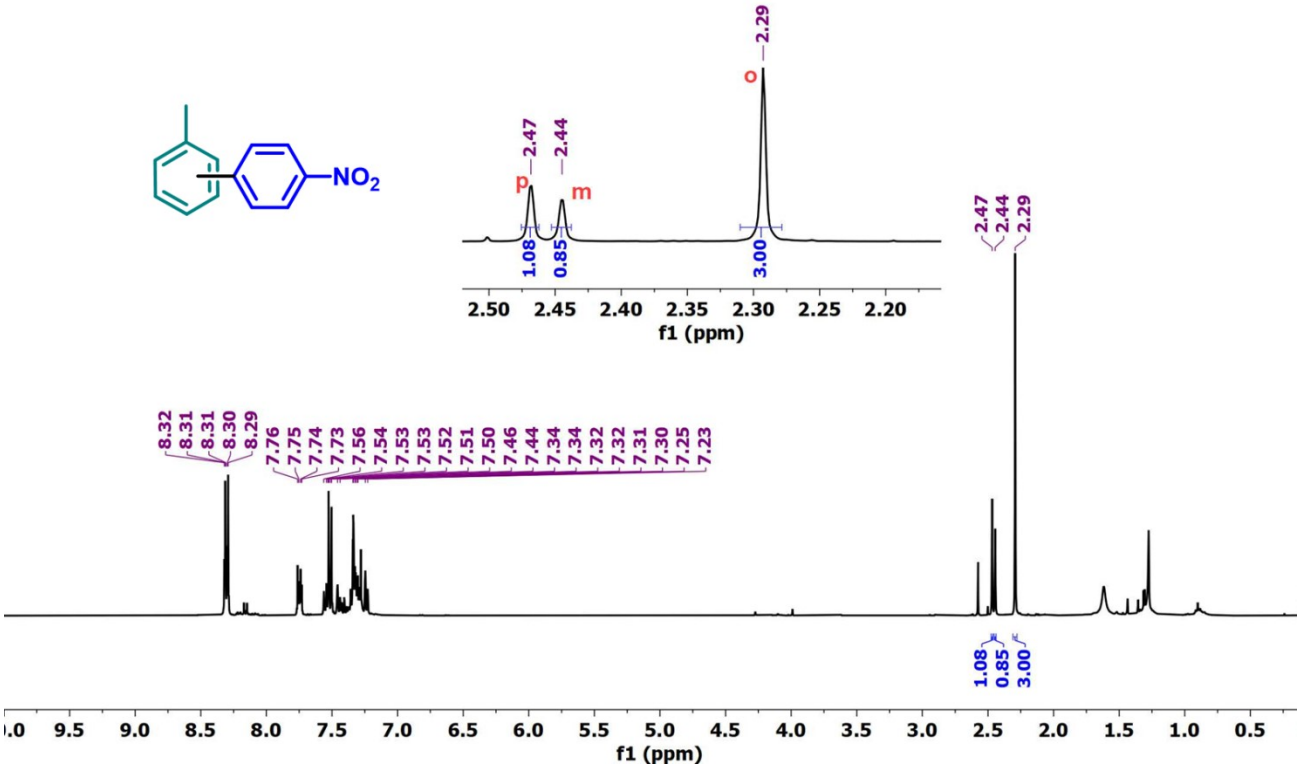

Figure S74: ^{1}H NMR spectrum of **8c**.

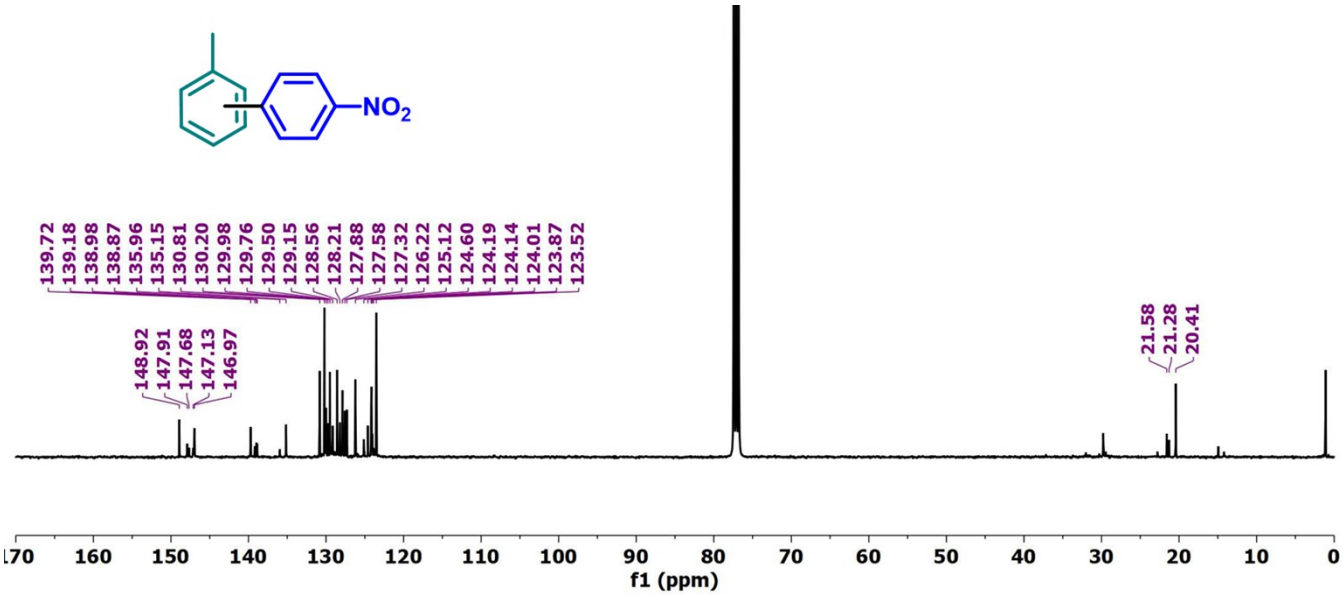

Figure S75: ^{13}C {^{1}H} NMR spectrum of **8c**.

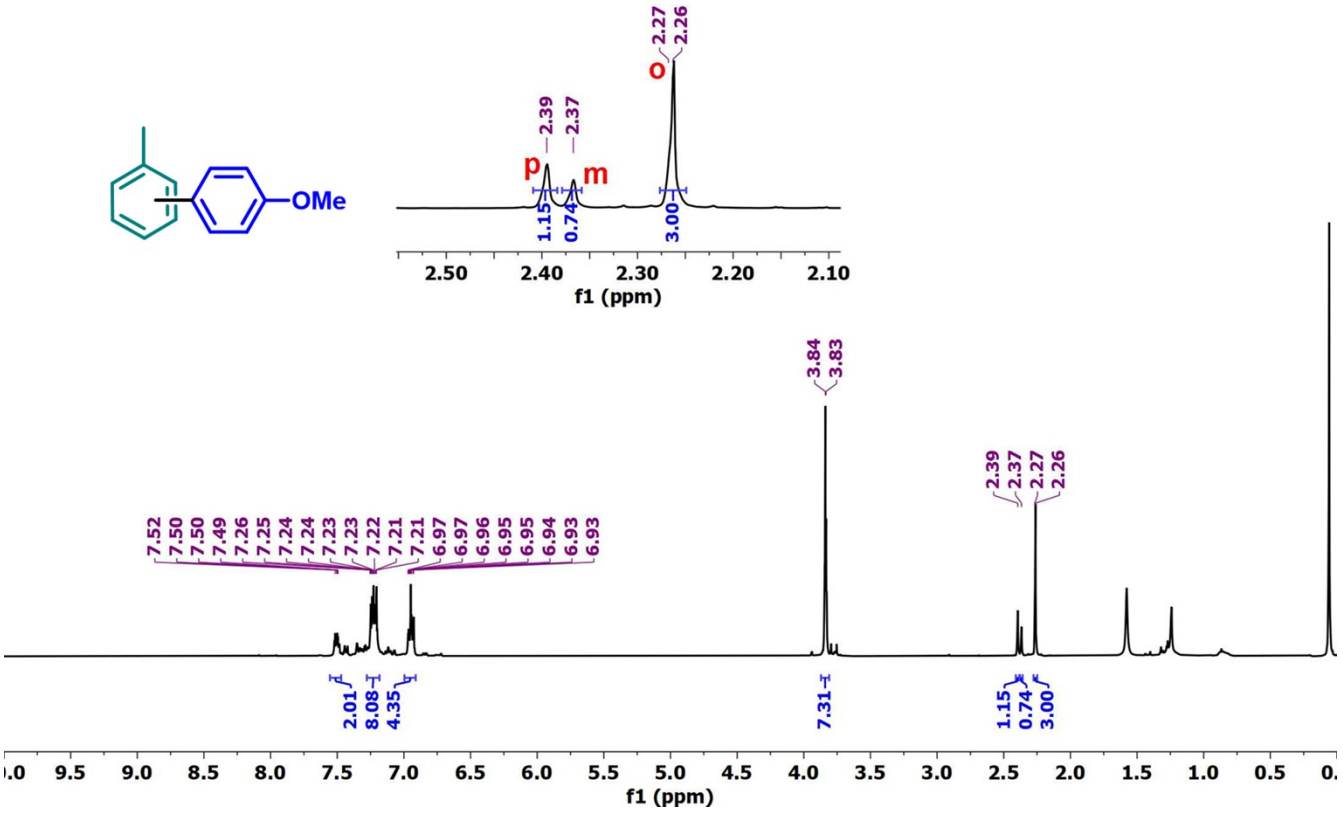

Figure S76: ^{1}H NMR spectrum of **8d**.

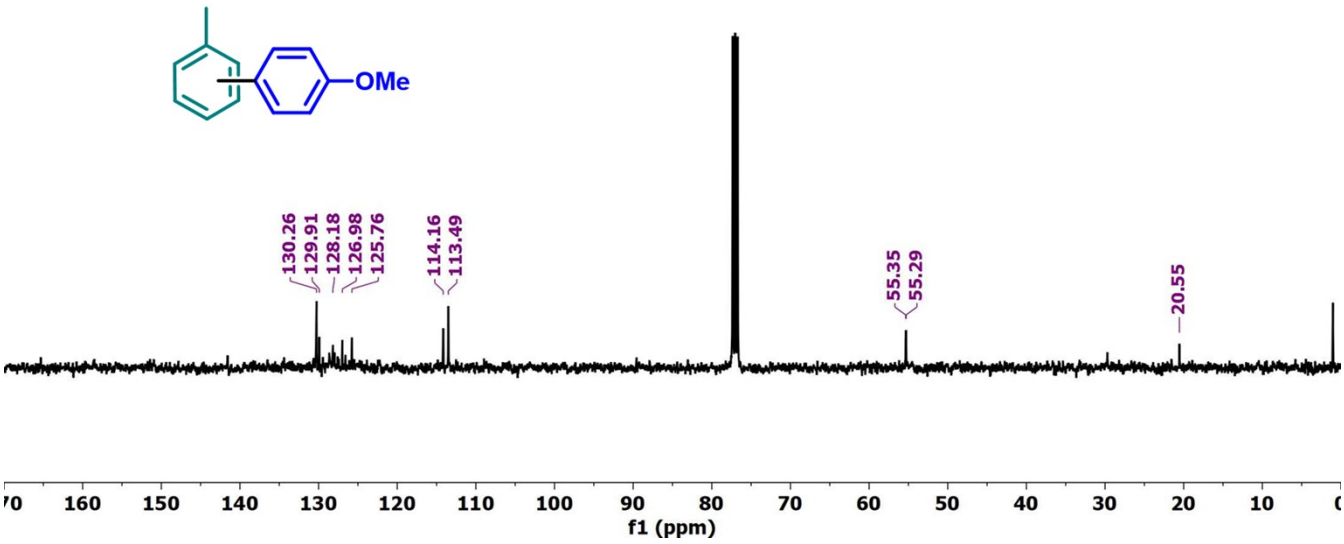

Figure S77: ^{13}C {^{1}H} NMR spectrum of **8d**.

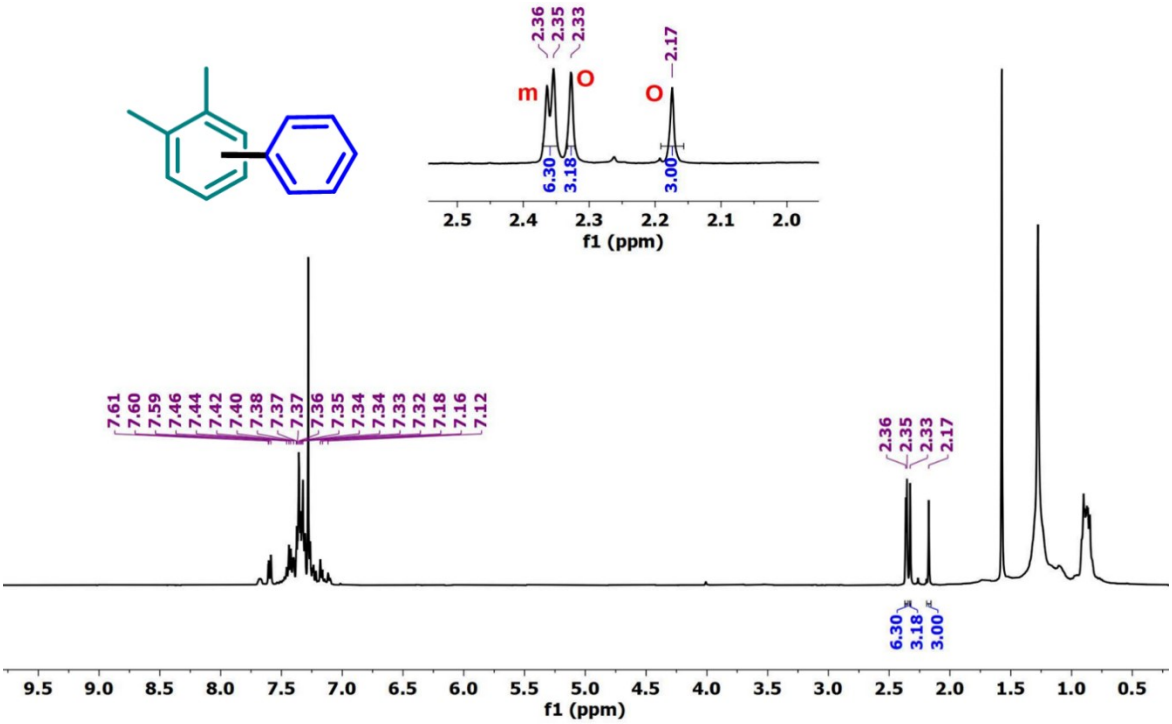

Figure S78: ^{1}H NMR spectrum of **9a**.

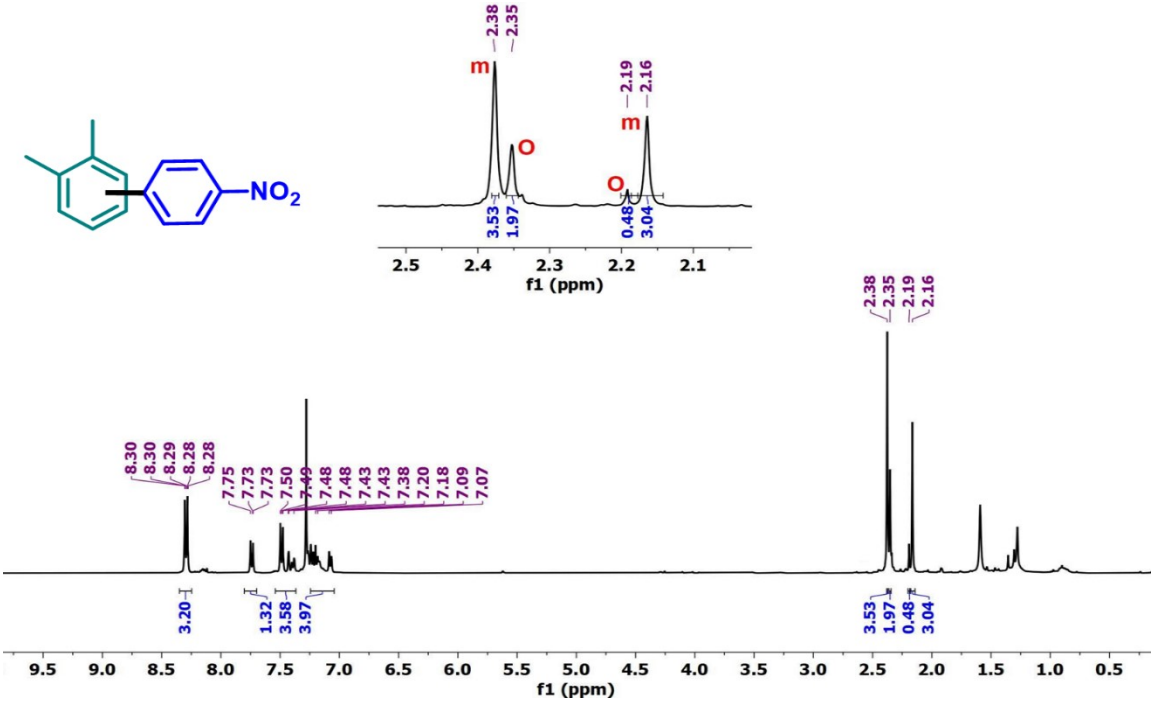

Figure S79: ^{1}H NMR spectrum of **9b**.

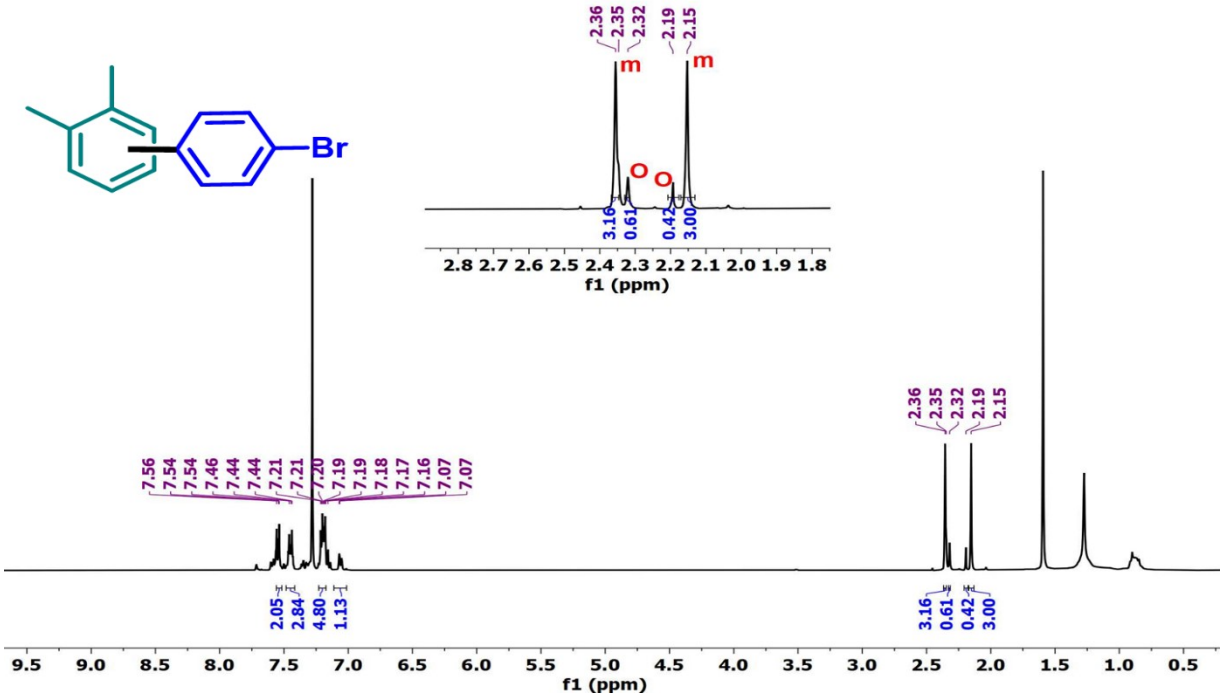

Figure 80: ^{1}H NMR spectrum of **9c**.

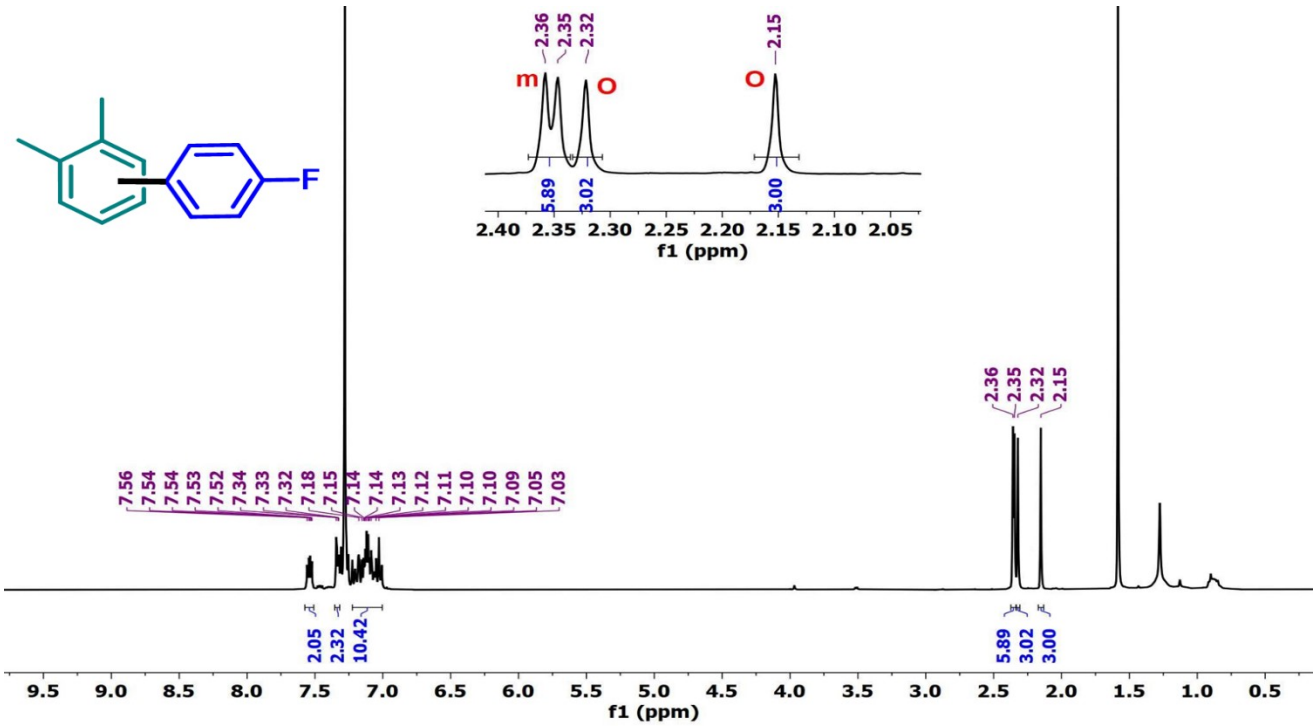

Figure S81: ^{1}H NMR spectrum of **9d**.

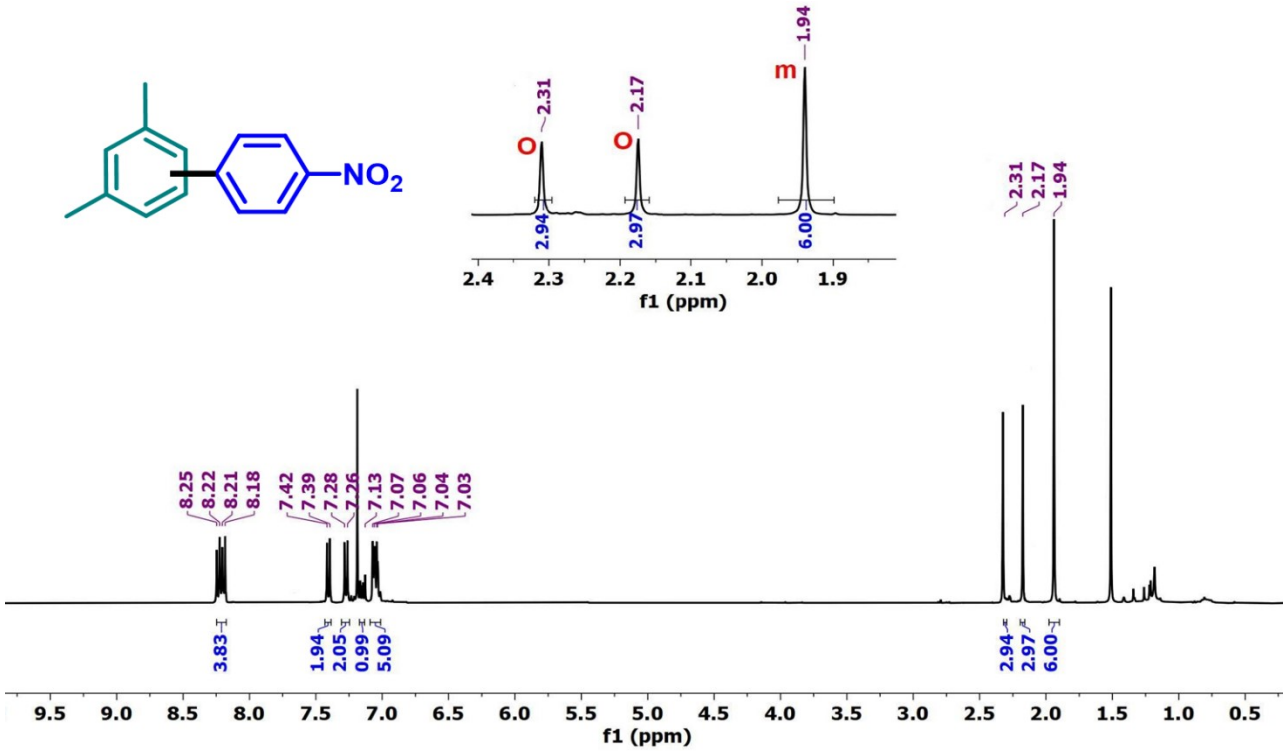

Figure S82: ^{1}H NMR spectrum of **10a**.

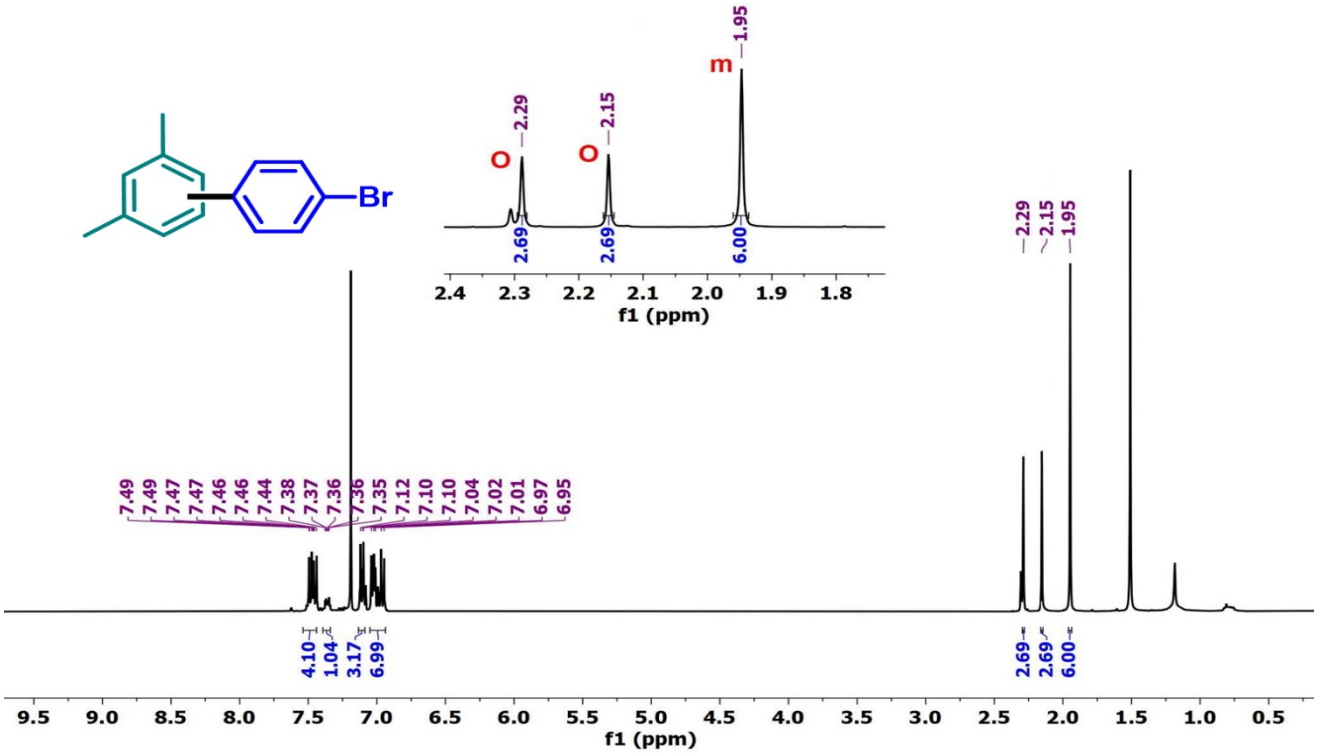

Figure S83: ^{1}H NMR spectrum of **10b**.

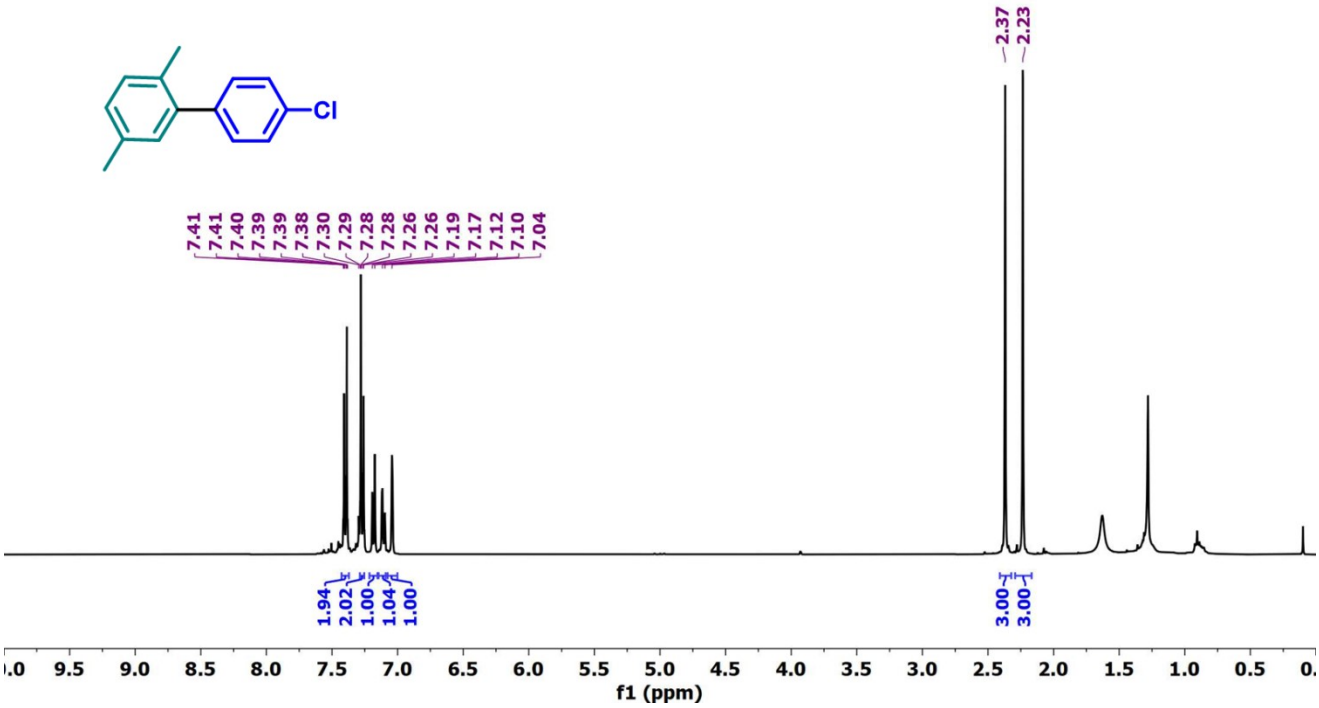

Figure S84: ^{1}H NMR spectrum of **11a**.

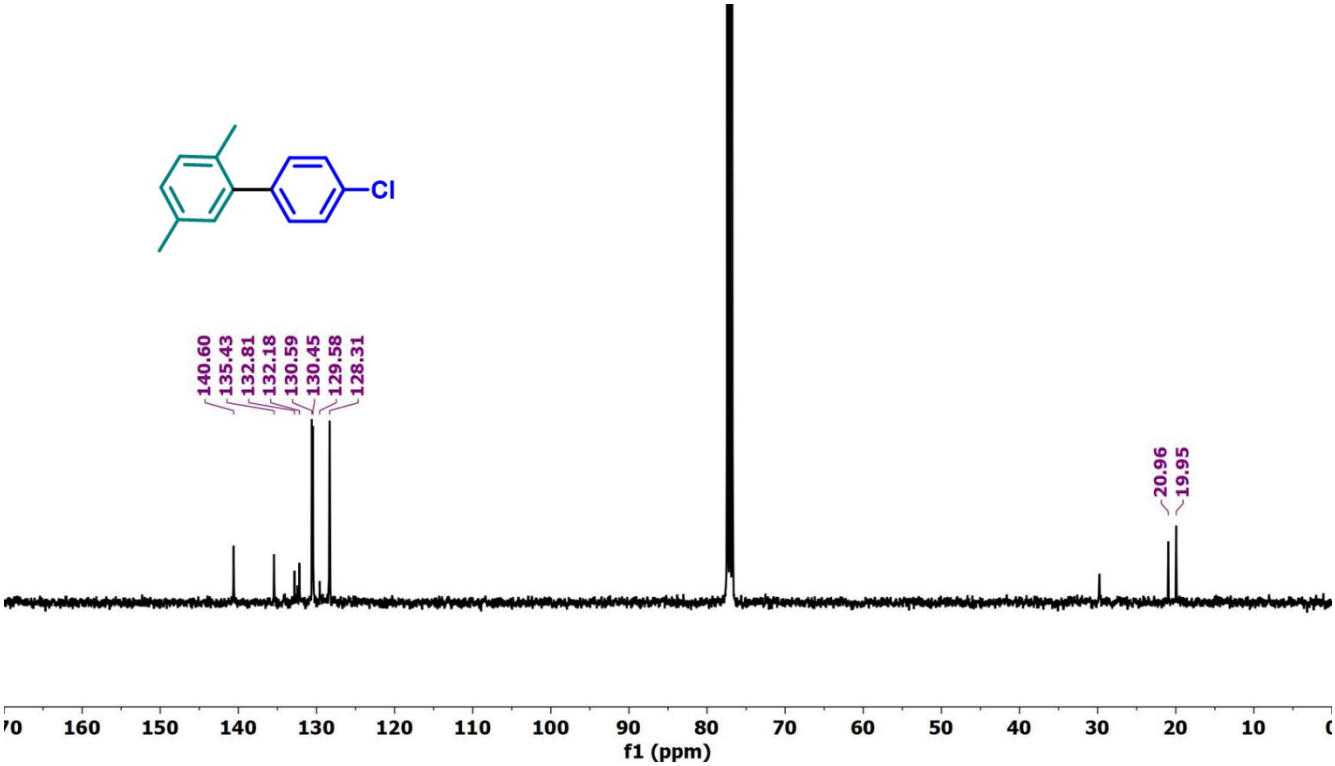

Figure S85: ^{13}C {^{1}H} NMR spectrum of **11a**.

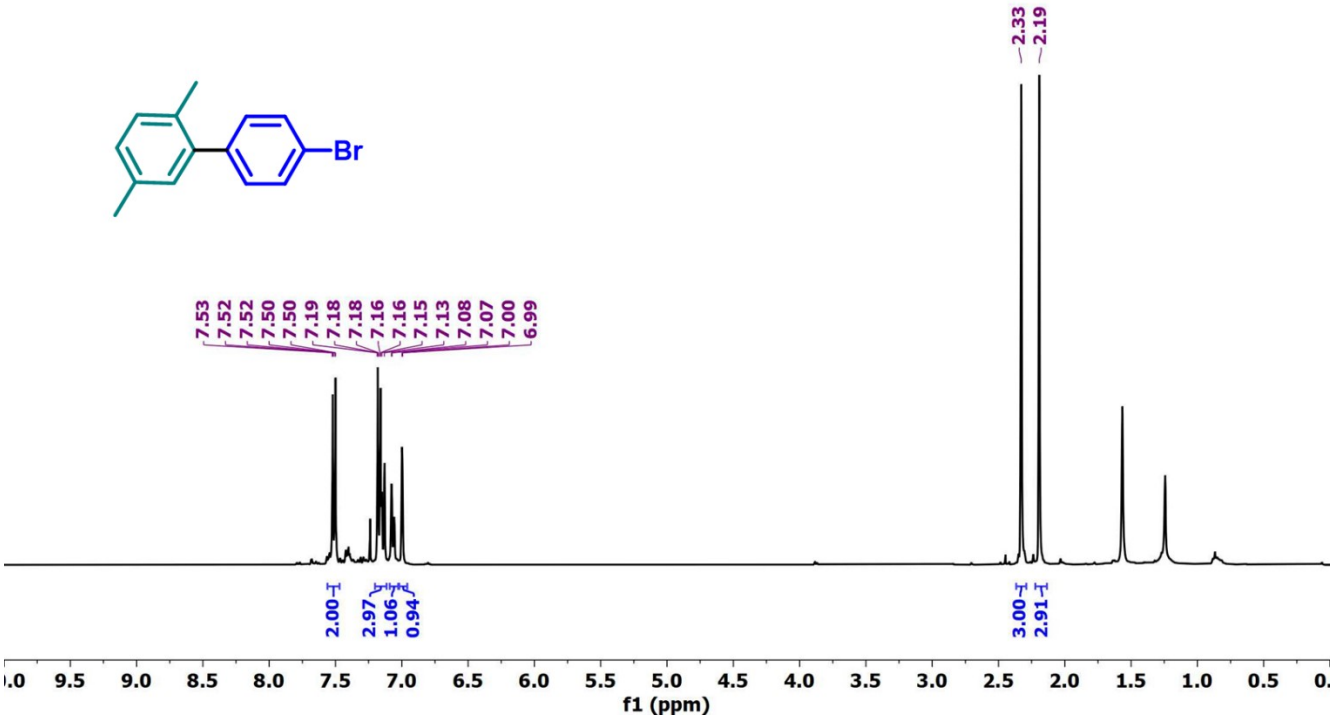

Figure S86: ^{1}H NMR spectrum of **11b**.

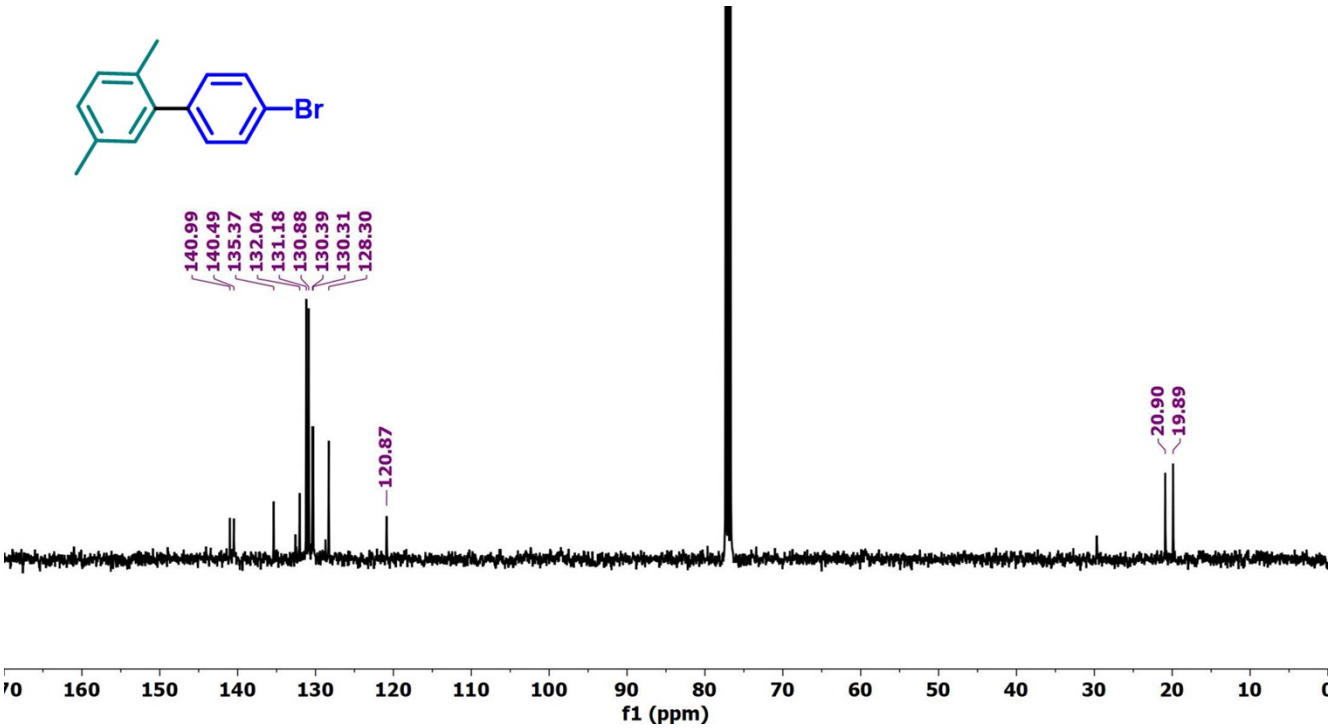

Figure S87: ^{13}C {^{1}H} NMR spectrum of **11b**.

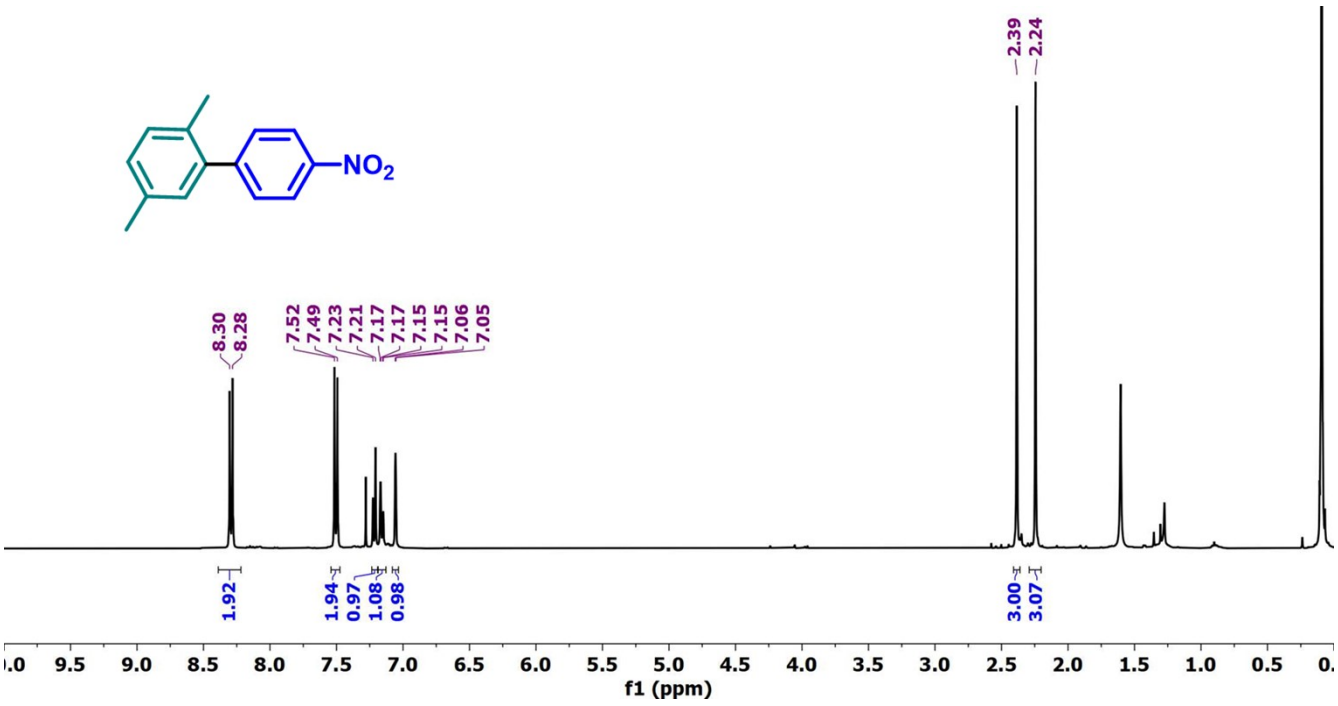

Figure S88: ^{1}H NMR spectrum of **11c**.

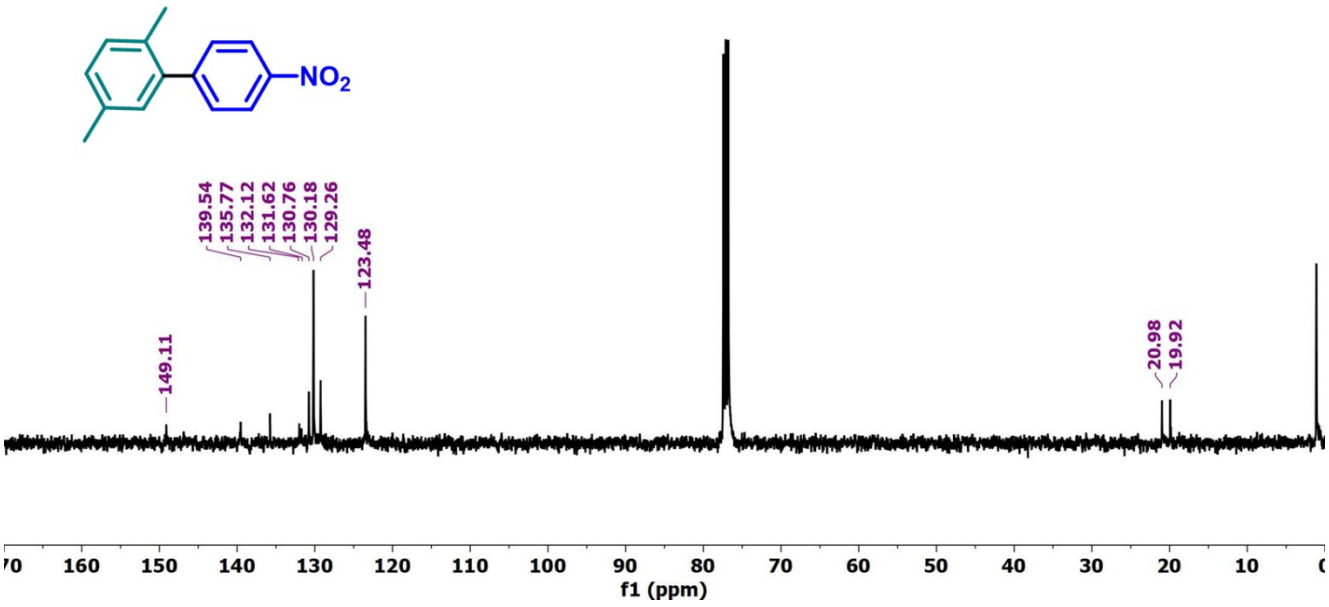

Figure S89: ^{13}C {^{1}H} NMR spectrum of **11c**.

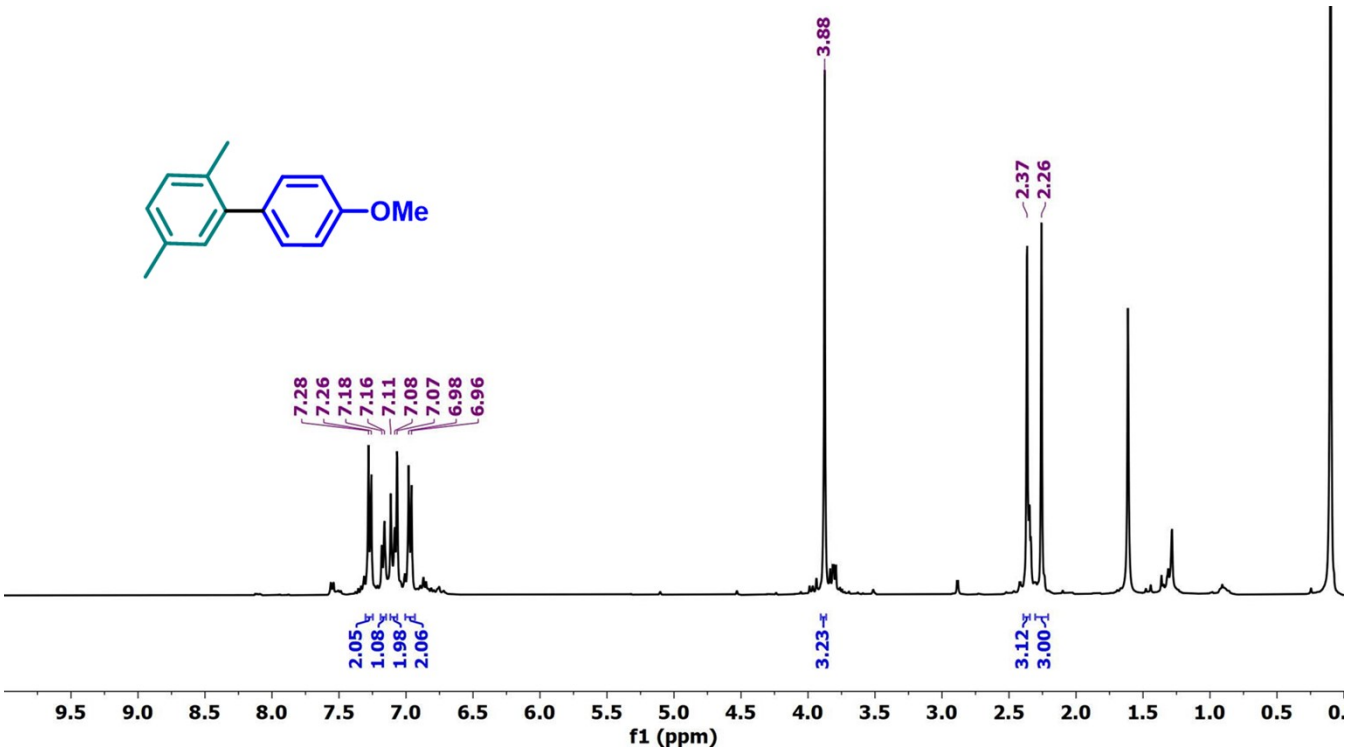

Figure S90: ^{1}H NMR spectrum of **11d**.

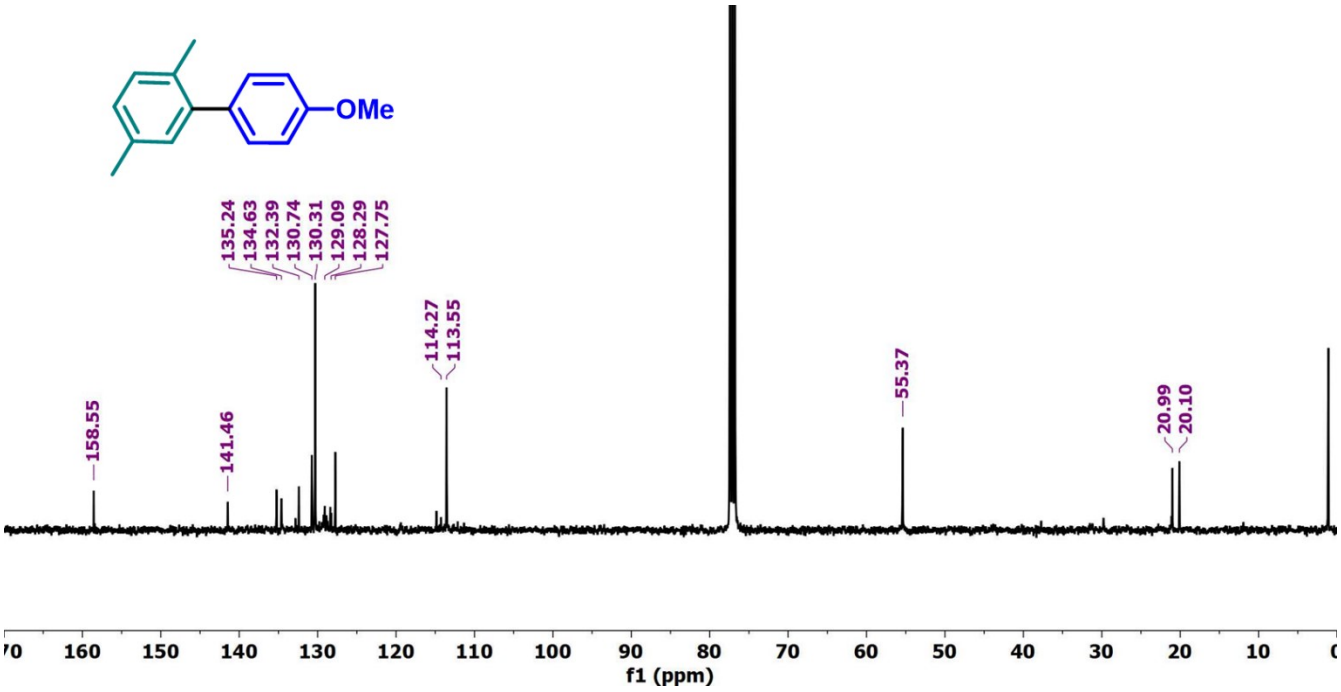

Figure S91: ^{13}C {^{1}H} NMR spectrum of **11d**.

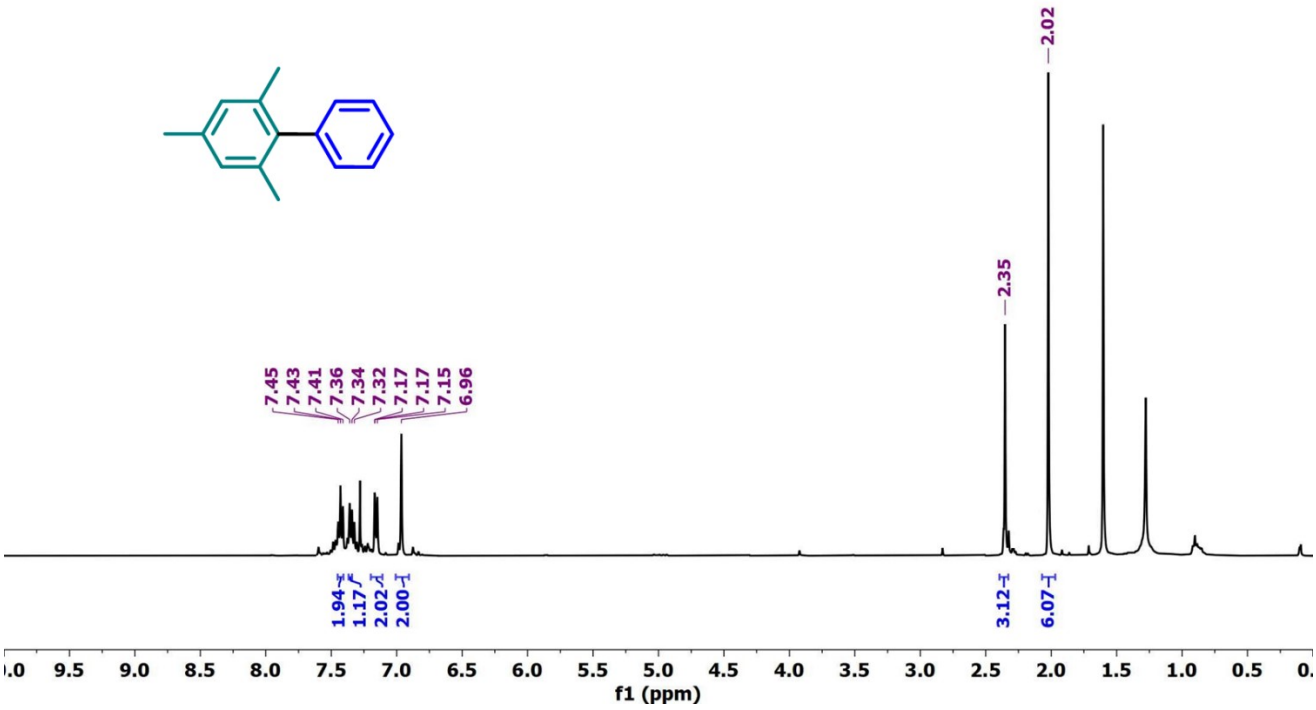

Figure S92: ^{1}H NMR spectrum of **12a**.

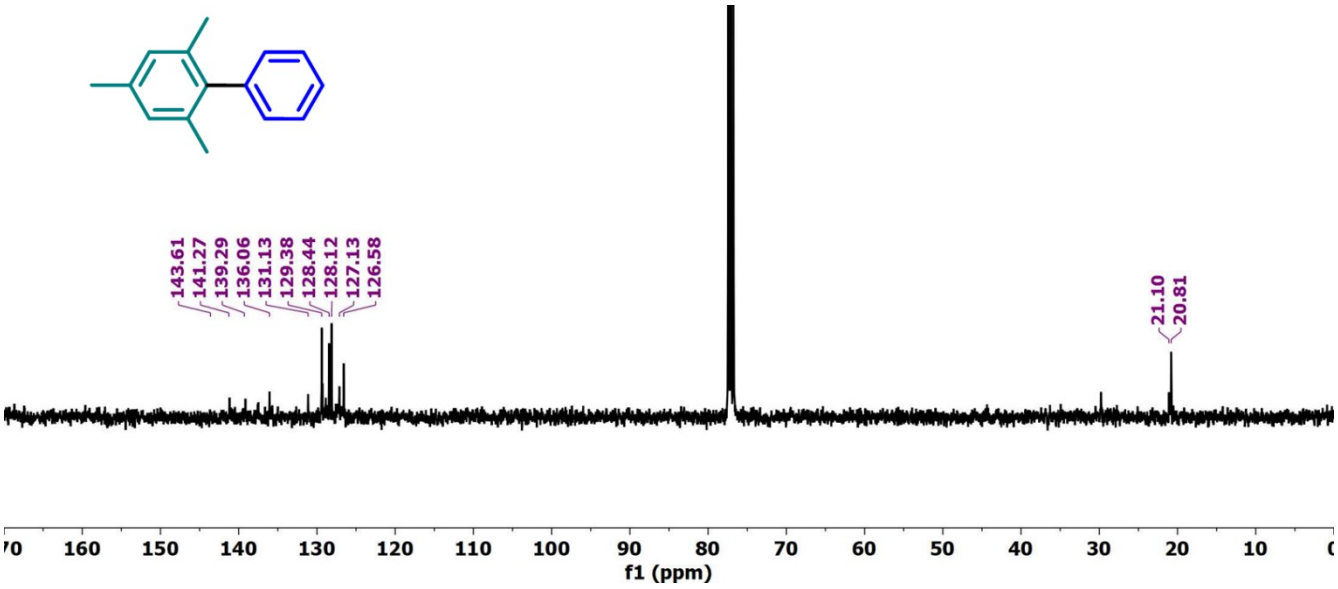

Figure S93: ^{13}C {^{1}H} NMR spectrum of **12a**.

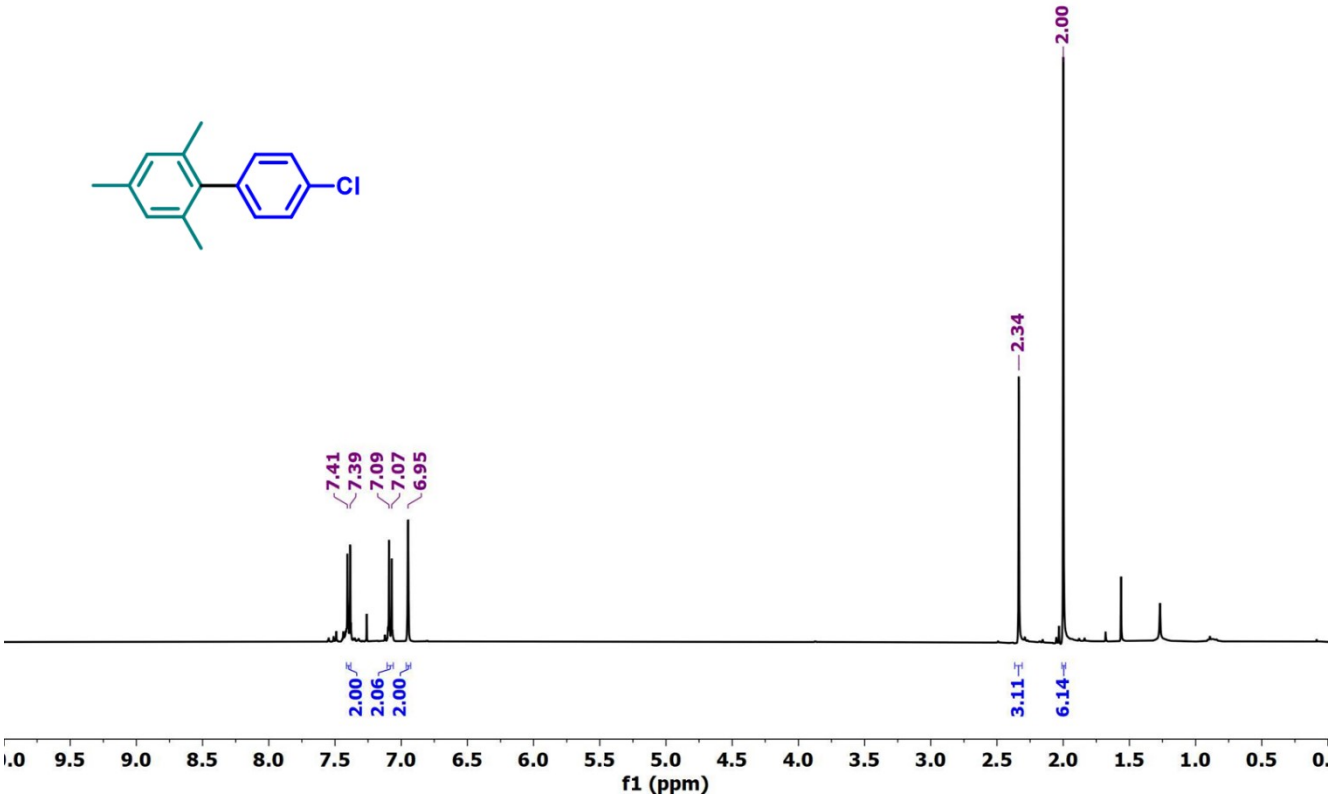

Figure S94: ^{1}H NMR spectrum of **12b**.

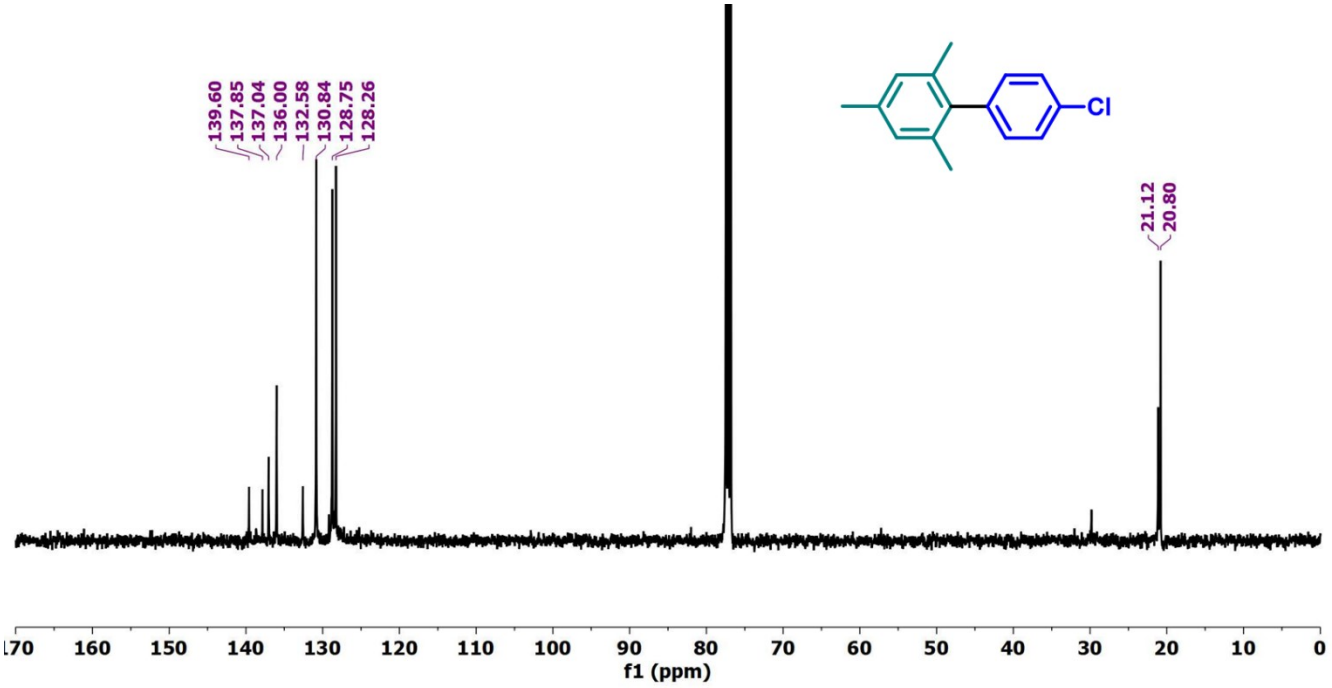

Figure S95: ^{13}C {^{1}H} NMR spectrum of **12b**.

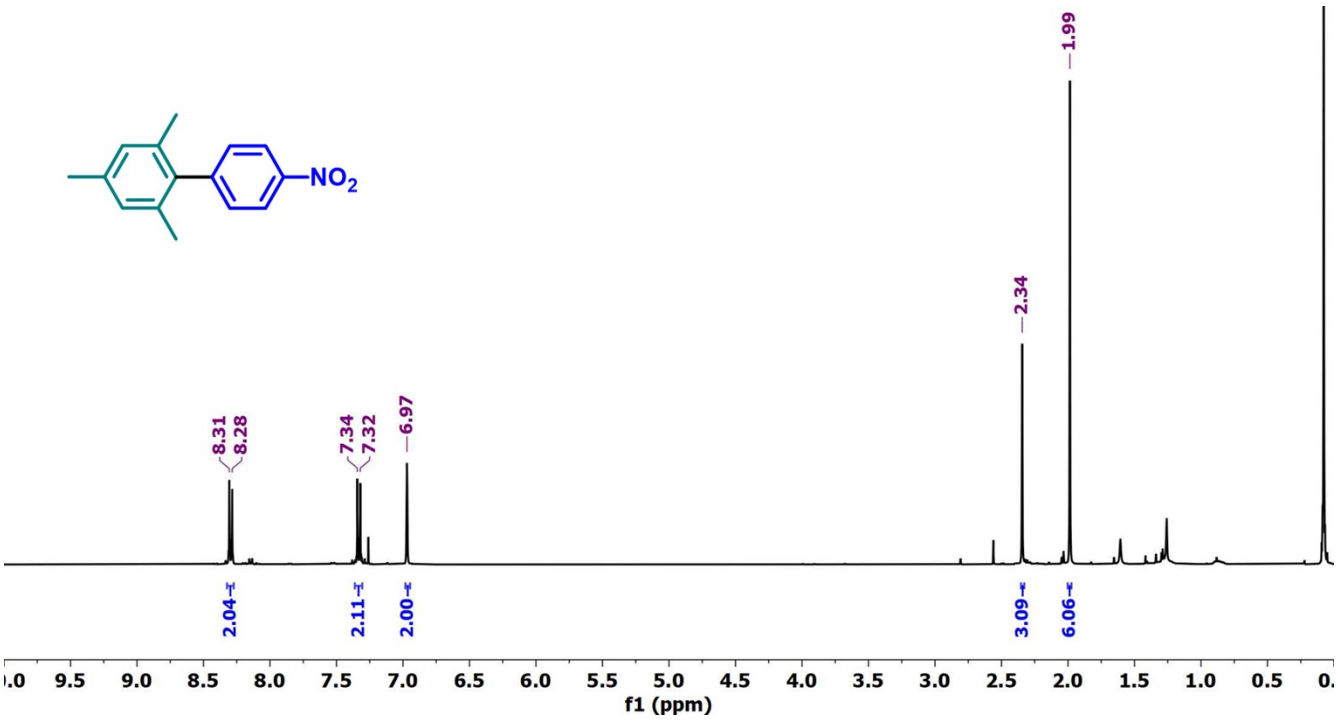

Figure S96: ^{1}H NMR spectrum of **12c**.

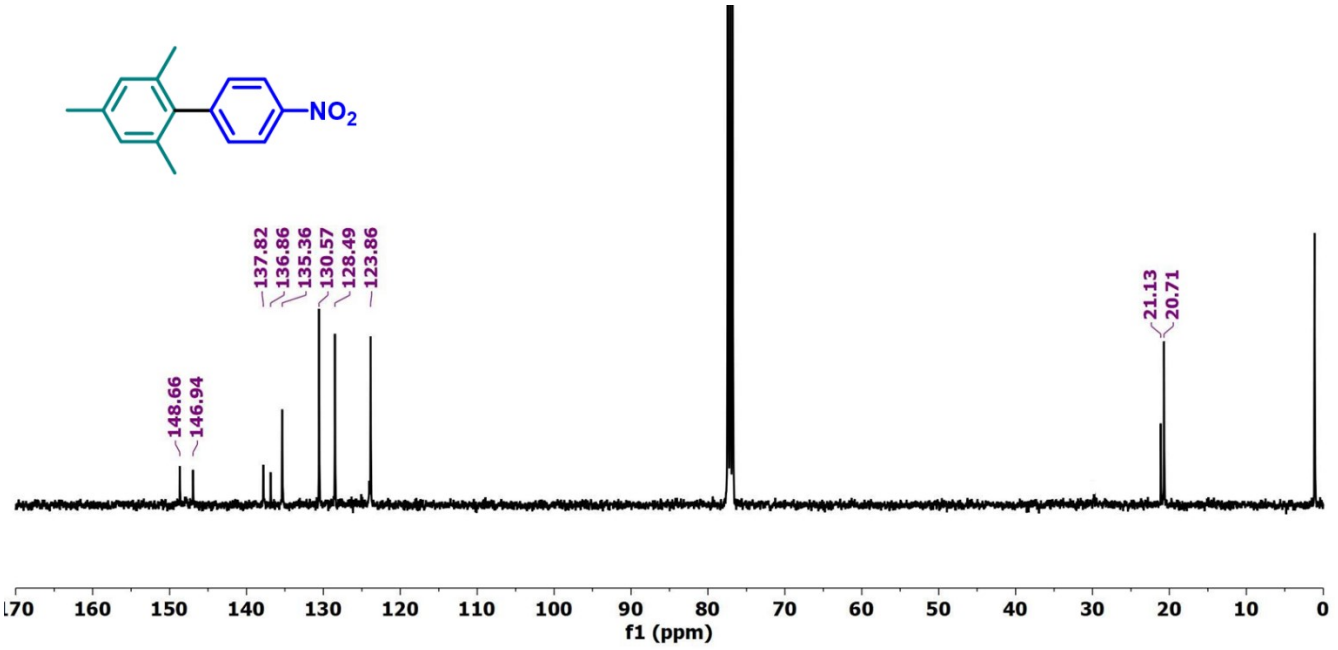

Figure S97: ^{13}C {^{1}H} NMR spectrum of **12c**.

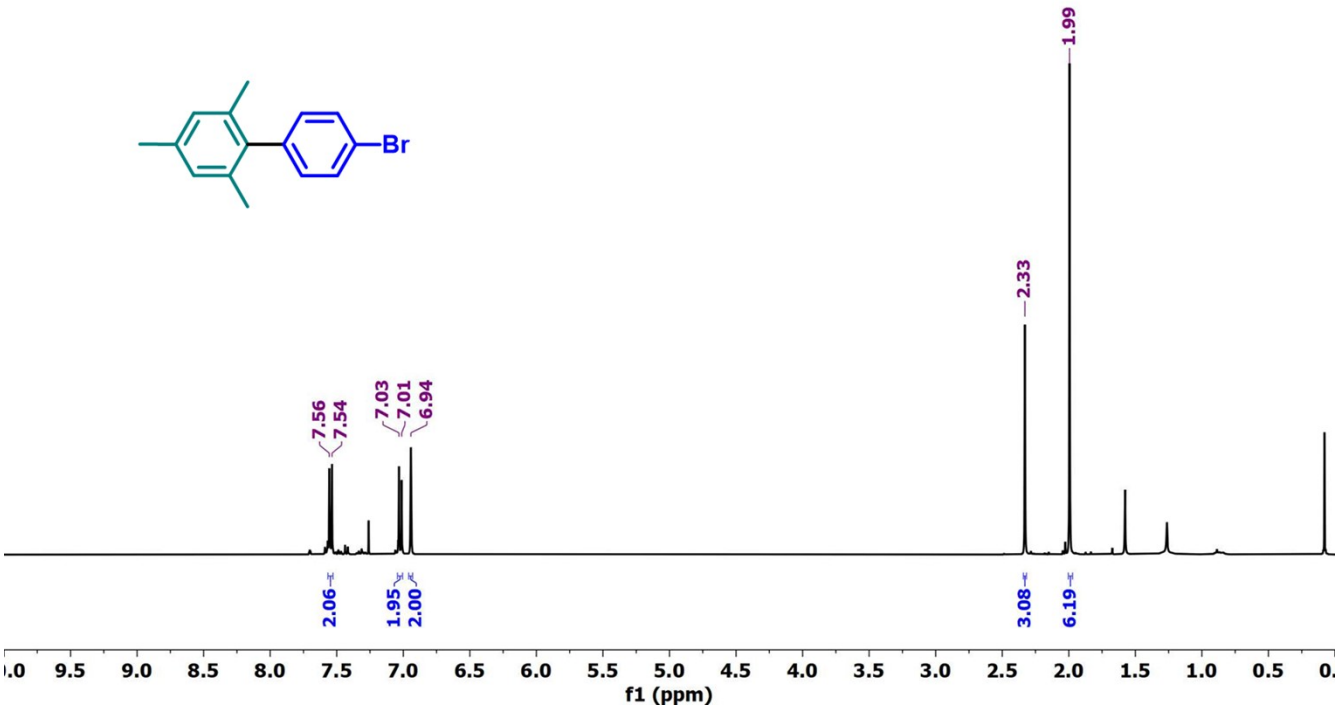

Figure S98: ^{1}H NMR spectrum of **12d**.

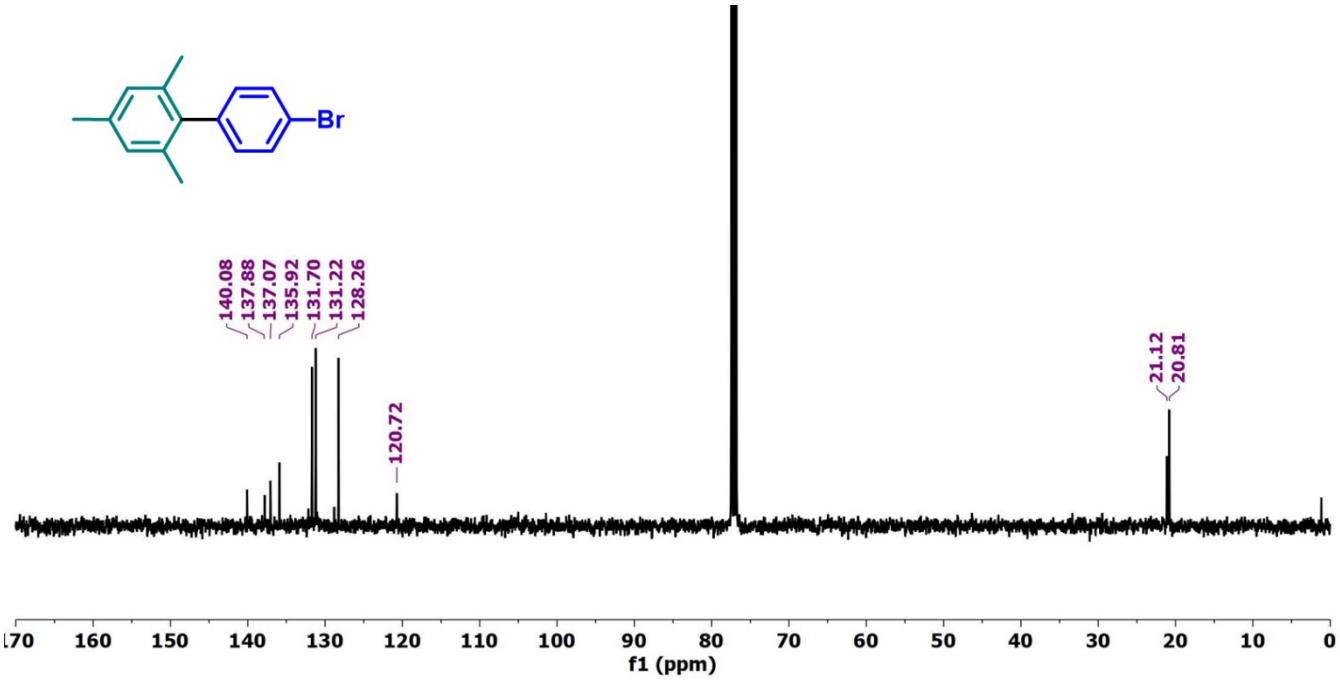

Figure S99: ^{13}C {^{1}H} NMR spectrum of **12d**.

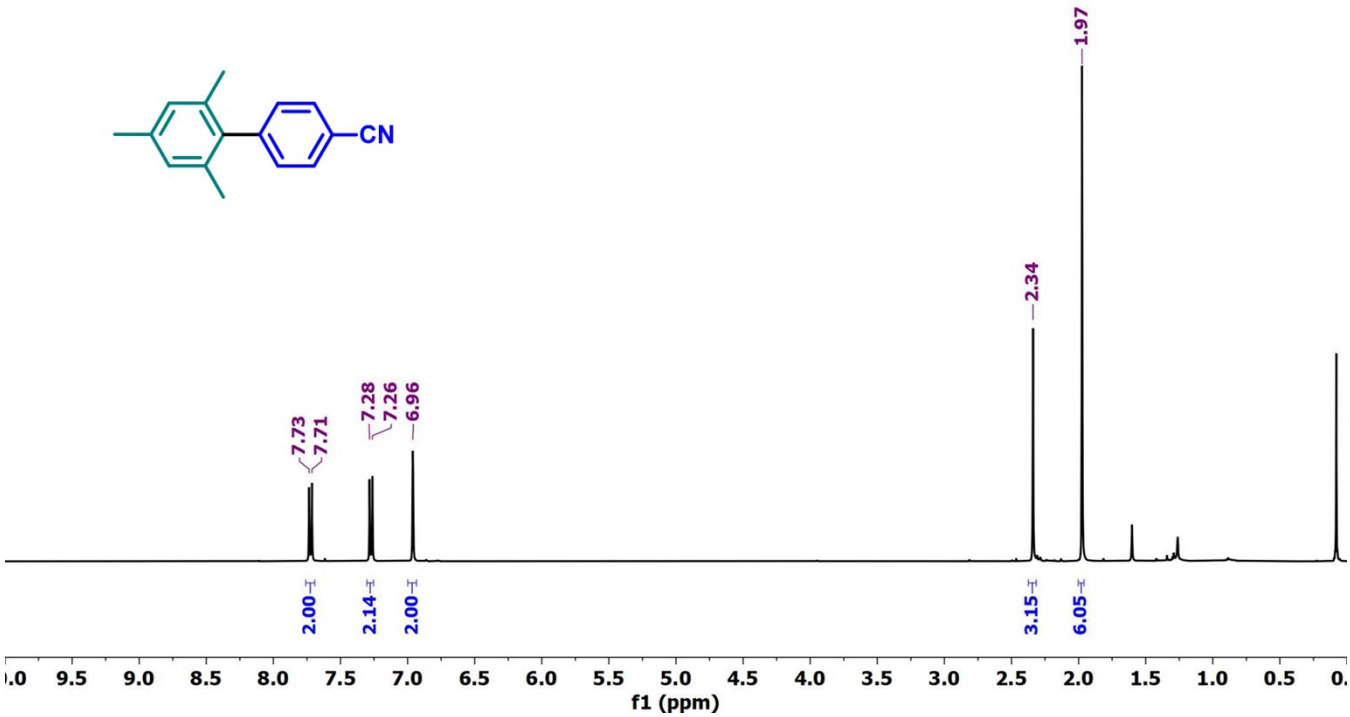

Figure S100: ^{1}H NMR spectrum of **12e**.

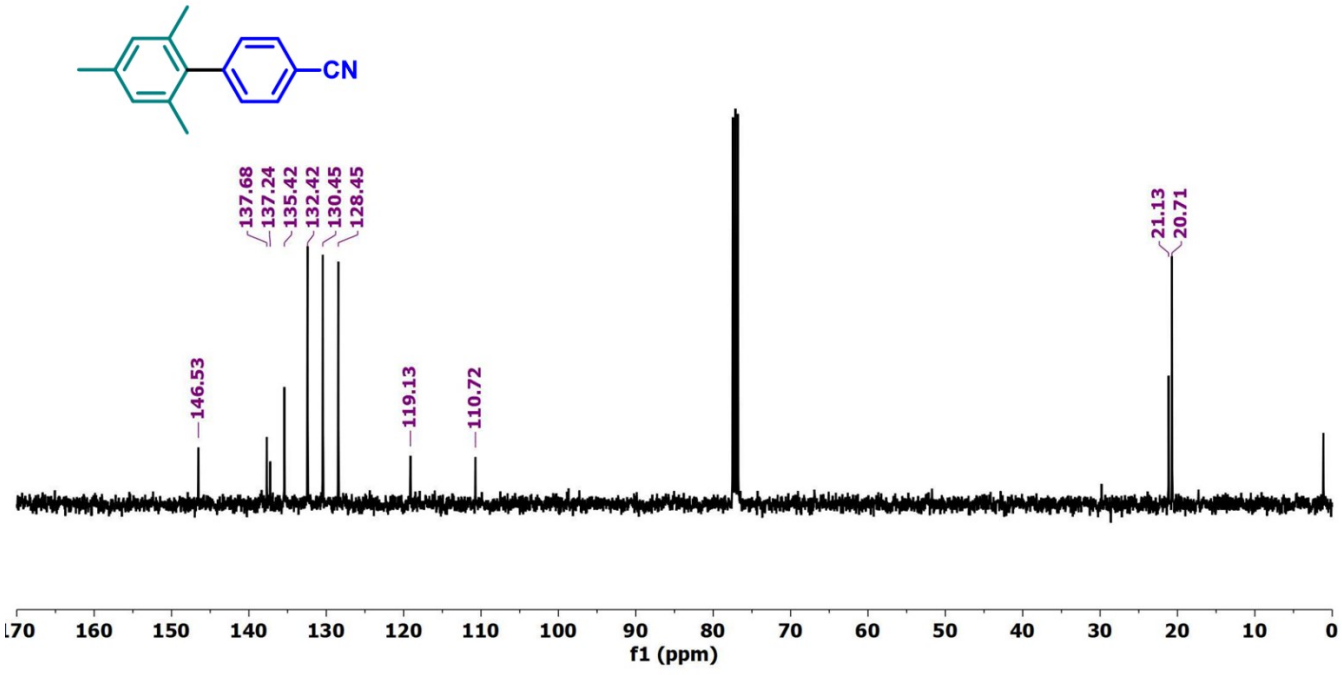

Figure S101: ^{13}C {^{1}H} NMR spectrum of **12e**.

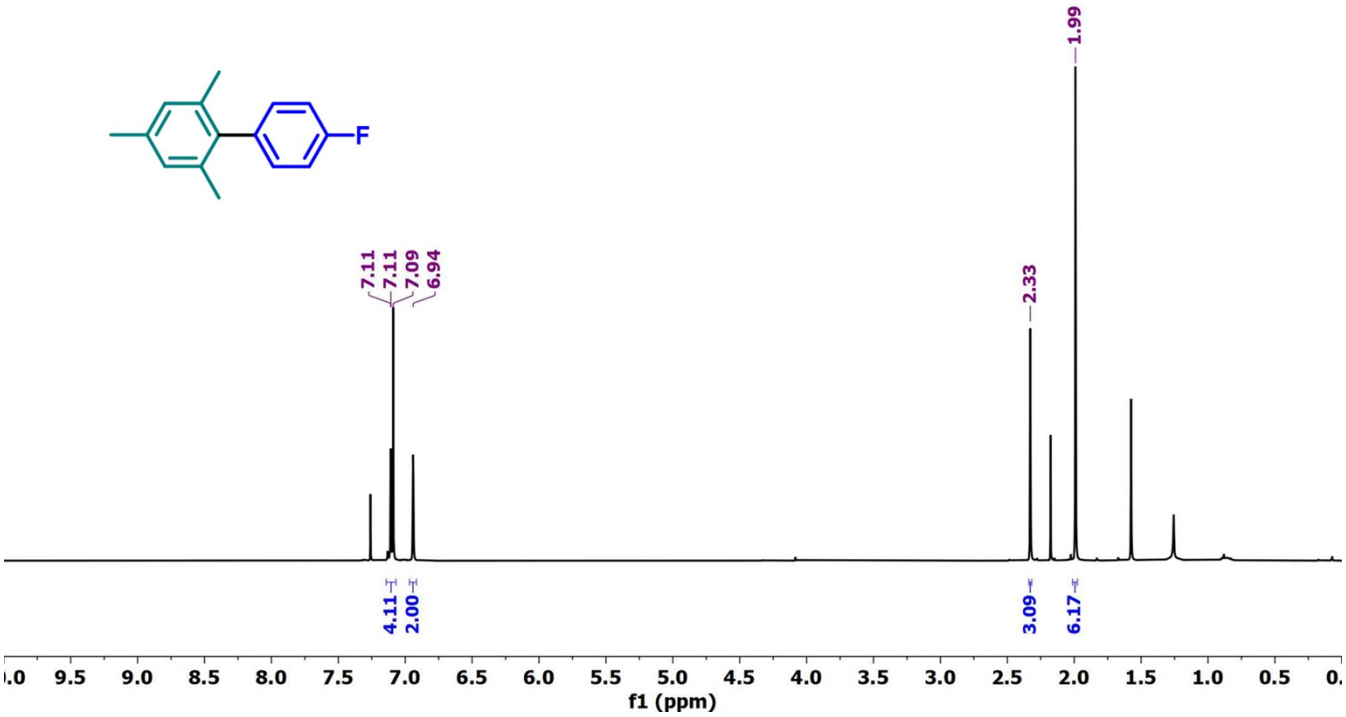

Figure S102: ^{1}H NMR spectrum of **12f**.

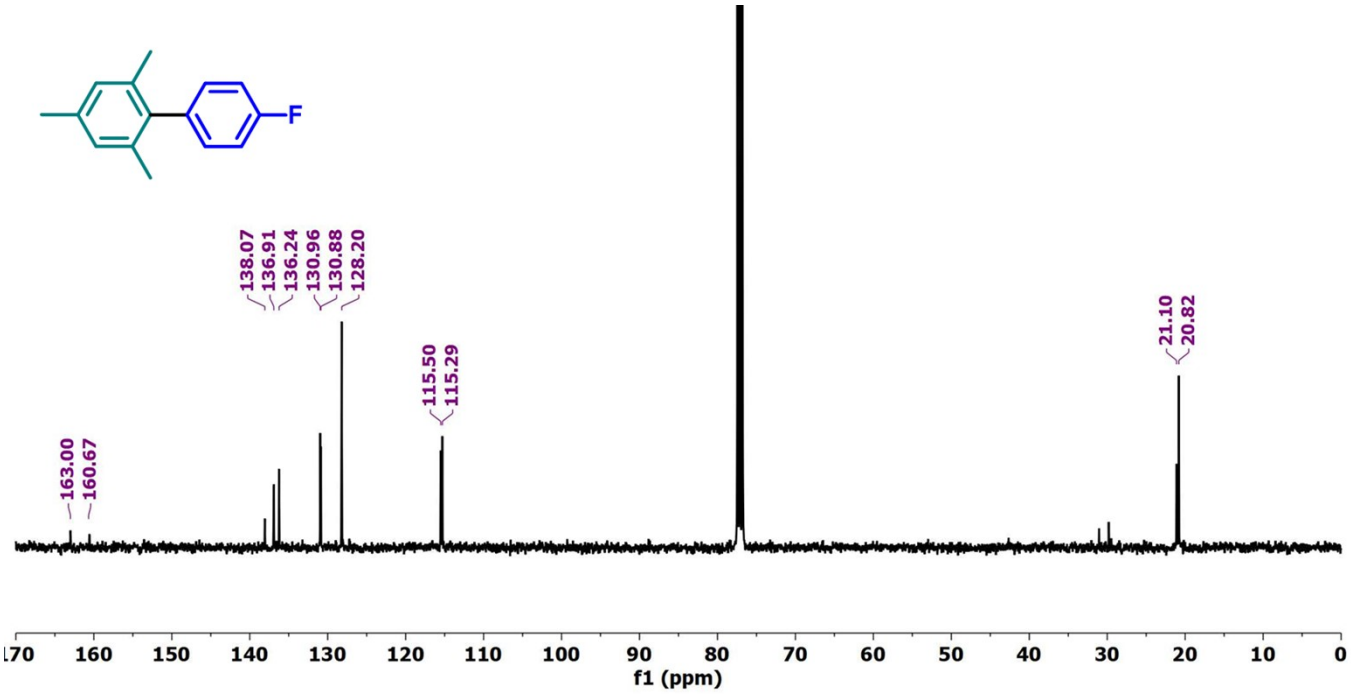

Figure S103: ^{13}C {^{1}H} NMR spectrum of **12f**.

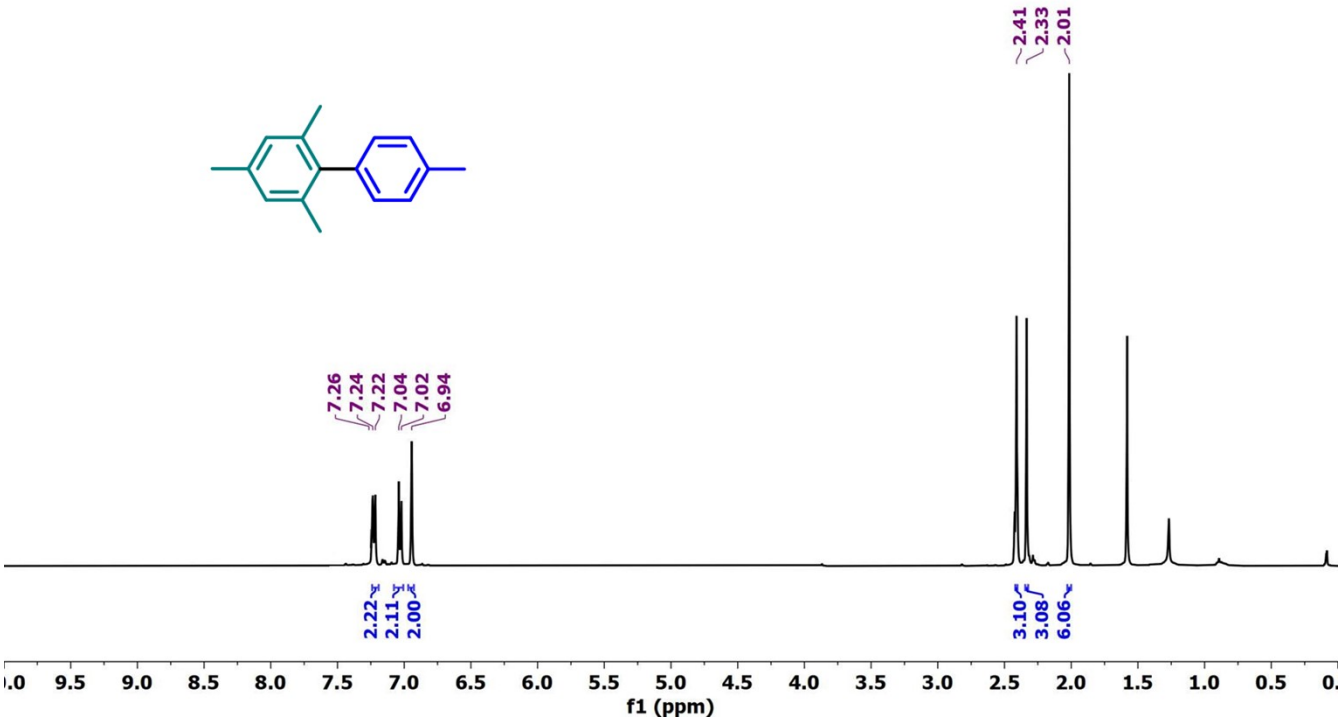

Figure S104: ^{1}H NMR spectrum of **12g**.

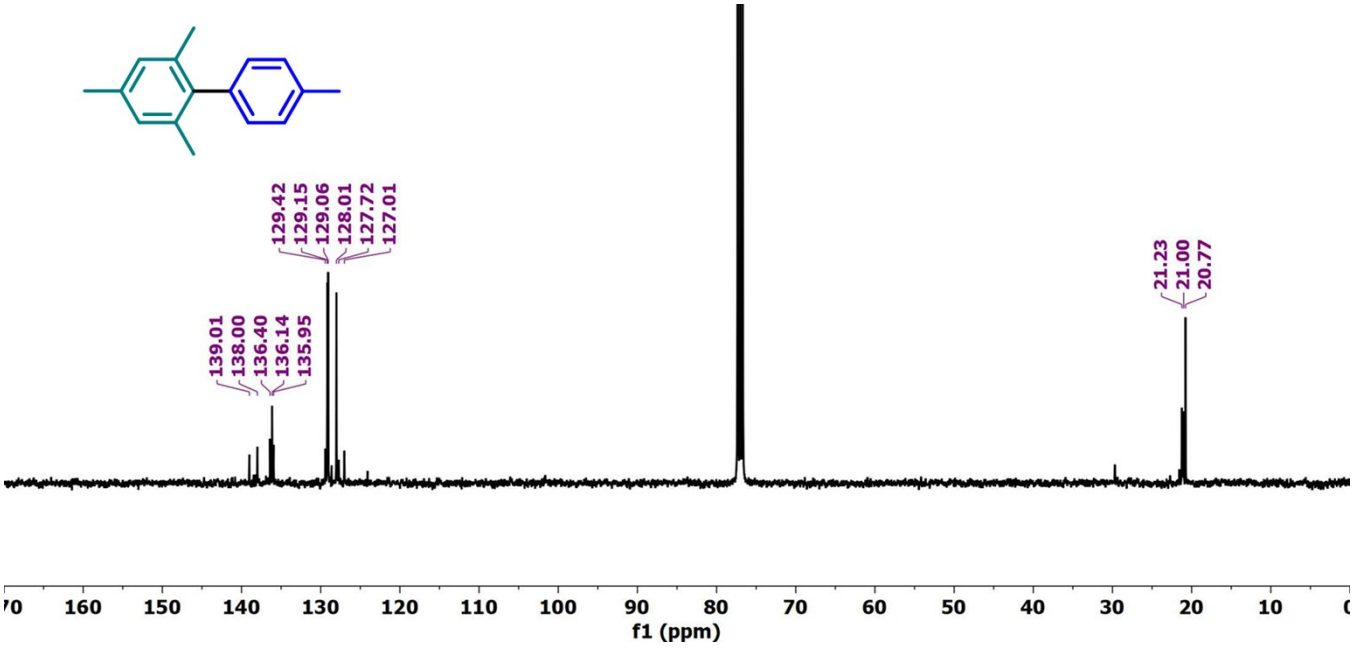

Figure S105: ^{13}C {^{1}H} NMR spectrum of **12g**.

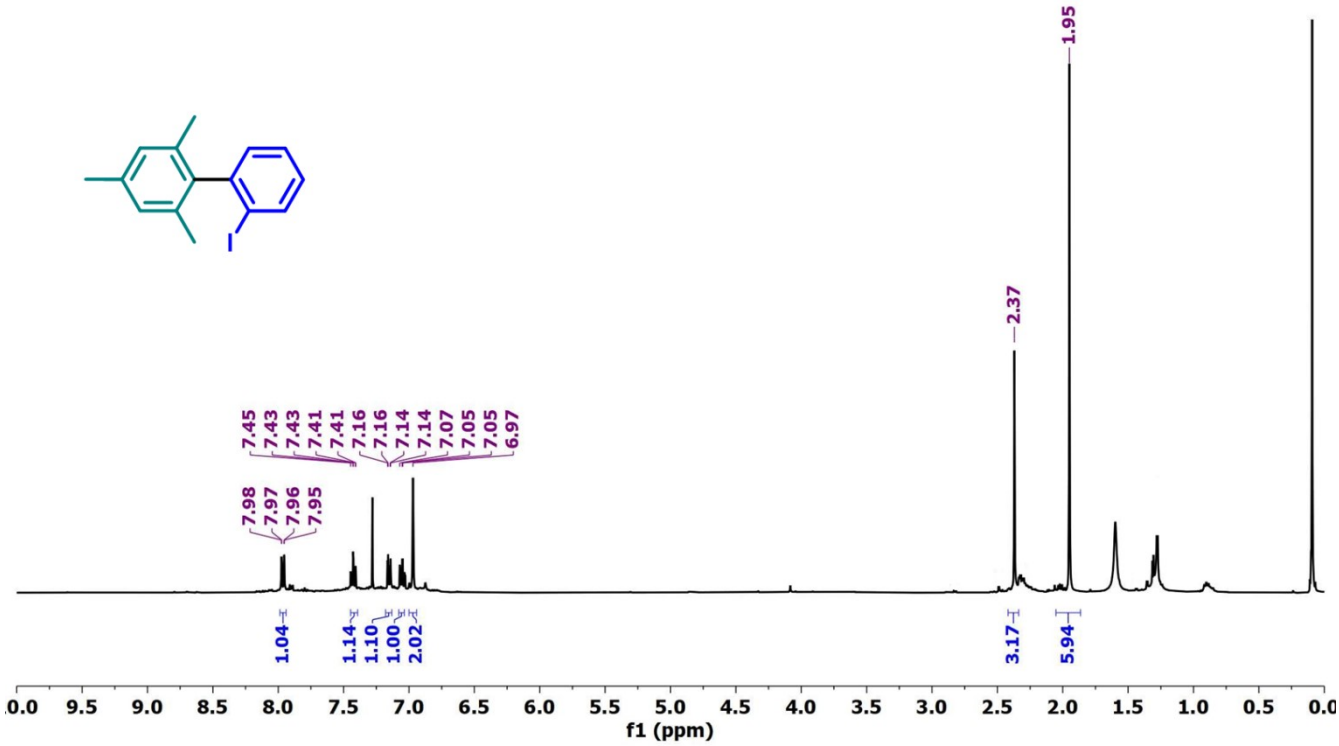

Figure S106: ^{1}H NMR spectrum of **12h**.

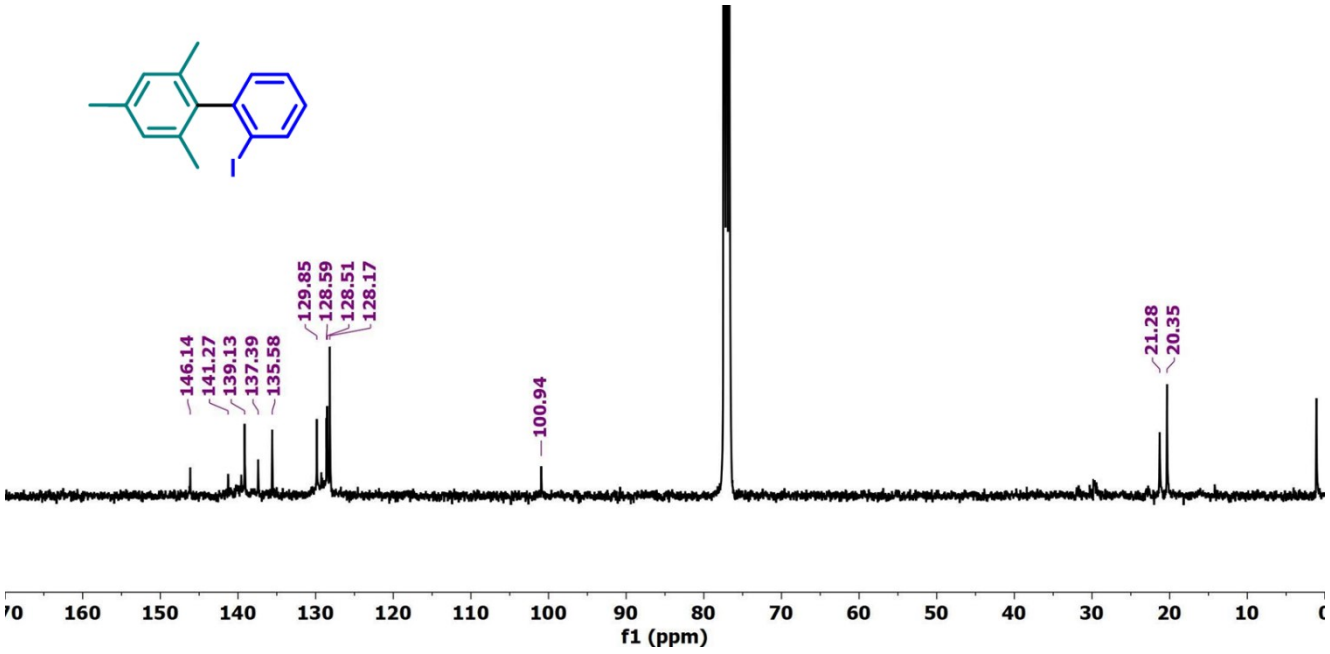

Figure S107: ^{13}C {^{1}H} NMR spectrum of **12h**.

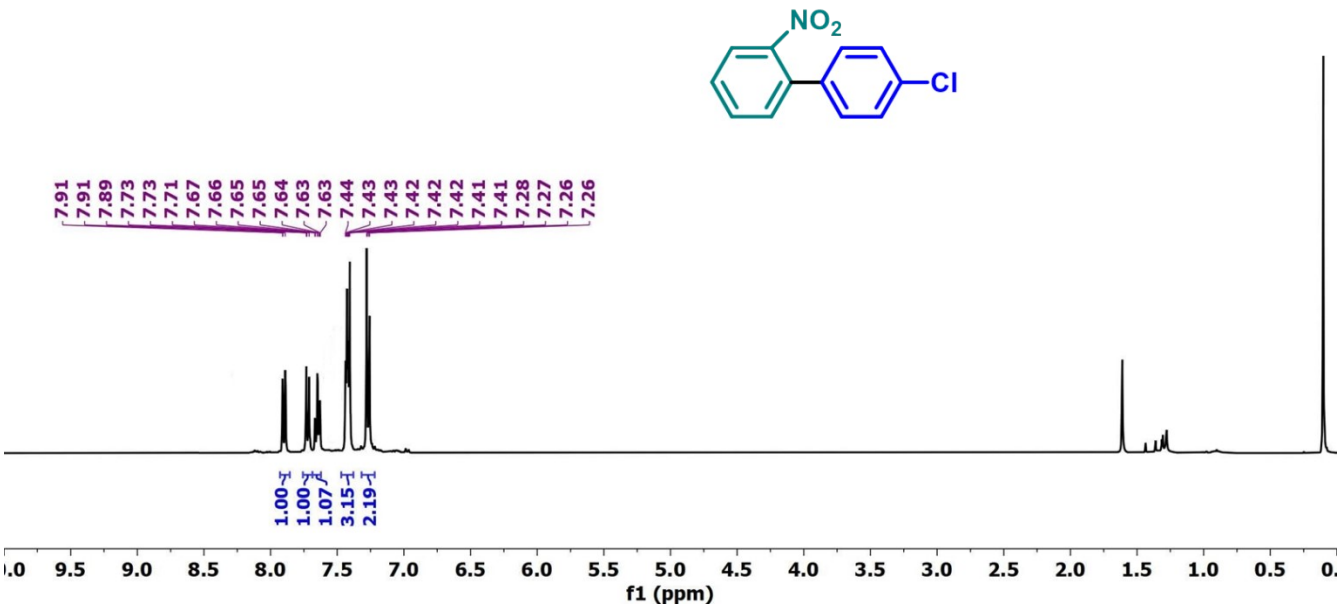

Figure S108: ^{1}H NMR spectrum of **13a**.

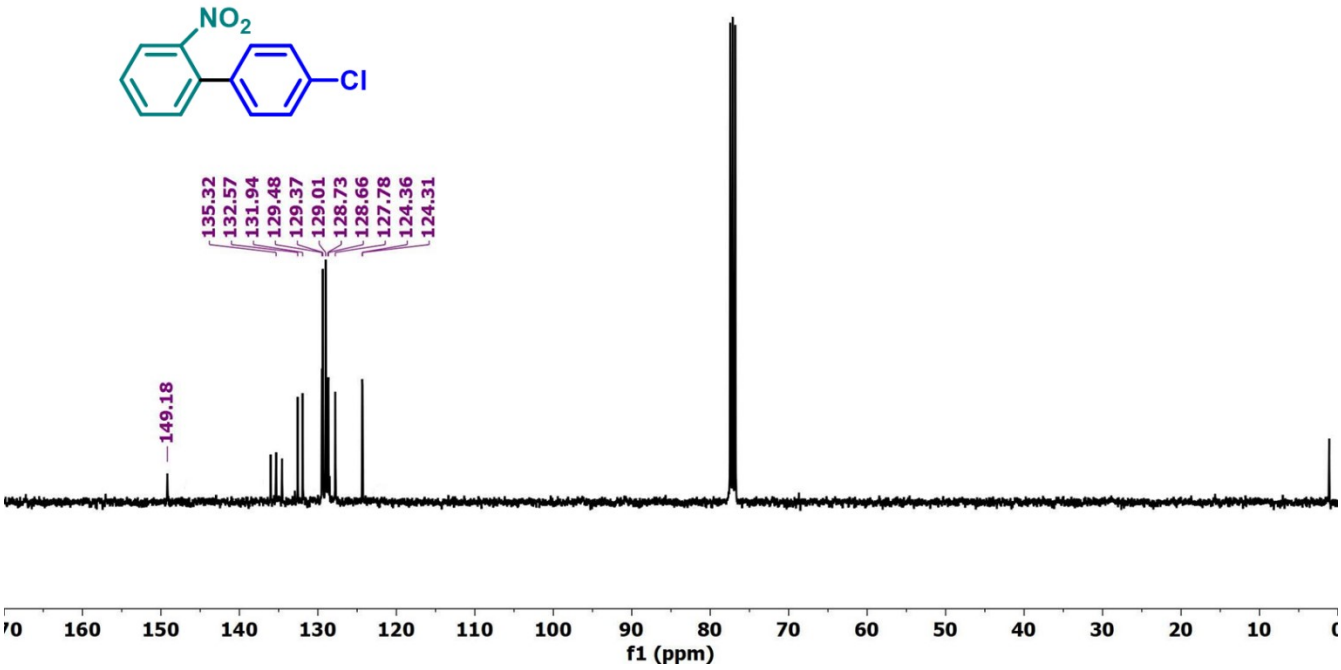

Figure S109: ^{13}C {^{1}H} NMR spectrum of **13a**.

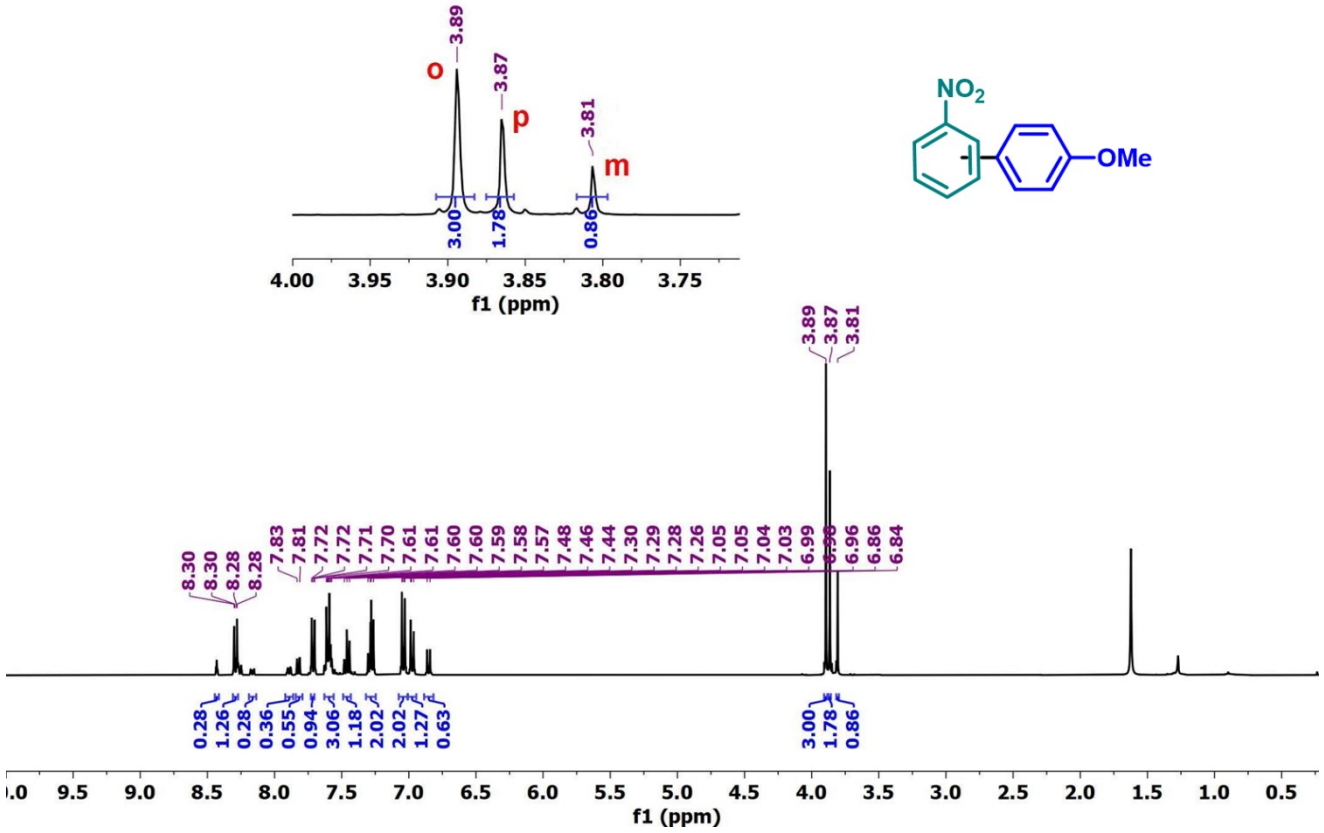

Figure S110: ^{1}H NMR spectrum of **13b**.

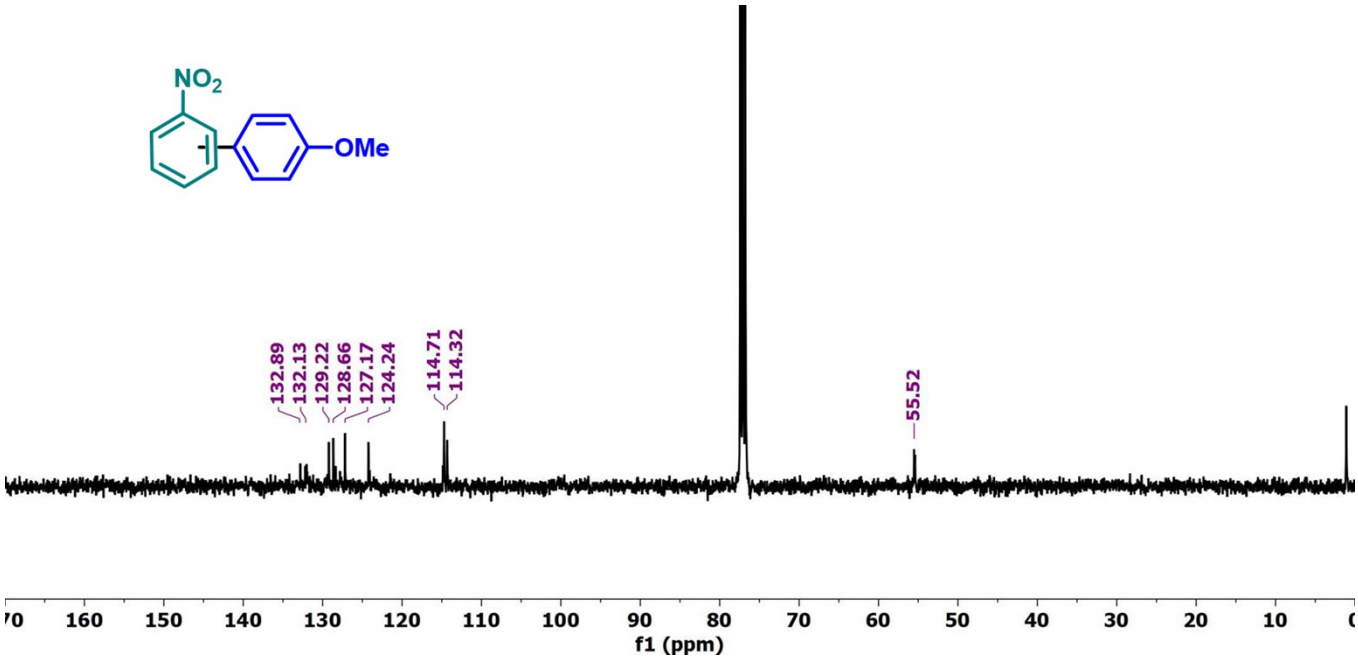

Figure S111: ^{13}C {^{1}H} NMR spectrum of **13b**.

11. Computational details:

Coordinates of all the optimized geometries:

Complex 1:

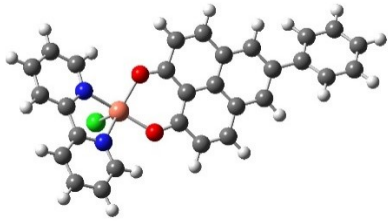

Cu	-2.358147	-0.009533	0.386461
Cl	-2.797074	-0.156195	2.695441
O	-1.071221	-1.307821	-0.323206
O	-1.042233	1.380176	0.317646
N	-3.852428	-1.265270	-0.120608
N	-3.798731	1.327917	-0.366421
C	0.201341	-1.193851	-0.330361
C	0.970768	-2.368191	-0.683825
C	0.403100	-3.262290	-0.919274
C	2.329357	-2.360141	-0.700606
H	2.878452	-3.263564	-0.955651
C	3.073703	-1.175174	-0.385750
C	4.474470	-1.161558	-0.409655
H	4.996323	-2.074452	-0.683952
C	5.214444	-0.005120	-0.125592
C	4.501204	1.161205	0.182121
H	5.044410	2.070130	0.426403
C	3.100216	1.191828	0.215955
C	2.382890	2.393906	0.525300
H	2.951404	3.294621	0.744430
C	1.024178	2.421926	0.547018
H	0.476610	3.327756	0.784447
C	0.230798	1.242592	0.281570

C	0.921182	0.017582	-0.026039
C	2.351009	0.010731	-0.061460
C	6.699027	-0.015498	-0.154674
C	7.422510	-1.125354	0.313727
H	6.887317	-1.974641	0.728105
C	8.815947	-1.136709	0.284845
H	9.353889	-2.002806	0.659623
C	9.518462	-0.036605	-0.209570
H	10.604168	-0.044583	-0.230354
C	8.813783	1.074056	-0.676573
H	9.349715	1.932451	-1.071473
C	7.420275	1.083496	-0.651233
H	6.882333	1.941364	-1.043857
C	-3.757436	-2.589726	0.034840
H	-2.780740	-2.953427	0.331315
C	-4.838540	-3.438997	-0.181477
H	-4.724134	-4.508403	-0.045615
C	-6.056781	-2.880648	-0.564146
H	-6.923996	-3.510232	-0.736800
C	-6.153444	-1.501129	-0.723494
H	-7.092908	-1.051253	-1.021029
C	-5.024641	-0.710044	-0.492070
C	-4.997758	0.766872	-0.621690
C	-6.105309	1.546038	-0.968473
H	-7.066948	1.088829	-1.168484
C	-5.957836	2.928547	-1.047008
H	-6.805982	3.551839	-1.312577
C	-4.714941	3.497868	-0.776171
H	-4.562170	4.570332	-0.822446
C	-3.659283	2.655143	-0.434941
H	-2.666129	3.024444	-0.202384

12. Reference:

1. R. C. Haddon, R. Rayford and A. M. Hirani, *J. Org. Chem*., 1981, **46**, 4587-4588.
2. L. Bensch, I. Gruber, C. Janiak, T. J. J. Mueller, *Chem.-Eur. J*., 2017, **23**, 10551-10558.
3. F. Mohr, S. A. Binfield, J. C. Fettinger and A. N. Vedernikov, *J. Org. Chem*., 2005, **70**, 4833-4839.
4. SMART, Version 5.0, Bruker AXS, Inc., Analytical X-ray Systems, 5465 East Cheryl Parkway, Madison, WI 53711 5373, 2000.
5. SAINT, Version 6.02, Bruker AXS, Inc., Analytical X-ray Systems, 5465 East Cheryl Parkway, Madison, WI 53711 5373, 2000.
6. G. M. Sheldrick, SADABS, Program For Empirical Correction of Area Detector Data, University of Gottingen, Germany, 2000.
7. G. M. Sheldrick, SHELXS97 and SHELXL97, Program For Crystal Structure Refinement, University of Gottingen, Germany, 1997.
8. S. Chakraborty, J. Ahmed, B. K. Shaw, A. Jose, and S. K. Mandal, *Chem. Eur. J*., 2018, **24**, 17651.
9. A. Nagaki, K. Hirose, Y. Moriwaki, K. Mitamura, K. Matsukawa, N. Ishizukac and J. Yoshida, *Catal. Sci.Technol.*, 2016, **6**, 4690.
10. K. Funaki, T. Sato and S. Oi, *Org. Lett*., 2012, **14**, 6186.
11. E. L. Kolychev, A. F. Asachenko, P. B. Dzhevakov, A. A. Bush, V. V. Shuntikov, V. N. Khrustalevc and M. S. Nechaev, *Dalton Trans*., 2013, **42**, 6859.
12. S. Paul, K. K. Das, S. Manna and S. Panda, *Chem. Eur. J*., 2020, **26**, 1922.
13. P. K. Vardhanapu, J. Ahmed, A. Jose, B. K. Shaw, T. K. Sen, A. A. Mathews and S. K. Mandal, *J. Org. Chem*., 2019, **84**, 289.
14. E. Shirakawa, K. -i. Itoh, T. Higashino and T. Hayashi, *J. Am. Chem. Soc*., 2010, **132**, 15537.
15. J. Ahmed, S. Chakraborty, A. Jose, P. Sreejyothi and S. K. Mandal, *J. Am. Chem. Soc*., 2018, **140**, 8330.
16. P. Klein, V. D. Lechner, T. Schimmel and L. Hintermann, *Chem. Eur. J*., 2020, **26**, 176.
17. Y. Liu, Y. Feng, J. Nie, S. Xie, X. Pen, H. Hong, X. Chen, L. Chen and Y. Li, *Chem. Commun*., 2023, **59**, 11232.
18. G.-Q. Chen, W. Fang, Y. Wei, X.-Y. Tang and M. Shi, *Chem. Commun*., 2016, **52**, 10799.
19. Arumugam, W. Kaminsky, N. S. P. Bhuvaneshc and D. Nallasamy, *RSC Adv*., 2015, **5**, 59428.
20. T. Yoshida, Y. Honda, T. Morofuji and N. Kano, *Org. Lett*., 2021, **23**, 9664.
21. C. Fricke, A. Dahiya, W. B. Reid and F. Schoenebeck, *ACS Catal*., 2019, **9**, 9231.
22. D. Kim, G. Choi, W. Kim, D. Kim, Y. K. Kang and S. H. Hong, *Chem. Sci*., 2021, **12**, 363.
23. X.-B. Lan, F.-M. Chen, B.-B. Ma, D.-S. Shen and F.-S. Liu, *Organometallics.*, 2016, **35**, 3852.

24. A. Operamolla, O. H. Omar, F. Babudri, G. M. Farinola and F. Naso, *J. Org. Chem*., 2007, **72**, 10272.
25. T. E. Storr and M. F. Greaney, *Org. Lett*., 2013, **15**, 1410.
26. C. Qin and W. Lu, *J. Org. Chem*., 2008, **73**, 7424.
27. H. Zhao, J. Shen, J. Guo, R. Ye and H. Zeng, *Chem. Commun*., 2013, **49**, 2323.
28. D. Dey, A. Kundu, M. Roy, S. Pal and D. Adhikari, *Catal. Sci. Technol*., 2022, **12**, 1934.
29. V. Gauchot, D. R. Sutherland and A.-L. Lee, *Chem. Sci*., 2017, **8**, 2885.